INFORMATION TO USERS

This manuscript has been reproduced from the microfilm master. UMI films the text directly from the original or copy submitted. Thus, some thesis and dissertation copies are in typewriter face, while others may be from any type of computer printer.

The quality of this reproduction is dependent upon the quality of the copy submitted. Broken or indistinct print, colored or poor quality illustrations and photographs, print bleedthrough, substandard margins, and improper alignment can adversely affect reproduction.

In the unlikely event that the author did not send UMI a complete manuscript and there are missing pages, these will be noted. Also, if unauthorized copyright material had to be removed, a note will indicate the deletion.

Oversize materials (e.g., maps, drawings, charts) are reproduced by sectioning the original, beginning at the upper left-hand corner and continuing from left to right in equal sections with small overlaps.

Photographs included in the original manuscript have been reproduced xerographically in this copy. Higher quality 6" x 9" black and white photographic prints are available for any photographs or illustrations appearing in this copy for an additional charge. Contact UMI directly to order.

ProQuest Information and Learning
300 North Zeeb Road, Ann Arbor, MI 48106-1346 USA
800-521-0600

Université d'Ottawa · University of Ottawa

Low Density Lipoprotein Receptor: Interaction with Ligands and Molecular Chaperone Proteins

Written by
Vinita Chauhan

A thesis presented to the School of Graduate Studies
In partial fulfillment of the requirements of the degree of Doctor of Philosophy

Department of Biochemistry, Immunology and Microbiology, Faculty of Medicine,
University of Ottawa
October, 2001

ABSTRACT

The low density lipoprotein receptor (LDLr) is a complex multi-domain protein that is involved in the maintenance of cholesterol homeostasis. To study the kinetics of interaction of lipoproteins to the LDLr, we produced truncated forms of the LDLr that included the ligand-binding domain with and without the EGF homology domain. In the absence of the EGF precursor homology domain the receptor was secreted from Chinese hamster ovary (CHO-K1) cells as inactive, disulfide-linked multimers. In contrast, in the presence of the EGF precursor homology domain the receptor was secreted as a functional monomeric species. These observations led us to believe that inter-domain interactions may be involved in producing an active receptor. Since many mutations that cause familial hypercholesterolemia (FH) map to the EGF precursor homology domain, we expressed the EGF precursor homology domain as a separate polypeptide in order to determine if it could act *in trans* to assist in the proper folding of the ligand-binding domain. We propose a model, whereby an initial co-translational stabilization of the ligand-binding domain by chaperone proteins is followed by a post-translational interaction of the EGF repeats with the ligand-binding domain to yield a properly folded and functional receptor.

Low density lipoproteins (LDL) are heterogeneous in terms of size, lipid composition and protein conformation. These factors influence the ability of LDL to bind to the LDLr. The binding of lipoproteins to the LDLr is also modulated by a number of other factors including ligand conformation, cell surface proteoglycans and steric

hindrance. Surface plasmon resonance (SPR) was used to determine the affinity and kinetics of the LDL-LDLr interaction. This technology allows for interactions to be continuously monitored in real time and generates binding profiles from which rate constants can be derived. To minimize lattice effects and to exclude the participation of other cell surface components, a soluble N-terminal 692 amino acid LDLr fragment was stably produced in mammalian cells. The LDLr was expressed at 10 μg/ml and could be immuno-purified to homogeneity using the anti-LDLr monoclonal antibody, C7. The LDLr bound biotinylated LDL on a ligand blot and, when monitored by SPR, it could bind native but not acetylated LDL, which demonstrates its physiological specificity. The kinetics of binding fit a model in which a conformational change in the receptor and/or the ligand occurs following the initial binding that converts a low affinity complex to a high affinity complex with a slow dissociation rate. To determine the effect of LDL heterogeneity on the kinetics of binding, LDL from hypertriglyceridemic patients was tested. The small, dense and triglyceride-enriched particles bound the LDLr with similar conformational kinetics as native LDL.

DEDICATIONS

I dedicate this thesis to my "Lily"

ACKNOWLEDGEMENTS

I would like to express my appreciation to everyone who has contributed to the successful completion of my education. Firstly, my supervisor Dr. R. W. Milne who has provided me with the freedom to excerise my abilities and guided me along the journey. Under his supervision, I have learned patience and the art of tact. I would like to thank my committee members, Dr J. Van Huysse, Dr. Y. Marcel and Dr. Z. Yao for providing me with critical insights into the direction of my project. The studies conducted at the NRC would not have been complete without the expertise of Dr. R. Mackenzie and Tomoko Hirama. Lastly, I would like to acknowledge past and present members of the lipoprotein and atherosclerosis group. Particularly, Dr. K. Ko, Dr. Y. Wang, Dr. X. Wang, Dr. K. Tran, Vivian Franklin, Ann Nyugen, Reema Harish, Viken Tenkejian, Stephanie Walter, Rita Kohen and Jelena Vukmirica.

TABLE OF CONTENTS

ABSTRACT ii
DEDICATION iv
ACKNOWLEDGEMENTS v
TABLE OF CONTENTS vi
LIST OF TABLES viii
LIST OF FIGURES ix
ABBREVIATIONS xii

CHAPTER I: General introduction

LDL receptor function 2

Cholesterol influx
SR-B1 3
LRP 4
LDLr pathway 4

The low density lipoprotein receptor
Genes 9
Multidomain protein 10

Insights into the structure/function of the LDLr
Biochemical techniques 18
Circular dichroism 20
NMR & X-ray crystallography 22

LDLr interaction with ligands
Apolipoprotein B100 29
Apolipoprotein E 35

LDL heterogenity and binding to the LDLr 41

LDLr binding kinetics 43

Diseases Pertaining to LDLr
Familial hypercholesterolemia 44
Acquired defects in the LDLr pathway 47

Rationale and objective 48

CHAPTER II: Expression and secretion of a soluble LDLr

Introduction 50
Materials and experimental procedures 54
Results 63
Discussion 86

CHAPTER III: Components required for the proper folding of the LDLr

Introduction 93
Materials and experimental procedures 96
Results 100
Discussion 113

CHAPTER IV: Kinetics of LDL-LDLr interaction

Introduction 119
Materials and experimental procedures 122
Results 127
Discussion 150

CHAPTER V: General discussion & future perspectives 156

REFERENCES 166

LIST OF TABLES

Table 4-1 Mass percentage composition of LDL and HTG-LDL 130

Table 4-2 Rate constants 149

LIST OF FIGURES

Figure 1-1 LDLr pathway 8

Figure 1-2 The multidomain structure of the low density lipoprotein receptor 12

Figure 1-3 Amino acid sequence of ligand-binding domain 1 (LB1) and ligand-binding domain 2 (LB2) 13

Figure 1-4 Binding of calcium to the LDLr 15

Figure 1-5 Ribbon diagrams of β-propeller domain predicted for the YWTD domain of nidogen 27

Figure 1-6 Structure of human apoB100 31

Figure 1-7 Putative receptor-binding sites 34

Figure 1-8 "Ribbon and Bow" model for the conformation of apoB100 on the LDL surface 36

Figure 1-9 Schematic representation of helix 4 and helix 3 of the receptor-competent ApoE3 and receptor incompetent apoE2 40

Figure 2-1 Features of pPICZαB 52

Figure 2-2 Agarose gel analysis of $LDLr^{331}$ 64

Figure 2-3 PCR analysis of genomic DNA isolated from *Pichia* recombinants using 5' and 3' AOX1 primers 65

Figure 2-4 Immunoblot analysis of $LDLr^{331}$ (non reducing) 67

Figure 2-5 Immunoblot analysis of $LDLr^{331}$ (reducing) 68

Figure 2-6 Agarose gel analysis of $LDLr^{692}$ 70

Figure 2-7 PCR analysis of genomic DNA isolated from *Pichia* recombinants using 5' and 3' AOX1 primers 72

Figure 2-8 Representative immunoblot analysis of $LDLr^{692}$ 73

Figure 2-9 Agarose gel analysis of $LDLr^{331\text{-His}}$, $LDLr^{331}$ & $LDLr^{292}$ 74

Figure 2-10 Agarose gel analysis of purified DNA from positive $LDLr^{331\text{-}His}$, $LDLr^{331}$ & $LDLr^{292}$ transformants 76

Figure 2-11 Immunoblot analysis of $LDLr^{331\text{-}His}$ 77

Figure 2-12 Immunoblot analysis of $LDLr^{331}$ & $LDLr^{292}$ 78

Figure 2-13 Immunoblot analysis of $LDLr^{692}$ 79

Figure 2-14 Western blot analysis of $LDLr^{692}$ after adaptation to serum-free media 81

Figure 2-15 Analysis of purified $LDLr^{692}$ 82

Figure 2-16 Competitive ELISA 83

Figure 2-17 Schematic of constructs 88

Figure 3-1 Immunoblot analysis of RAP transfected $LDLr^{292}$ and $LDLr^{331}$ 101

Figure 3-2 Immunoblot analysis of $LDLr^{292}$ cells at different DNA concentrations 102

Figure 3-3 Immunoblot analysis of media from RAP and $LDL^{692/292}$ transfected cells 103

Figure 3-4 Immunoblot analysis of media from $LDLr^{292}$ transfected cells 105

Figure 3-5 Agarose gel analysis of PCR amplification product and restriction digest of positive $LDLr^{EGF\text{-}His}$ and W556S transformants 106

Figure 3-6 Immunoblot analysis of media & cells from W556S mutant transfected cells 108

Figure 3-7 Immunoblot analysis of media from $LDLr^{EGF}$ and $LDLr^{692/292}$ transfected cells 111

Figure 3-8 Immunoblot analysis of media from CETP, $LDLr^{EGF}$ and $LDLr^{692/292}$ transfected 112

Figure 4-1 Non denaturing gradient gel electrophoresis 128

Figure 4-2 Agarose gel analysis 129

Figure 4-3 Non-specific binding of LDL to F1 sensor chip 132

Figure 4-4 Sensorgram for binding of acetylated LDL and normal LDL 133

Figure 4-5 Curve fitting using 1:1 langmuire model 135
Figure 4-6 Curve fitting using bivalent model 136
Figure 4-7 Curve fitting using heterogeneous ligand model 137
Figure 4-8 Curve fitting using conformational change model 138
Figure 4-9 Components of conformational change model 139
Figure 4-10 LDL-LDLr interaction as a function of injection time 140
Figure 4-11 LDL-LDLr interaction as a function of [LDL] 143
Figure 4-12 LDL-LDLr interaction as a function of temperature 146
Figure 4-13 Curve fitting at different [HTG-LDL] 147
Figure 4-14 HTG-LDL & LDLr interaction as a function of injection time 148
Figure 4-15 Schematic of conformational change model 155
Figure 5-1 Point mutations in the β-propeller domain 164
Figure 5-2 Model depicting the post-translational folding of $LDLr^{692}$ 165

ABBREVIATIONS

ACAT	acyl-coenzyme A cholesterol acyltransferase
AOX	alcohol oxidase
Apo	apolipoprotein
Arg	arginine
Asp	aspartic acid
bHLH-ZIP	basic helix-loop-helix leucine zipper
Bip	binding protein
BMGY	buffered media glycerol
BMMY	buffered media methanol
BSA	bovine serum albumin
CETP	cholesteryl ester transfer protein
CHD	coronary heart disease
CHO-K1	Chinese hamster ovary
CMV	cytomegalovirus
Cys	cysteine
DMPC	dimyristoylphosphatidylcholine
E.coli	*Escherichia coli*
ECL	enzyme chemiluminescence
EDC	ethyl-dimethylaminopropyl carbodiimide hydrochloride
EGF	epidermal growth factor
ELISA	enzyme linked immunoassay
FDB	familial defective apolipoprotein B100
FH	familial hypercholesterolemia
GADPH	glyceraldehyde-3-phosphate dehydrogenase
Gln	glutamine

Grp78	glucose stress regulatory protein
HDL	high density lipoprotein
HMG-CoA	hydroxymethyl-glutyrl coenzyme A
HRP	horse-radish peroxidase
HTG	hypertriglyceridemic
IDL	intermediate density lipoprotein
Kb	kilobase
kDa	kiloDalton
LBB	ligand blot buffer
LCAT	lecithin cholesterol acyltransferase
LDL	low density lipoprotein
LDLr	low density lipoprotein receptor
LRP	low density lipoprotein receptor related protein
NGF	nerve growth factor
NHS	N-hydroxysuccinimide
Ni-NTA	nickle-triacetic acid
NMR	nuclear magnetic resonance
P. pastoris	*Pichia pastoris*
PBS	phosphate buffered saline
PCR	polymerase chain reaction
PLTP	phospholipid transfer protein
PMSF	phenylmethylsulfonyl fluoride
RAP	receptor associated protein
S2P	site 2 protease
SCAP	SREBP cleavage activating protein
SDS-PAGE	sodium-docecyl polyacrylamide gel electrophoresis
SPR	surface plasmon resonance
SRE	sterol regulatory element
SREBP	sterol regulatory element binding protein

TBS	tris buffered saline
TGF	transforming growth factor
TIR	totally internally reflected
TMB	terra-methyl-benzidine
VLDL	very low density lipoprotein
WHHL	Watanabe heritable hyperlipidemia
YPD	yeast peptone dextrose

Chapter I

General Introduction

Coronary heart disease (CHD) is currently the largest single cause of death in western societies, and by the year 2020 it is estimated to be the biggest single cause of death worldwide (Stemme et al., 2000). CHD is a chronic, progressive, and usually silent disorder, which kills about one third of those who suffer their first coronary event.

High plasma levels of cholesterol are known to be a hallmark for the development of CHD among other risk factors such as hypertension and smoking. In 1913, Anitschkow (Goldstein et al., 1983) demonstrated that rabbits, which were fed cholesterol, developed hypercholesterolemia. However, dietary cholesterol is only an indirect, aggravating factor. Human hypercholesterolemia is caused by genetic or acquired abnormalities in the degradation or synthesis of plasma lipoproteins. Lipoproteins are the fundamental shuttle mechanism of endogeneous cholesterol between body tissues. In laboratory animals, hypercholesterolemia is produced exogenously when normal mechanisms of lipoprotein clearance are overwhelmed by large amounts of dietary cholesterol. In 1983, Goldstein and Brown (Buja et al., 1983) discovered a new model to study endogenous hypercholesterolemia. A strain of rabbits designated Watanabe heritable hyperlipidemic (WHHL) rabbits were shown to develop massive hypercholesterolemia. It was found that WHHL rabbits have mutations in a gene that encodes the low density lipoprotein receptor (LDLr). This gene is also known to be mutated in patients with familial hypercholesterolemia. WHHL rabbits, like patients with

FH, have an elevation in cholesterol-carrying lipoproteins. These rabbits also exhibit a pattern of atherosclerosis that is indistinguishable from human disease. In 1988, Scanu et al. introduced a second animal model for FH in a pedigree of rhesus monkeys with hypercholesterolemia inherited in an autosomal dominant pattern. Fibroblasts from the hypercholesterolemic monkeys showed a half normal level of LDL receptor activity, protein and mRNA. These findings and studies of the WHHL rabbit have highlighted the important role that the LDLr plays in controlling both the production and the clearance of lipoproteins.

LDLr function:

The LDLr is a cell surface glycoprotein that binds apolipoprotein B100, the single protein component of low density lipoproteins (LDL) and apolipoprotein E, a protein associated with chylomicron remnants, very low density lipoproteins (VLDL), intermediate density lipoproteins (IDL) and a minor subclass of high density lipoproteins (HDL). It delivers vital nutrients into cells and removes LDL particles from the extracellular environment. The receptor also acts to deliver cholesterol into cells to be utilized as a structural component of membranes. The LDL-derived cholesterol is also used as precursor for the production of steroid hormones in steroidogenic tissues that express relatively high level of LDL receptors. In the liver, LDL receptors serve to remove LDL particles from the plasma, targeting the cholesterol either for assembly into VLDL for resecretion back into the plasma or excretion from the body as bile acids.

Thus, the hepatic LDLr pathway is responsible for the maintenance of steady-state plasma concentrations of LDL cholesterol (Brown and Goldstein, 1986).

Cholesterol influx:

Free cholesterol can enter cell compartments through a number of mechanisms. Described below is a brief overview of a few important receptors involved in cholesterol uptake with an emphasis on the LDLr pathway.

SR-BI:

SR-BI is a high affinity, cell-surface HDL receptor that mediates physiologically relevant selective cholesterol transport. It plays a key role in controlling plasma HDL cholesterol concentration and delivery of cholesterol to steriodogenic tissues. Krieger and colleagues have shown HDL to bind SR-BI and mediate the selective transfer of lipids, specifically cholesteryl esters (Rigotti et al. 1996). However, the mechanism of SR-BI-mediated selective lipid uptake has yet to be defined. SR-BI has been shown to cluster within caveolae on the surfaces of cultured cells. Caveolae are clathrin-free invaginations of the plasma membrane. This raises the possibility that specialized membrane domains (caveolae) may play a role in the selective uptake process.

SR-BI binds native LDL with high affinity, although LDL does not effectively compete with HDL binding (Acton et al., 1994). It is possible that SR-BI may serve as an alternative receptor to the critically important, classic LDLr.

Low density lipoprotein receptor related protein (LRP):

LRP is an endocytic plasma membrane receptor. It is a modular protein consisting of an unusually large extracellular domain, a transmembrane domain, and a short cytoplasmic tail. LRP is known to bind to a number of different ligands. These ligands include proteins involved in protease and lipoprotein metabolism specifically, lipid-associated apolipoprotein E, activated α_2-macrogobulin, vitellogenin, and receptor associated protein (RAP) (Krieger and Herz, 1994).

Experimental evidence has demonstrated that the LRP plays a role in chylomicron remnant metabolism (Ishibashi et al., 1996, Rohlmann et al., 1998). Chylomicron remnants are defined as large lipoproteins that are enriched in apolipoprotein E and have a buoyant density of less than 1.006 mg/ml. The initial step in binding remnant particles involves heparin sulfate proteoglycans at the plasma membranes. Proteoglycans most likely tether lipoproteins near the receptor prior to internalization. This model is based on the observation that lipoproteins appear to be captured by plasma membrane proteoglycans before being metabolized (Cooper, 1997). Upon internalization the particles undergo lysosomal hydrolysis similar to the LDLr pathway, which is described in detail below.

LDLr pathway:

The removal of LDL from the plasma is mediated by the high affinity LDLr pathway (Figure 1-1). The rate of uptake of LDL by this pathway is a function of the number of LDL receptors clustered within clathrin-coated pits. Coated pits are invaginations of the plasma membrane stabilized on the cytoplasmic surface by

interlocking clatherin trimers (triskelions). Clathrin is composed of three heavy (180 kDa) and three light (33 kDa) chain molecules. The carboxy-terminus of three clathrin heavy chains are linked together to form the hub of the triskilion, while the amino-terminus of each has a flexible globular domain. Triskelions assemble into a lattice with the globular domain protruding inwardly towards the membrane. This domain, as well as the hub, is stabilized by adaptor proteins (AP-1 and AP-2) that are bound to the membrane by a high-affinity binding site. Therefore, globular domains of each triskelion in an assembled lattice are in close proximity to the plane of the membrane. The globular domain of the clathrin triskelion is the principle site of interaction during LDLr clustering in coated pits (Ybe et al., 1999).

Clustered LDLrs localized within coated pits are internalized by vesicle budding. An early step of vesicle formation involves the self-assembly of a restricting annulus of dynamin subunits in response to GTP binding. Dynamin, a 100 kDa member of the GTPase superfamily, is the mammalian homologue of the Drosophilia Shibaura gene product. Dynamic has been shown to spontaneously self-assemble into rings and stacks of interconnected rings. Unvaccinated coated pits become constricted by the assembly of dynamic into rings around their necks. A concerted conformational change then closes the rings and pinches off the budding coated vesicles (Hinshaw and Schmid, 1995).

Upon budding, the coated vesicles lose their coat. Uncoating of clathrin is essential for the further metabolism of primary coated endosomes. An ATP-binding chaperone (uncoating ATPase, hsc70) promotes the disassembly of clathrin. The protein co-factor, auxilin is also required (Holstein et al, 1996). Auxilins and the beta-subunits of

AP-1 and –2 bind to independent sites on the heavy chain of clathrin. Auxilin has an attachment site for hsc70 and also promotes the attachment of hsc70 to the clathrin heavy chain. The product of these reactions is an uncoated vesicle, from which dissociated clathrin monomers return to the cell surface for assembly into new coated pits. The uncoated vesicles then fuse with endosomes, where the acidic environment causes the uncoupling of receptor and ligand. Endosomes containing ligand, fuse with lysosomes, while the receptor is recycled back to the surface of the plasma membrane. Within lysosomes, cholesterol esters are hydrolyzed, and cholesterol is released into the cytoplasm. The mechanism responsible for exit of LDL-cholesterol from lysosomes involves the NPC1 protein (Cruz and Chang, 2000). NPC1 is a multispanning membrane protein. It contains a sterol-sensing domain in the membrane spans and is involved in directing cholesterol binding. The NPC1 protein may also function to remove cholesterol from the degradative endosomal compartments by facilitating sterol transport to the Golgi. Mutations in the sterol-sensing domain results in an inactive protein, which causes cholesterol and other lipids to accumulate in lamellar bodies derived from lysosomes (Simons and Ikonen, 2000).

LDL-derived cholesterol is cycled to the cell surface for use in plasma membranes. When the amounts of unesterified cholesterol exceed the need for cell membranes, the excess cholesterol inhibits the cells' own synthesis of cholesterol, and cholesterol can be converted to inert cholesteryl ester for intracellular storage by the intracellular enzyme, acyl-coenzyme A cholesterol acyltransferase (ACAT). The

formation of free cholesterol initiates several regulatory events that prevent an overload of cells with cholesterol (Goldstein et al., 1986).

Homeostasis is achieved by modulating the transcription of genes encoding enzymes of cholesterol biosynthesis and uptake from plasma lipoproteins. The modulators are a family of membrane-bound transcription factors called sterol regulatory element binding proteins (SREBPs) (Brown and Goldstein, 1999). The SREBPs are members of the basic helix-loop-helix leucine zipper (bHLH-ZIP) family of transcription factors. Members of this family are known to bind DNA either as homodimers or heterodimers. The basic region mediates DNA binding, and dimerization is mediated by the helix-loop-helix and leucine zipper structure. SREBP is associated with the membrane of the nuclear envelope and endoplasmic reticulum, through two transmembrane domains, and exists as a looped structure with the amino- and carboxy-terminus exposed to the cytoplasm. When intracellular sterol concentrations decrease, SREBP becomes the substrate for proteolytic cleavage by two specific intracellular proteases. The first cleavage is catalyzed by a membrane-bound serine protease, designated Site-1 protease (S1P). S1P clips SREBPs at a leucine-serine bond within the luminal loop that links the two transmembrane domains. Cleavage of SREBPs by S1P requires the action of SREBP cleavage activating protein (SCAP), a polytopic membrane protein of 1276 amino acids that is found in tight complex with SREBPs in cells. SCAP possesses a sterol-sensing domain that shows homology to similar domains in hydroxy-methyl-glutaryl CoA (HMG CoA) reductase and in NPC1. In sterol-depleted cells, SCAP promotes budding of SREBP from the endoplasmic reticulum membrane and migration of the SREBP-SCAP-

Figure 1-1: LDLr pathway. Receptor-mediated uptake of LDL: pathways for uptake and degradation of LDL at the cellular level. For details, see text.

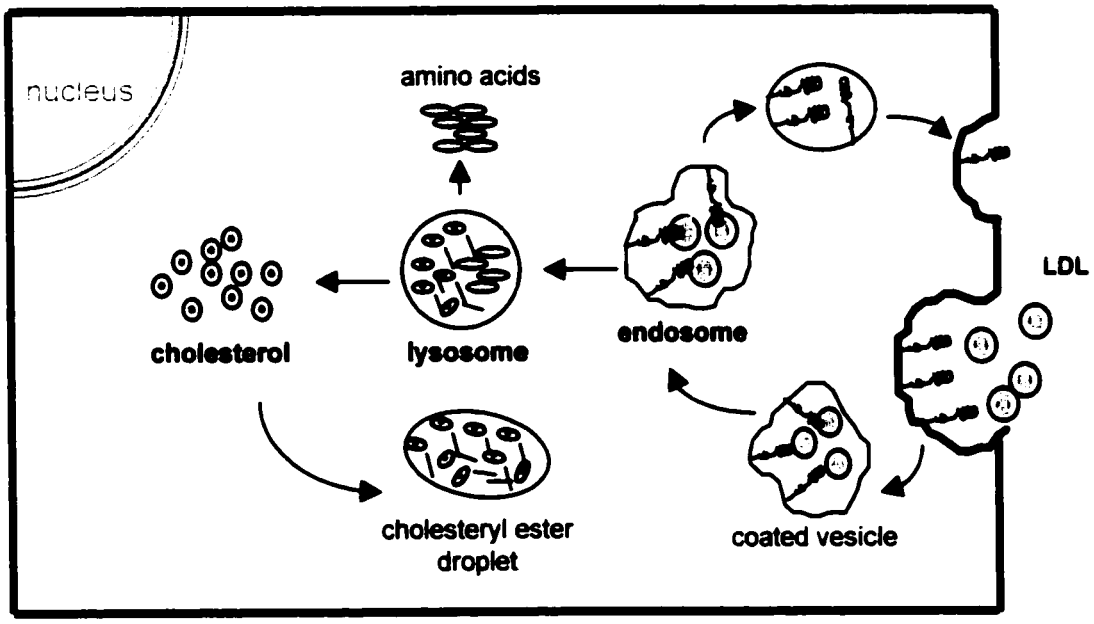
nucleus
amino acids
LDL
cholesterol
lysosome
endosome
cholesteryl ester
droplet
coated vesicle

containing vesicles to the Golgi where S1P is located (Nohturfft et al.,2000). Cleavage of SREBP by S1P generates a substrate for a second enzyme, a membrane-bound zinc metalloprotease, designated Site-2 protease (S2P) that cleaves the amino-terminal fragment of SREBP at a point that is three amino acids into the first transmembrane domain. The amino-terminal fragment of SREBP is released and is transported to the nucleus, where it associates with a sterol regulatory element (SRE) in the promoters of multiple genes encoding enzymes of cholesterol biosynthesis, unsaturated fatty acid biosynthesis, triglyceride biosynthesis and lipid uptake. In the cholesterol biosynthetic pathway, the target genes include, HMG CoA reductase, HMG CoA synthase, farnesyl diphosphate synthase and squalene synthase. The SREBPs also enhance transcription of the LDLr through an interaction with a SRE in the promoter of the LDLr gene (Brown and Goldstein, 1997).

LDL receptor genes:

The LDLr cDNA was cloned by Russell et al. (1983) and Yamamoto et al. (1984), and its gene was isolated and characterized in 1985 by Sudhof et al.. The LDLr mRNA is 5.3 kilobases in length and encodes a protein of 860 amino acids that includes a 21 residue signal sequence (Hobbs et al., 1990). The human LDLr gene is located on the distal short arm of chromosome 19, spans 45 kb and is divided into 18 exons and 17 introns (Sudhof et al., 1985). The active promoter of the LDLr is composed of a 200 base pair segment located upstream of the methionine codon. This region of the receptor contains *cis* acting DNA sequences that are responsible for the sterol regulation of the

gene (Goldstein et al., 1985a). Three imperfect direct repeats consisting of 16 base pairs each, two A/T rich sequences and a cluster of mRNA initiation sites, all function in the regulated transcription of the gene. Exon 1 encodes a short 5' untranslated region and 21 hydrophobic amino acids that comprise the signal sequence, which is cleaved during translocation into the endoplasmic reticulum. The mature protein is 839 amino acids in length. Exons 2-6 encode the ligand-binding domain. This domain is composed of seven imperfect repeats of forty amino acids. Exons 7-14 encode a 400 amino acid sequence that is 33% identical to a portion of the human epidermal growth factor precursor gene. Exon 15 encodes 58 amino acids that are enriched in serine and threonine residues. Exon 16 and the 5'-end of exon 17 encode hydrophobic amino acids that comprise the membrane-spanning domain. The remainder of exon 17 and the 5'-end of exon 18, encode the 50 amino acids that comprise the cytoplasmic domain.

LDLr as a multi-domain protein:

The LDLr belongs to a gene family that includes the VLDL receptor, apoER2 receptor, LRP, megalin and the LDLr. Members of the LDLr gene family are mosaic proteins comprised of tandemly-arranged recurring protein modules. The receptors differ in the arrangement and number of their individual modules.

The LDLr contains a number of different domains or modules arranged in tandem on a single polypeptide chain (Figure 1-2). In order of appearance from the amino-terminus these domains are: the ligand-binding domain, the epidermal growth factor homology domain, a transmembrane domain and a short cytoplasmic region.

Ligand-binding domain:

The first domain of the mature LDLr consists of the amino terminal 292 amino acids. This domain is composed of a sequence of 40 amino acids that is repeated, with some variation, seven times. This domain is located on the external surface of the plasma membrane. Each of the seven 40-amino acid repeats contains six cysteine residues that form three intra-repeat disulfide bonds. The disulfide bond pattern was shown to consist of residues Cys 6 bound to Cys 18, Cys 13 to Cys 31, and Cys 25 to Cys 42 (Figure 1-3) (Bieri et al., 1995). A striking feature of the cysteine-rich repeat sequence is a cluster of negatively charged amino acids, Asp-X-Ser-Asp-Glu (DxSDE) near the carboxy-terminus of each repeat. It was originally thought that the charges on these sequences interact with a cluster of positively charged residues that are believed to occupy one face of a single α-helix in apolipoprotein E, the best studied of the LDLr ligands. More recently, however, it has been proposed that the DxSDE motif forms a calcium-binding site, that is essential for the proper folding of the repeat. Support of this latter concept has come from recent determination of the crystal structure of the cysteine-rich repeat 5 of the ligand-binding domain of the LDLr (Figure 1-4). In this structure, most of the negatively-charged residues within the DxSDE motif are coordinated with calcium and are, therefore, unavailable to bind apoB or apoE (Blacklow and Kim., 1996). It is possible, nevertheless, that positively charged residues within the respective LDL receptor-binding sites of apoB and apoE interact with negatively charged residues that are situated elsewhere in the LDL receptor-binding domain. It could also be possible that, during binding of ligands to the LDLr, calcium is released that would free negatively charged

Figure 1-2: The multidomain structure of the low density lipoprotein receptor. The ligand-binding domain is composed of seven imperfect repeats that are characterized by 6 highly conserved cysteine residues and a series of acidic residues at the carboxy-terminus. The EGF precursor homology domain contains three short motifs that have homology to the epidermal growth factor precursor. Between EGF B and C is a structural motif known as a β-propeller. This domain is followed by a short region that is rich in serine and threonine residues. The last two domains are the transmembrane domain and cytoplasmic tail.

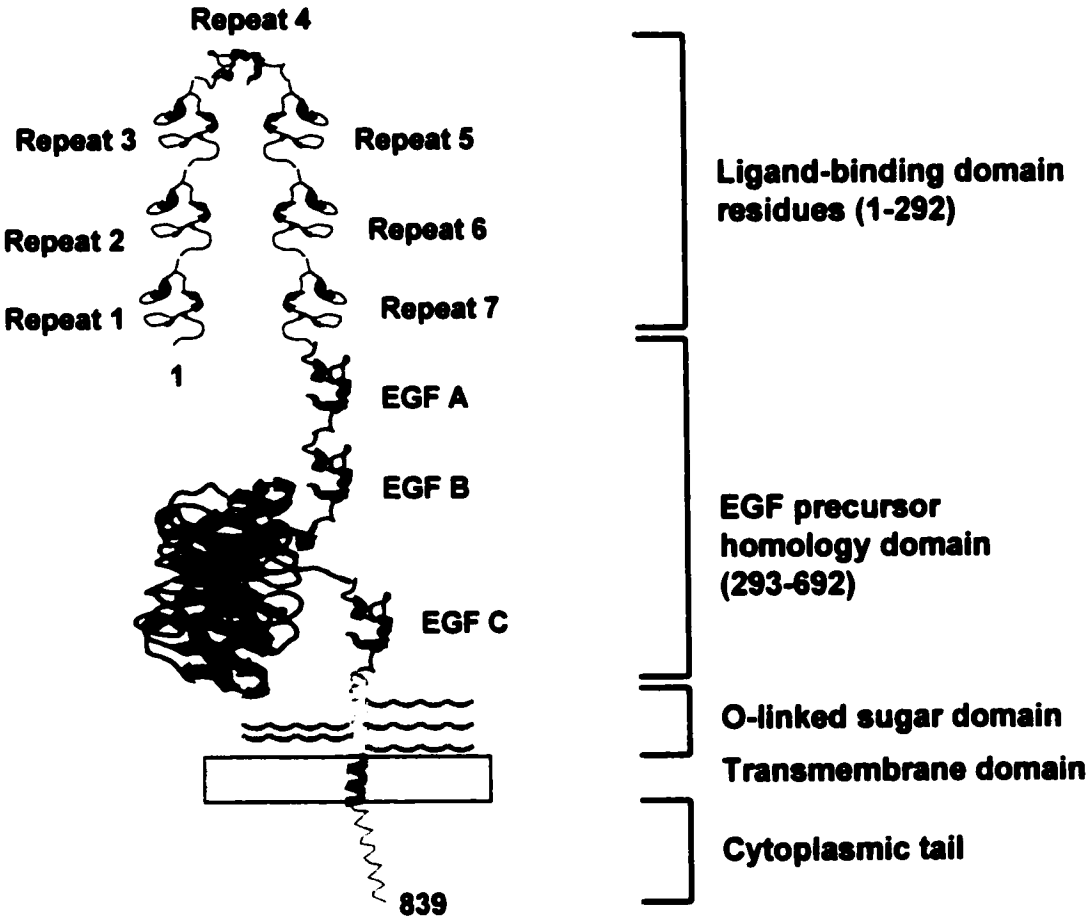
Repeat 4
Repeat 3
Repeat 5
Repeat 2
Repeat 6
Repeat 1
Repeat 7
1
EGF A
EGF B
EGF C
839
Ligand-binding domain residues (1-292)
EGF precursor homology domain (293-692)
O-linked sugar domain
Transmembrane domain
Cytoplasmic tail

Figure 1-3: Amino acid sequence of ligand-binding domain 1 (LB1) and ligand-binding domain 2 (LB2). The sequence contains the first 83 amino acids of the mature LDLr with an amino-terminal Glycine-Serine extension. Acidic residues are shown in red and cysteine residues in yellow. Predicted pepsin cleavage sites are indicated by a line. Adapted from Bieri et al., 1995.

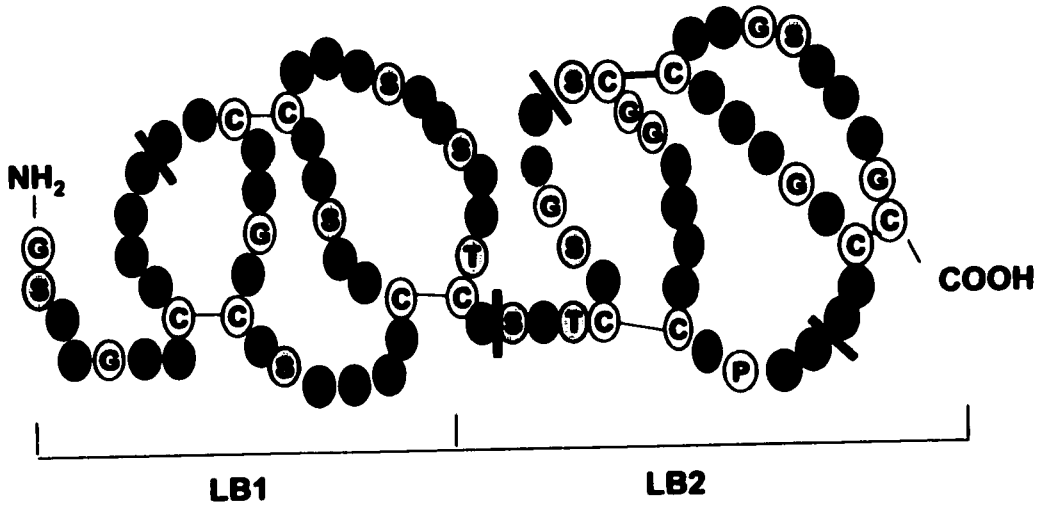
NH2
COOH
LB1
LB2

residues to interact with positively charged residues in apoB or apoE (Gaus et al., 2001). The repeats in the ligand-binding domain are not functionally equivalent (Esser et al., 1988, Russell et al., 1989). Repeat 1 plays no detectable role in the binding of LDL or β-VLDL. Repeats 2 & 3 and repeats 6 & 7 are required for maximal binding of LDL but not β-VLDL. Repeat 5 appears crucial for binding of both ligands.

Epidermal growth factor homology domain:

The second domain of the LDLr, consists of 400 amino acids and has 35% homology to a portion of the extracellular domain of the precursor for epidermal growth factor (Yamamoto et al., 1994). This region includes three growth factor repeats, which are 40 amino acid cysteine-rich sequences that differ from the cysteine-rich sequences in the ligand- binding domain. The first two growth factor repeats, designated A and B, are contiguous and separated from the third (C) by a 280 amino acid sequence that contains five copies of a conserved motif (YWTD) repeated once each 40-60 amino acids. YWTD repeats are always found in groups of six and appear to have a globular rather than an extended structure in electron microscopy. Receptors, which lack YWTD repeats and surrounding EGF domains bind β-VLDL but not LDL (Springer et al., 1998). The EGF precursor homology domain is required for the acid dependent dissociation of proteins from the receptor in the endosome during receptor recycling (Miyake et al., 1989, Davis et al., 1987). It also serves to position the ligand-binding domain so that it can bind ligand on the cell surface (Esser et al, 1988). LDL receptor variants with mutations within this domain frequently fail to fold properly and undergo degradation within the endoplasmic reticulum or show retarded transport to the cell surface (Hobbs et al., 1990).

Figure 1-4: Binding of calcium to the LDLr. Coordination of calcium by acidic residues of the cysteine-rich repeat five of the LDLr. Atomic coordinates from Fass et al., 1997 (Protein Data Bank accession number 1AJJ).

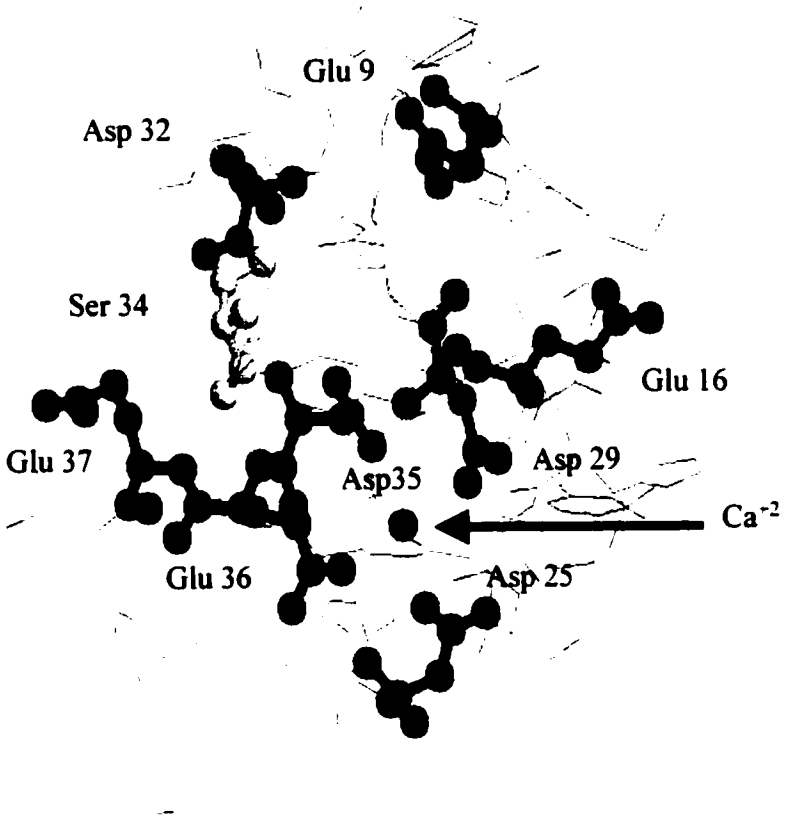
Glu 9
Asp 32
Ser 34
Glu 16
Glu 37
Asp35
Asp 29
Ca^{+2}
Glu 36
Asp 25

Oligosacharide domain:

The third domain of the LDLr lies immediately external to the membrane spanning domain and consists of a stretch of 58 amino acids that contains 18 serine or threonine residues (Yamamoto et al., 1984). This region contains the clustered O-linked sugar chains. Absence of this domain has no significant functional consequences when the mutant receptor is transfected into cultured hamster fibroblasts. Nevertheless, deletion of the exon encoding this domain does lead to a heterozygous FH phenotype (Kuwano, et al., 1991). The O-linked sugar chain may play a role in maintaining the stability of the receptor by protecting it from proteolytic cleavage (Kozarsky et al., 1988). It has also been postulated that the extensive glycosylation at this site may permit interactions with cell surface heparin proteoglycans. This interaction facilitates receptor accessibility to circulating plasma lipoproteins (Brown and Goldstein, 1985).

Transmembrane domain:

The fourth domain consists of a stretch of 22 hydrophobic amino acids that span the plasma membrane, as demonstrated by proteolysis experiments (Yamamoto et al. 1984). This region is poorly conserved amongst seven mammalian species. The deletion of this domain in certain naturally occurring mutations leads to secretion of truncated receptors from mutant cell lines.

Cytoplasmic domain:

The fifth domain is the cytoplasmic tail, which constitutes a short stretch of 50 amino acid residues. This domain is important in the localization of the receptor in clathrin-coated pits on the cell surface (Goldstein et al., 1979). The cytoplasmic sequence

is strongly conserved among species. Of the 50 amino acids in this domain, only four differ between human and cow, and each of these substitutions is conservative with respect to charge. Naturally occurring mutations and site-specific mutagenesis have led to the identification of an "internalization sequence", FXNPXY or NPXY (Chen et al., 1990).

The FXNPXY has been predicted to form a reverse turn conformation, which interacts with clathrin terminal domains in coated pits (Kibbey et al., 1998). Adaptor proteins have also been shown to bind to the cytoplasmic portion of the LDLr, or to modulate the interaction of NXPY motif with clathrin. The adaptor protein 2 (AP-2) is also believed to interact with other endocytosis signals, the YXXL and dileucine internalization motifs. YXXL and dileucine motifs may target receptors to plasma membrane, late endosome, lysosome, and trans golgi network structures via combinatorial interactions with AP complexes and possibly other membrane coats (Kibbey et al., 1998). By contrast, the FXNPXY motif may be needed for efficient clathrin-mediated recycling of LDLr between the plasma membrane and endosome (Kibbey et al., 1998). However the exact conformational determinants of the sorting motifs have yet to be determined.

The FDNPXY in the human LDLr, and the tetrapeptide NPXY has now been found in all structurally elucidated members of the LDLr family. The motif is also present among many other receptors including insulin receptor, and G protein-coupled receptors like integrins (Rapoport et al., 1998). However, in the insulin receptor the NPXY motif does not serve as an internalization signal. Similarly, in LRP, an YXXL and a di-leucine motif serves as the dominant signal for endocytosis, not the NPXY motifs

(Hobbs et al., 1990, and Li et al., 2000). This was shown by a study (Li et al., 2000) in which substitution of tyrosine or leucine within the YXXL motif with alanine significantly reduced the rate of LRP endocytosis. In this same study the investigators showed that the distal di-leucine motif in LRP contributes to LRP endocytosis, and functions independently of the YXXL motif. Therefore, it appears that each member of the LDLr family may utilize different potential signals within their cytoplasmic tails for receptor-mediated endocytosis.

Insights into the structure/function of the LDLr:

Biochemical techniques:

To gain insight into the structure and function of the LDLr, many investigators have expressed purified and truncated forms of the LDLr. Dirlam et al., in 1996 employed a baculovirus expression system to produce a truncated LDLr containing the ligand-binding domain, as well as regions of the EGF precursor homology domain. The recombinant virus encoded a 354 amino acid pro-protein, which upon cleavage of the signal peptide was predicted to yield a 333-amino acid mature protein. The truncated receptor was secreted in a water-soluble form and appeared to form high-ordered multimers. However, these receptor aggregates bound LDL and calcium. This study was able to demonstrate that the ligand-binding domain of the LDLr can fold into a functionally active protein.

The following year, Simmons et al. (1997) produced a truncated LDLr comprising the ligand-binding domain in order to study the interaction of apoE with the receptor at

the molecular level. The first 292 amino acids of the receptor were produced in *Escherichia coli* as a thrombin-cleavable, heat stable thioredoxin fusion protein. After cleavage of the fusion protein with thrombin, the receptor fragment could be refolded under oxidative conditions with an efficiency of 10%. The active receptor fragment was isolated and purified by using LDL affinity chromatography. The refolded receptor fragment exhibited properties similar to the intact native receptor. The receptor was able to bind calcium, LDL and could distinguish between isoforms of apoE.

In 1999 Marlovits et al., produced the entire ligand-binding domain of the LDLr in a soluble form and demonstrated that this region is sufficient for recognition by minor group human rhinoviruses (HRV). Previous studies have shown that minor group HRV's bind to the LDLr. The exact binding site to the receptor remains elusive. In order to identify the smallest structural element of the LDLr molecule required for viral recognition, soluble LDLr fragments encompassing various numbers of the complement type repeats with a hexa-histidine tag in the baculovirus system were expressed and tested for binding to HRV. The recombinant truncated proteins were affinity purified from the tissue culture by nickel chromatography. The study showed that soluble receptors with more than two repeats are sufficient for attachment of minor group HRV to immobilized receptors. However three repeats are required to protect HeLa cells against viral infection.

Together the above studies have provided insight into the structural units within the LDLr that are required to produce a functional protein. However, detailed studies

using biophysical and physicochemical techniques have further enhanced our knowledge of the relationship between LDLr structure and function.

Circular dichroic (CD) analysis on purified LDLr:

The LDLr has been studied extensively in intact cultured cells and in membranes from animal tissues. The highest concentration of the LDLr is found in the cortex of the adrenal gland. The adrenal glands use cholesterol for steroid hormone synthesis. In 1979, Brown and Goldstein described a method for the solubilization and partial purification of the receptor from bovine adrenal cortex (Schneider et al., 1979). The purification procedure involved the use of non-ionic detergents. The receptor was initially solubilized with octyl-β-D-glucoside. The solubilized receptor was purified by ionic exchange chromatography. The receptor was 5% pure. The exact molecular weight of the receptor could not be estimated due to receptor-bound octyglucoside.

In 1981, Brown and Goldstein modified their initial receptor purification procedure and described a rapid two-step method for the isolation of the LDLr from bovine adrenal cortex (Schneider et al., 1981). After solubilizing the receptor with non-ionic detergents, the receptor was isolated by using two chromatography columns. The first purification step made use of the acidic pK of the receptor while the second purification step was dependent on the high affinity binding of the receptor for LDL. The chromatography columns that were employed were an ionic exchange column followed by a LDL affinity column. The sequential use of these two procedures yielded a preparation of LDLr that was homogenous. A 164,000 Da protein was the predominant

protein in the eluted fraction. The purified receptor retained all of the binding properties of the receptor of intact cells and crude membranes.

Studies of the full-length receptor using prediction algorithm and circular dichroism methods have provided information on its secondary structure (De Loof et al., 1986 and Saxena and Shipley, 1997). Based on CD spectroscopy, the detergent–solubilized bovine LDLr is particularly rich in β-structure (40%) and 40% coil, with a significantly smaller proportion of α-helix (20%). The whole LDLr and its individual five domains have been analyzed by using predictive algorithms. The secondary structure of the whole LDLr is high in β-structure (40% β-turn and 25% β-sheet) with lesser amounts of α-helix (20%); similar results were obtained by De Loof et al. (1986).

In addition, the five individual domains of the human LDLr have also been analyzed. The ligand-binding domain was predicted to be rich in β-turns (50%) and β-sheet (20%) with less (15%) α-helix. This agrees with the experimentally determined structures of cysteine-rich repeats, which all contain an N-terminal β-hairpin followed by several β-turns. The EGF precursor homology domain was predicted to be mostly β-structure (60%).

NMR and X-Ray crystallography:

Recent studies using NMR and x-ray crystallography have provided structural insights into certain repeats in the ligand-binding domain and EGF precursor homology domain of the LDLr.

The first glimpse into repeat one of the LDLr was derived from two-dimensional NMR spectroscopy. This pioneering study was carried out by Daly et al. in 1995. The three-dimensional structure of the first and second repeat was shown to consist of a β-hairpin motif, followed by a series of β-turns. Furthermore, this study confirmed the position of the three disulfide bonds within the repeat that had previously been identified by biochemical techniques (Bieri et al., 1995) and demonstrated the clustering of acidic residues along one face of the module. The study provided the first experimental evidence that each of the repeats in the ligand-binding domain has a similar global fold but differs somewhat in backbone topology and structural flexibility.

In 1997, the crystal structure of repeat 5 was determined by Fass et al.. The striking feature of repeat 5 was that it was organized around a calcium ion. Although the overall topology of repeat 5 was similar to that of homologous modules 1 and 2 determined by NMR, the NMR structures did not show evidence of calcium binding. The residues in repeat 5 that coordinated the calcium ion through their side chains were Asp 25, Asp 29, Asp 35 and Glu 36, the same acidic residues that are conserved among the repeats 1 and 2. The backbone carbonyls of Trp 22 and Gly 27 completed an octahedral coordination geometry (Figure 1-4). The ion-binding site provided a rationale for the calcium-binding requirement in lipoprotein binding. However, the structure of repeat 5 was not consistent with a number of the existing models for normal LDLr function. In these models binding of ligand to the LDLr occurred through ionic interactions between positively charged residues on the apolipoprotein and negatively charged residues on the receptor. However the crystal structure of repeat 5 showed that many of these negatively

charged amino acids were occupied and were coordinating calcium ions and, as a consequence, were not exposed on the surface of the domain. Therefore, the structure of repeat 5 suggested an alternative model for LDLr function in which a hydrophobic concave face provided a lipoprotein-binding surface.

By using NMR, North and Blacklow (2000) provided the solution structure of repeat 6. This module retains the essential structural features observed in the crystal structure of repeat 5. Three disulfide bonds, a pair of buried residues forming a hydrophobic core, and a calcium-binding site. Two mutations that cause FH, E219K and D245E are localized within repeat 6. The first mutation is located near the amino-terminal end of repeat 6 while the second mutation alters one of the aspartate side chains that contributes to the coordination of a bound calcium ion. NMR analysis of these mutants showed that neither E219K nor D245E was able to fold to a unique disulfide isomer. This study provided the first evidence that FH mutations both within and distant from the calcium binding site give rise to protein-folding defects.

Analysis of LDLr variants with naturally occurring and engineered mutations have shown that the binding of apoB-100 requires a combination of repeats 2-7, while the binding of apoE-containing lipoproteins depends critically on repeat 5 (Esser et al. 1988). Furthermore, the LDLr can distinguish between isoforms of apoE. To understand how different modules interact with one another, Bieri et al. (1998) expressed and characterized a concatemer of the first two ligand-binding modules of the LDLr. The repeats folded spontaneously in the presence of calcium and had the characteristic 1-3, 2-5 and 4-6 disulfide-bonding pattern. In the folded state, the concatemer showed two high-

affinity calcium-binding sites. Furthermore, the concatemer was very similar to individual modules, and showed no evidence for strong interactions between modules. Such a structure would provide a great deal of flexibility and could allow modules to rearrange to bind a variety of ligands such as apoB and apoE. Similar results were obtained from a study conducted by North et al., in 1999. This group studied repeats five and six of the LDLr and showed by using NMR solution studies that in solution these repeats are independent of each other. These results support the hypothesis that specific residues in structurally independent repeats are more important for receptor function than module organization. The concept that individual repeats fold essentially independently of each other is supported by another study, which showed that FH causing mutations in one cysteine-rich module only caused misfolding in that module and did not impact on the structure of remaining neighbouring repeats (North et al., 1999). The mutations occurred in LDLr repeat 5 and within LDLr repeat 6. For each mutation, a folding defect persisted in the module pair, but remained restricted to the module containing the mutation. It had also previously been proposed that the each cysteine-rich module folds independently based on mutagenesis studies of the full-length LDL receptor (Russell et al., 1989).

The seven ligand-binding domains of the LDLr account for only 40% of the entire protein. The EGF precursor homology domain containing the YWTD motif is 400 amino acids in length and plays an important role in the pH-dependent release of LDL from the receptor after internalization in the endosome (Davis et al., 1987 and Miyake et al., 1989). The structural organization of this domain has remained relatively unclear until recently. In 1998, experimental and computational data suggested that the six YWTD repeats

flanked by the EGF repeats were likely to form a six-bladed compact β-propeller structure (Figure 1-5) (Springer, 1998). β-propellers are large circular domains that contain six β-sheets arranged radially about a pseudo-symmetry axis. Many point mutations that cause FH map to YWTD repeats (Springer, 1998). Blacklow and et al., (2001) recently solved the crystal structure of the YWTD domain and the carboxy-terminal EGF repeat of the LDLr and confirmed the earlier model proposed by Springer. This domain indeed formed a β-propeller structure. By crystallizing this domain new insights have been gained into the possible mechanisms of the pH-dependent release of ligand.

One possible mechanism might involve aspartic acids. Mutations in this residue could result in the destabilization of hydrogen bonds that form the backbone structure of the β-strands. A second mechanism could involve the histidine residues that stabilize an interaction between the bottom of the β-propeller and the third EGF module. These histidine residues are located at crucial positions at the interface between the propeller and the third EGF repeat. A number of FH mutations occur in residues that stabilize this interface, thereby supporting a potential role of this interface in the acid-induced conformational change of the receptor. The last potential mechanism was provided by a study conducted by Malby et al. (2001). By using a combination of biophysical methods, the investigators were able to characterize the calcium binding properties of EGF A and EGF B. The study showed that both modules were stabilized with respect to each other by a calcium ion that was chelated by residues at the amino-terminal end of the second EGF module. A change in calcium concentration and a decrease in pH similar to what

Figure 1-5: Ribbon diagrams of β-propeller domain predicted for the YWTD domain of nidogen. β-propellers are large circular domains that contain six β-sheets arranged radially about a pseudo symmetry axis. Adapted from Springer et al., 1999.

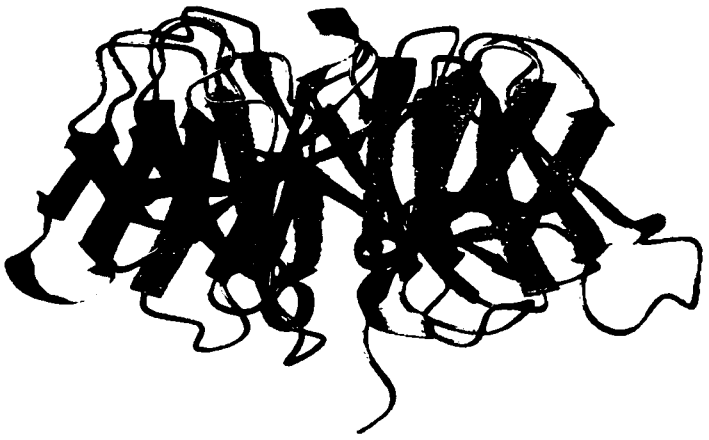

occurs within the endosome were predicted to induce a conformational change in the tandem EGF modules. This conformational change could cause a destabilization in the structural backbone of the receptor with a concomitant release of ligand.

Together these studies have provided insights into the individual domains of the receptor. However, due to the characteristically complex structure of the receptor it has been difficult to crystallize it in its entirety. As a consequence, considerable structural information on the full-length LDLr remains to be elucidated.

Cryoelectron microscopy (cryoEM):

Recently, Shipley and colleagues were able to provide low-resolution pictures of the LDLr within intact membranes by using cryoEM. In these studies purified bovine LDLr was incorporated into pre-formed large unilamellar egg yolk phosphatidylcholine vesicles. The reconstituted receptor alone and bound to LDL was visualized by cryoEM (Jeon et al., 2000a and 2000b). The studies thereby provided a low-resolution structural picture of the bovine LDLr. The receptors alone were found in stick-like, bent stick-like and Y-shaped configurations. The various orientations represented the extracellular domain of the receptor based on its experimentally determined length and width parameters. The elongated, stick-like projections had maximum dimensions 120 Å length by 45 Å width (Jeon et al., 2000a). The Y-shaped configurations could represent dimerized forms of the receptor. Receptors bound to the LDL particles were also visualized. Images showed bound LDL particles at the surface of the LDL receptor-containing vesicles. Many individual LDL particles were bound to the outside surface of the receptor-containing vesicles, and in some images, the stick-like extracellular domain

of the LDLr was visible, extending from the membrane surface to the bound LDL particle.

The location of the ligand-binding domain of the LDLr was determined by gold labeling of reduced cysteines in this domain (Jeon et al., 2000b). CryoEM images of reduced, Nanogold-labeled LDLr localized the amino-terminal cysteine-rich repeats to the distal end of the observed receptor images. Based on these results the investigators were able to propose four possible arrangements of the 7 cysteine-rich repeats in both the monomeric and dimeric forms. The proposed arrangements comprised a 2+5- and a 4+3-type arrangement of the cysteine-rich modules. Binding of LDL to the LDLr is severely affected by mutations in repeats 3 to 7 (Esser et al., 1988, Russell et al., 1989). This would imply that, in the 2+5 arrangement, the first and the second repeats would be located away from the binding site for LDL. In the 4+3-type arrangement, the presence of a long linker sequence (12 amino acids vs 4 amino acids) between repeats 4 and 5 suggests a turn may occur after the fourth repeat in the ligand-binding domain. It had been previously shown that deletion of the 12-residue linker impairs LDL binding to the LDLr (apoB100-mediated) but not β-VLDL binding (apoE-mediated) (Russell et al., 1989).

LDLr interaction with ligands:

Apolipoprotein B100:

Apolipoprotein B100 is one of the largest known proteins. It is a major protein component of VLDL, IDL and LDL (Schumaker et al., 1994). The human apoB gene

contains 29 exons and 28 introns and spans approximately 43 kilobase of the genome. The primary sequence of mature human apoB100 consists of 4536 amino acids. It contains 19 potential N-linked glycosylation sites, of which 16 are glycosylated. There are 25 cysteine residues distributed asymmetrically within apoB100. Sixteen of the cysteine residues are involved in disulfide linkages of which six are located within the amino-terminal 500 residues (Figure 1-6). ApoB naturally exists in two forms, apoB100 and apoB48, which in man are secreted primarily by the liver and the intestine in association with VLDL and chylomicrons, respectively. ApoB48 is identical in amino acid sequence to the amino-terminal 48% of apoB100 but is truncated due to a mRNA editing complex present in the intestinal enterocytes that causes codon 2180 of apoB100 mRNA to be converted to a translational stop codon. Mature apoB48 consists of 2152 amino acids (Chan, 1992).

Studies of the structure-function relationships within apoB100 have proven to be difficult, mainly because of its enormous size and extreme hydrophobicity (Chan, 1992). ApoB secondary structure has been predicted on the basis of the primary amino acid sequence. Steele and Reynolds (1979) used the method of Greenfield and Fasman (1969) to analyze the secondary structure of apoB in LDL and predicted that the structure would contain 43% α-helix, 21% β-sheet, 20% random coil, and 16% β-turns. Segrest et al. (1994) used computer analysis to predict the presence of two domains of amphipathic β-strand alternating with three domains of amphipathic α-helices within apoB100. This has been called the pentapartite model of apoB100 secondary structure (NH_2–α_1-β_1-α_2-β_2-α_3-

Figure 1-6. Structure of human apoB100. *A*, the position of apoB amino acid residues (*top*) in comparison to the nomenclature of apoB using the centile system (*bottom*) (Kane et al., 1980). B48 refers to the N-terminal 48% of full-length apoB, whereas B100 refers to the full-length apoB. The centile system of apoB will be used in this Thesis. *B*, positions of the N-linked glycosylation sites within B100. There are 19 N-x-T/S sites within B100, 16 of which are glycosylated (*closed*) and 3 unglycosylated (*open*) (Yang et al., 1989). *C*, positions of cysteines within B100. Cysteines involved in disulfide linkages are connected together (Yang et al., 1989). *D*, the pentapartite model for the secondary structure of human B100 (Segrest et al., 1994).

A. Amino acid residues and the centile system

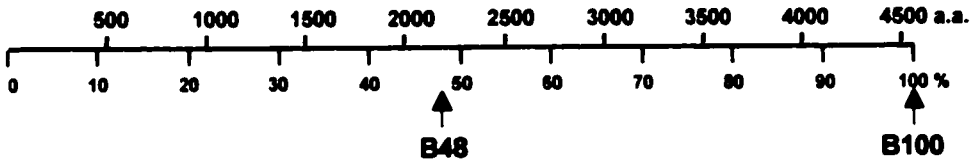

B. N-linked glycosylation sites

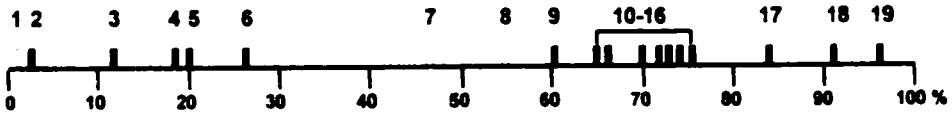

C. Disulfide linkages

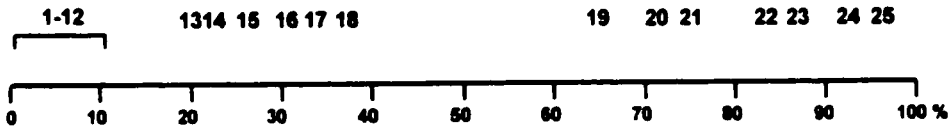

D. The pentapartite model

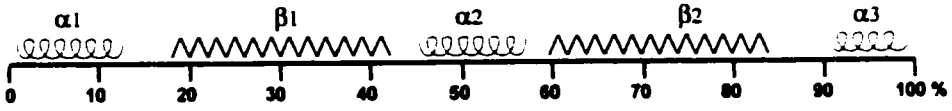

COOH) (Figure 1-6). It is also suggested that the pentapartite structure of apoB100 is conserved among nine vertebrate species. The α_1-helix, appears to form a globular domain with low affinity for lipids. The other two α-helix clusters, α_2 and α_3, may represent reversible lipid-binding domains. The extensive β-strands, β_1 and β_2, may represent irreversible lipid association domains. The function of the five putative apoB100 domains remains to be defined. However, it has been proposed that the β_1 and β_2 domains may directly bind to core lipids and provide a rigid backbone during lipoprotein assembly, whereas the α_2 and α_3 domains may be flexible in accommodating varying amounts of lipids during VLDL assembly and intravascular metabolism. Immunochemical evidence supports the pentapartide model of apoB100 secondary structure (Chauhan et al., 1998).

The amino-terminus of apoB shows primary structure homology to lipovitellin, a protein involved in chicken embryogenesis (Segrest et al., 1999). Since the crystal structure of lipovitellin has been determined at 2.8 Å resolution, the coordinates have been used to model the structure of the amino-terminal 300 amino acid residues of apoB100. It consists of three helices and a thirteen-stranded β-sheet; 11 of these strands form a β-barrel conformation, stabilized by disulfide linkages. The next 300 amino acid residues of apoB are predicted to form a double-layered α-helical structure containing 17 helices (Segrest et al., 1999).

An important physiological function of apoB is to serve as the ligand for the LDLr on cell surfaces. Thus, apoB has a crucial role in the metabolic pathway of cholesterol

and LDL. The sequence of apoB has been known since 1986 and a putative receptor-binding domain was described (Knott et al. 1985, Knott et al., 1986 and Yang et al., 1986). The receptor-binding domain was identified between amino acid residues 3345 and 3381. Yang et al. (1986) tested the ability of synthetic apoB peptides for binding to the LDLr on cultured fibroblasts. This study showed that a synthetic peptide composed of residues 3345-3381, but not a peptide spanning residues 4154-4189, could mediate binding of trypsin-digested VLDL to the LDLr, albeit with low affinity. Milne et al. (1989) and Pease et al. (1990) have demonstrated by immunochemical analysis that monoclonal antibodies whose epitopes mapped to a region between apoB residues 3000 and 3500 were able to block LDL binding to the LDLr present on cultured fibroblasts. Naturally occurring truncated apoB mutants that terminate at residue 3387 can mediate LDL binding to the LDLr (Krul et al., 1992) whereas a shorter variant that terminates at residue 3040 is unable to bind to the LDLr (Welty et al., 1995). Within this region, two short sequences residues 3147-3157 (Site A) and residues 3359-3369 (Site B), have been identified as potential regions that are able to bind to the LDLr (Knott et al., 1985). However, other additional apoB residues that have not currently been identified may also participate in binding to the LDLr. A disulfide bridge is thought to exist between cysteines 3167 and 3297 (Figure 1-7), which links Site A, and Site B into spatial proximity in apoB tertiary structure (Milne et al., 1989). These two cysteines are not, however, conserved in other species (Law and Scott, 1990). Site B in human apoB is enriched in positively charged amino acids and replacement of these basic residues by alanine residues disrupts apoB100-mediated binding of LDL to the LDLr (Borén et al.,

Figure 1-7: Putative receptor-binding sites. Depicted are the putative receptor-binding sites on apoB100-LDL (Site A and Site B) and regions which, when bound to monoclonal antibodies can block binding to the LDLr. A disulfide bridge between residue 3297 and 3167 may bring Site A and Site B into spatial proximity (Milne et al., 1989).

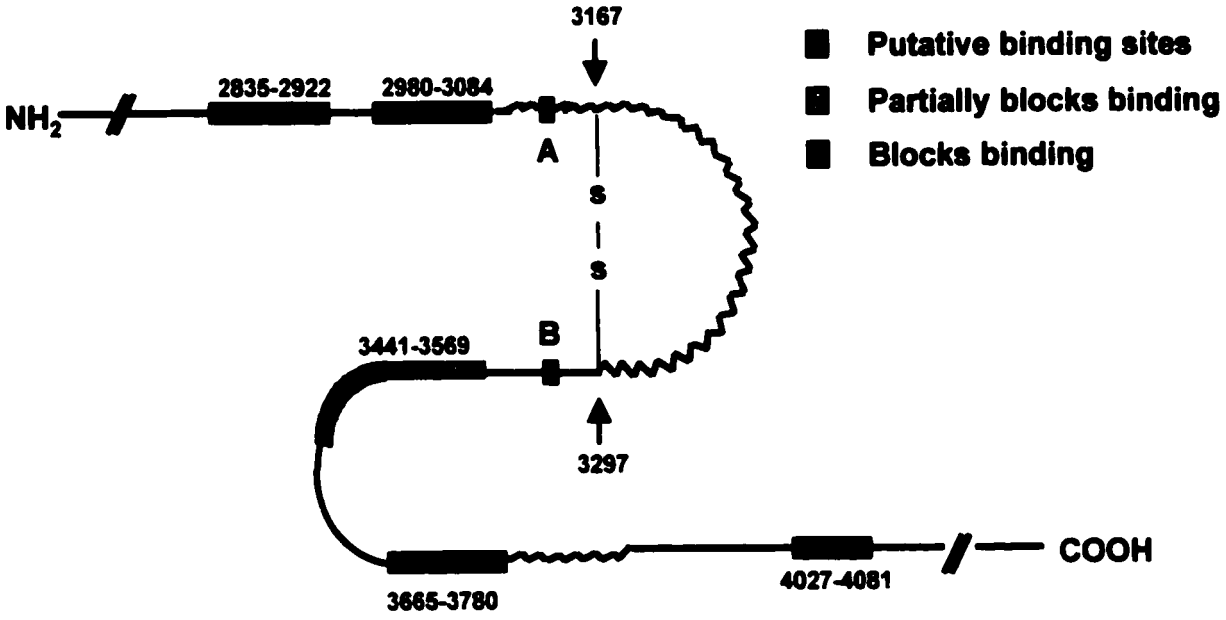
3167
Putative binding sites
Partially blocks binding
Blocks binding
NH2
2835-2922
2980-3084
A
S
S
B
3441-3569
3297
COOH
4027-4081
3665-3780

1998). Therefore, it is thought that basic amino acids of apoB participate in binding to the LDLr, possibly through ionic interactions with acidic residues within the ligand-binding domain of the receptor.

The configuration of apoB100 on the surface of human LDL has been proposed to be a "ribbon and bow" configuration. This was determined by Chatterton et al. (1995) using immunoelectron microscopy (Figure 1-8). In this model, the first 89% of apoB forms a ribbon encircling LDL completely, with an elongated configuration and a kink region. The final 11% of apoB constitutes a "bow", stretching back and crossing over the "ribbon" close to the putative LDL receptor-binding site (Site B). It was predicted that the "bow" might limit the accessibility of the LDL receptor-binding site and that a lateral movement of the extreme carboxy-terminus of apoB on the surface of the lipoproteins may expose the apoB LDL receptor-binding site. Borén et al., (1998 & 2001) have provided strong evidence that the interaction of arginine 3500 with tryptophan 4369 at the carboxy-terminus of apoB100 is important for receptor binding of LDL. The substitution of glutamine for arginine at residue 3500 abolishes this interaction, resulting in a conformational change, disrupted receptor binding and the clinical disorder familial defective apolipoprotein B100 (FDB). Truncation mutants that have insufficient carboxy tail to cross over near Site B do not need the arginine 3500 and tryptophan 4369 interaction and therefore bind normally to the LDLr. Furthermore, VLDL normally binds the LDLr with low affinity but removal of the carboxy-terminal tail increases receptor binding of VDL by more than sixfold. Wang et al., (2000) have shown that the carboxy-terminus of apoB100 undergoes major conformational changes during conversion of

Figure 1-8: "Ribbon and bow" model for the conformation of apoB100 on the LDL surface. A-D, the "ribbon" of N-terminal 89% of apoB100 on the LDL surface. These panels (from *A* to *D*) are related by sequential 90° rotations about a horizontal axis in the plane of the page. The numeric labels on the surface represent the centile nomenclature of apoB. *E*, the "bow" of apoB100. The orientation is the same as *D*. The C-terminal 11% of apoB100 moves "backward" from B89 into one hemisphere (at B92), and then crosses the ribbon near the LDL-receptor binding site and terminates in the other hemisphere (at B100). Figure reproduced from Chatterton et al., 1995.

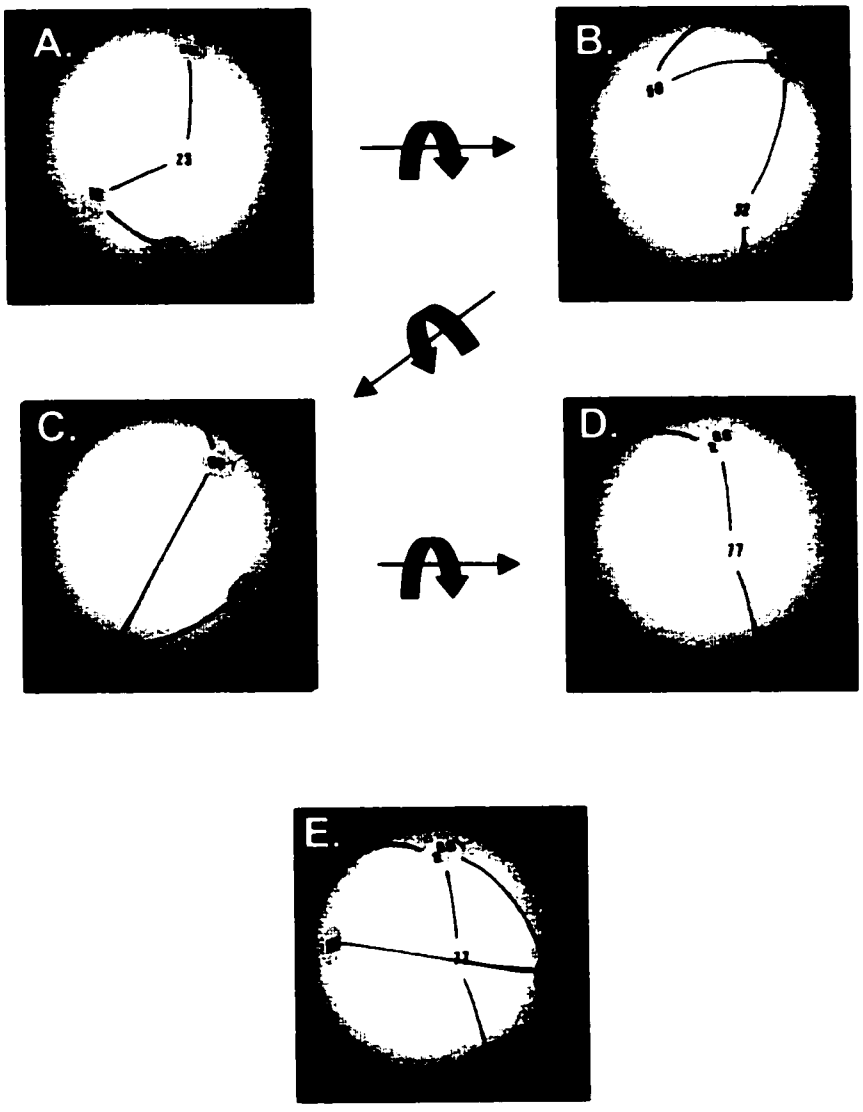
A.
B.
C.
D.
E.

VLDL to LDL. Together, these results suggest that the carboxy-terminus of apoB100 is a negative regulator of apoB-mediated binding to the LDLr by either modulating the conformation or limiting the accessibility of the apoB LDL receptor-binding site.

Apolipoprotein E:

Apolipoprotein E is an arginine-rich plasma protein found on VLDL particles. The 3.7 kilobase apoE gene is located on human chromosome 19 and is composed of 4 exons separated by three introns. The major site of apoE expression is in the liver, followed by the brain, where it is produced mostly by astrocytes. Human apoE is a 34 kDa protein that exists as three common isoforms. The isoforms are encoded by three co-dominantly expressed alleles termed ε2, ε3, and ε4. These alleles occur with an approximate frequency of 10, 70 and 20%, respectively, within the general population. Three homozygous phenotypes (apoE2/2, E3/3, and E4/4) and three heterozygous phenotypes (apoE3/2, E4/3, and E4/2) arise from the expression of any two of the three alleles (Mahley and Huang, 1999). Because of the frequency of the ε3 allele, apoE3 is considered to be the parent form of the protein, and apoE4 and apoE2 are variants. The molecular basis for apoE polymorphism was elucidated by analysis of the amino acid sequences of the three isoforms. Amino acid substitutions accounted for the differences among apoE4, E3 and E2 (Weisgraber et al., 1981). ApoE4 differs from apoE3 in that in apoE4, arginine is substituted for the normally occurring cysteine at amino acid residue 112. The most common form of apoE2 differs from apoE3 at residue 158, where cysteine is substituted for the normally occurring arginine. The charge differences among the three isoforms detected by isoelectric focusing are explained by the single amino acid

substitutions and differential sialyation at threonine 194 (Wernette-Hammond et al., 1989).

The structure of the amino-terminal 22 kDa domain of apoE has been solved at the atomic level. It forms a globular protein, composed of five helices, four of which form a tight bundle (Aggerbeck et al., 1988a, Aggerbeck et al., 1988b and Wetterau et al., 1988 Wilson et al., 1991). It exhibits low affinity for lipids and includes residues involved in LDLr and heparin interaction (Segelke et al., 2000). The carboxy-terminal 10 kDa fragment has high affinity for lipids but is not reactive with cell surface receptors. It is postulated to be composed of many small amphiphathic α-helices (Innerarity et al, 1983 and Weisgraber, 1994). Although the two domains of apoE appear to exist as independent entities in solution, there is increasing evidence for molecular co-operation between these domains on the surface of lipoproteins (Weisgraber, 1994).

The receptor-binding site of apoE was determined by Weisgraber et al., (1983). Although there is no apparent homology between the apoB and apoE sequences, clusters of positively charged amino acids, similar to those found on apoB are also present on apoE. The residues implicated in LDLr-binding reside on the fourth helix and are exposed to solvent (Wilson et al., 1991). The positive charges found on arginine, lysine and histidine residues, may all take an active part in interacting with the negatively charged residues present in the consensus sequence repeats found in the ligand-binding domain of the LDLr (Mahley and Huang, 1999, and Weisgraber et al., 1999). Early selective chemical modification experiments demonstrated that lysyl and arginyl residues were important in the interaction of apoE with the LDLr (Mahley et al., 1979). Substitutions of

single amino acids of apoE suggested that a number of the basic residues are involved in binding to the receptor. Since no single substituted mutant resulted in a dysfunctional receptor it would appear that the basic residues are cooperatively involved in the binding to the receptor and that there are multiple interactions between apoE and the receptor. ApoE polymorphism influences apoE-mediated binding to cell surface receptors (Rall et al., 1982). ApoE3 and apoE4 are receptor-competent when associated with lipids. ApoE2 is receptor-defective and differs from wild-type apoE3 by having an arginine (arg) to cysteine substitution at position 158. Since this residue lies outside the receptor-binding site (residues 136-150), its contribution to the receptor-binding has been thought to be indirect. It is believed that the replacement of Arg^{158} by cysteine disrupts salt bridges that normally exist between Arg^{158}, Asp^{154} and Gln^{96}. As a consequence, in apoE2, Asp^{154} interacts with Arg^{150}, which causes the side chain of Arg^{150} to deviate from the receptor-binding region thereby resulting in a low affinity LDLr interaction (Figure 1-9) (Wilson et al., 1994).

Interestingly, studies have shown that in the absence of lipid, the receptor-binding region of apoE does not interact with the LDLr on fibroblasts. Thus, it has been proposed that lipid-binding induces a conformational change in this domain that confers receptor recognition properties. Evidence based on infrared dichroism and x-ray crystallography support the view that defined helical segments in the four-helix bundle realign upon lipid association, orienting perpendicular to the phospholipid fatty acyl chains. This reorientation of the helices may be necessary for receptor-binding (Weisgraber et al., 1992 and Raussens et al., 1998).

Figure 1-9: Schematic representation of helix 4 and helix 3 of receptor-competent ApoE3 and receptor incompetent apoE2. Substitution of Arg^{158} for a Cys disrupt salt bridges that normally exist between Arg^{158}, Asp^{154} and Gln^{96}. Reproduced from Raffai et al., 2000.

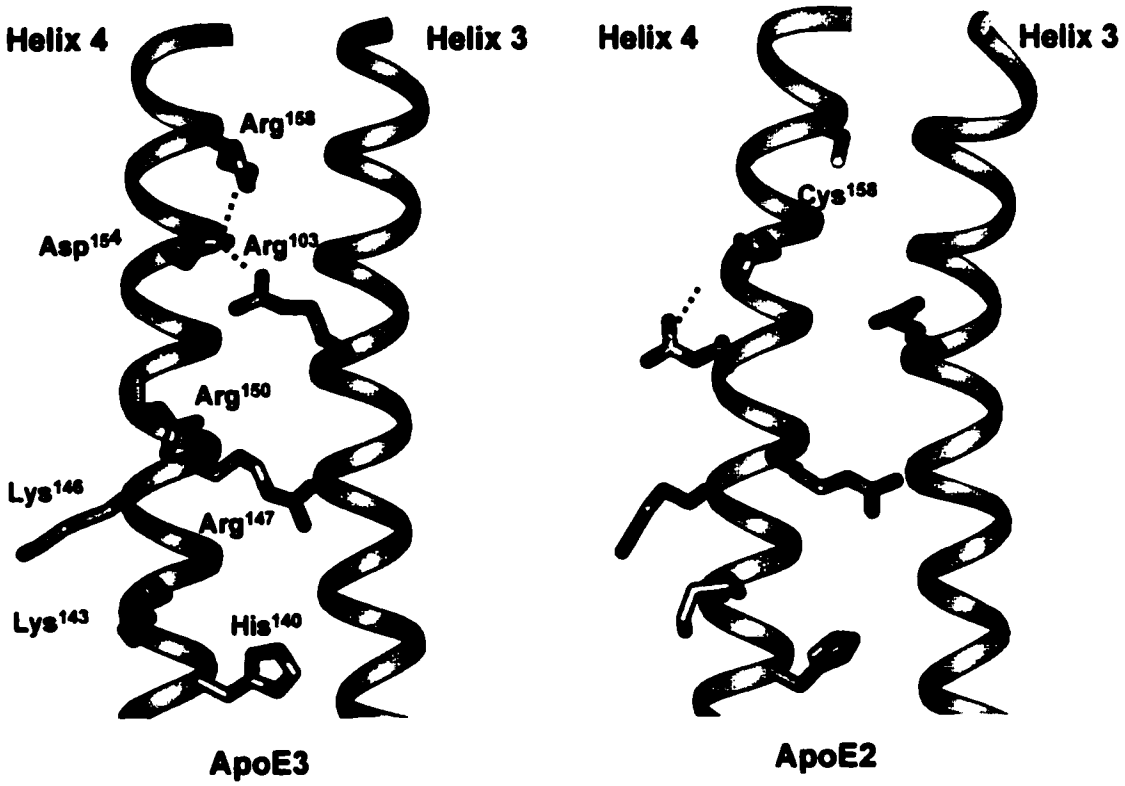
Helix 4
Helix 3
Arg158
Asp154
Arg103
Arg150
Lys146
Arg147
Lys143
His140
ApoE3
Helix 4
Helix 3
Cys158
ApoE2

Dysbetalipoproteinemia, also called type III hyperlipoproteinemia and broad-beta disease, is defined as the presence of VLDL particles that migrate at the beta position on electrophoresis (normal VLDL particles migrate in the pre-beta location) (Fazio, 1993). Beta-VLDL particles are chylomicron and VLDL remnants. Dysbetalipoproteinemia is caused in part by a homozygous inheritance of the apoE2 allele, which impairs the hepatic uptake of apoE-containing lipoproteins and slows the conversion of VLDL to IDL and LDL. An apoE defect combined with a second genetic or acquired defect that causes overproduction of VLDL, such as obesity, may alter the lipid composition of lipoproteins and thereby affect the conformation of apoE and its susceptibility to form an Arg^{150}-Asp^{154} salt bridge (Innerarity et al., 1986). Individuals with dysbetalipoproteinemia have elevations in both cholesterol and triglyceride levels and are likely to develop premature coronary artery disease.

LDL heterogeneity influences on receptor interaction:

Transformation of VLDL to LDL in plasma through lipolysis results in the creation of LDL particles that differ in size, composition and charge. These factors in turn affect the lipoproteins' ability to bind to the LDLr. Several classes of LDL have been identified and classified into two categories, pattern A and pattern B (Austin et al., 1988). Pattern A is characterized by a predominance of larger, more buoyant LDL particles while Pattern B consists predominantly of small LDL particles and is associated with increased triglyceride and reduced HDL cholesterol levels and an increase risk of coronary artery disease. A correlation has been found between differences in receptor-

mediated LDL catabolism, and subjects with pattern A and pattern B LDL. However, the exact nature of this correlation remains questionable due to inconsistency in findings. Swinkels et al., (1990) showed no differences in the receptor-binding of LDL subfractions to the LDLr on fibroblast and HepG2 cells, but other studies have found that both buoyant and dense LDL subfractions have reduced binding compared with medium density LDL subfractions (Chappell et al., 1991). Still other studies have found greater binding affinity for buoyant LDL subfractions compared with medium and dense LDL subfractions (Campos et al., 1996).

LDL heterogeneity also influences apoB conformation and function. Kinoshita et al. (1990) have shown that modification of core lipids of LDL produces selective alterations in the expression of apoB epitopes. Specifically, an increase in the triglyceride content of LDL results in a progressive decrease in immunoreactivity with antibodies distant from the putative receptor-binding site. Moreover, receptor-binding affinity decreases with increasing LDL triglycerides even though epitopes near the receptor-binding region are not affected. In another study by Aviram et al. (1988) it was shown that modification of LDL by lipoprotein lipase or hepatic lipase induced an enhanced uptake and cholesterol accumulation in macrophages. Both lipases modified LDL by substantially reducing core triglyceride content with no marked changes in size, charge or lipid peroxide content in comparison to native LDL. The concentration of triglyceride in LDL affected the chemical and physical properties of the lipoprotein surface thereby modifying the interaction of apoB with the LDLr.

In contrast to the above studies in which it was concluded that the LDL core composition is a primary determinant of apoB conformation and function, other investigators have shown that the ability of LDL to react with the LDLr on cultured fibroblasts is independent of core lipid composition but changes as a function of LDL size. During the metabolic conversion of VLDL to LDL many subspecies of LDL can be isolated. Chen et al., (1994) have shown conformation differences in apoB among these subspecies of LDL. These investigators found that the accessibility to protease attack in LDL from normolipidemic and hypertriglyceridemic subjects was altered in three regions of apoB. ApoB in hypertriglyceridemic LDL exposed more cleavage sites than native LDL. Analysis of circular dichroic spectra revealed an increase in the β-structure in the hypertriglyceridemic LDL (Galeano et al., 1994). Binding affinity for the LDLr of human fibroblasts decreased markedly with increasing density among hypertriglyceridemic LDL subspecies (McKeon et al., 1993). These changes were independent of lipid composition but rather varied as a function of LDL size. On the basis of the above observations, it can be seen that heterogeneity of the physical and chemical properties of LDL modulates apoB conformation and function. Subpopulations of particles can be isolated that differ in their apoB circular dichroic spectra, reactivity with certain anti-apoB monoclonal antibodies (Teng et al., 1985) and respective reactivity with the LDLr.

LDL-LDLr binding kinetics:

Most of our knowledge of the affinities and kinetics of binding of lipoproteins to the LDLr is based on studies from cultured human fibroblasts. In some of these studies

lattice effects have modulated the binding of lipoproteins to the cell surface. LDL particles are 20 times larger than the LDLr and 70-80% of LDLrs are clustered within coated pits. Robenek et al., (1991) under electron microscopy showed that receptor-bound LDL particles on the cell surface are in direct contact to each other. Furthermore, van Dreil et al. (1987) showed that up to 20% of the LDLr on the cell surface could be cross-linked by a cross-linking reagent and concluded that many LDLr existed as noncovalently attached dimers or higher ordered aggregates. A lattice model of binding implies that large LDL should produce steric effects at a lower receptor occupancy than should small LDL. Chappell et al. (1991) were able to show this by testing seven LDL fractions that differed in diameter from 20-27 nm. Fewer large than small LDL were bound to the cell surface of cultured fibroblasts at 4°C. At 37°C fewer large than small LDL particles were internalized and degraded. Another study conducted by Chappell et al. (1992) showed that large and small LDL bind to the LDLr by different mechanisms. ApoB-mediated binding was shown to follow binding kinetics that resulted in an initial low affinity site being converted over time to a higher affinity site. This rearrangement was referred to as an "isomerization" and was based on the observation that the dissociation rate constant of LDL-LDLr complexes decreased as a function of the duration of association. Curiously, large LDL, which bind predominantly by apoE did not undergo an isomerization. The structural basis for the isomerization is unknown but could involve a change in conformation of the apoB or the participation of additional or different cysteine-rich repeats of the LDLr in the ligand-receptor interaction.

Low density lipoprotein receptor and disease:

Familial hypercholesterolemia:

FH first described in 1938. The primary defect in this disorder is a deficient LDLr. Over 600 LDLr mutations have been described, of which 50 are point mutations that substitute individual amino acids within the seven cysteine-rich repeats of the ligand-binding domain (Goldstein et al., 1985b). Approximately 41% of FH homozygotes are true homozygotes as determined by haplotype mapping as well as mutational analysis. The remaining FH homozygotes are, in fact, compound heterozygotes, having inherited two different non-functional alleles. Five classes of LDLr mutations have been described in FH patients. These mutations can be classified according to their phenotypic effects on the protein (Brown et al., 1985b, Hobbs et al, 1990).

Class 1: no detectable precursor: This is the most common class of mutant alleles. These genes produce either no LDLr protein or only trace amounts as determined by reaction with monoclonal antibodies.

Class 2: slow or absent processing of precursor: For the class 2 mutants, receptor is synthesized but is either not transported or is transported slowly from the endoplasmic reticulum to the golgi apparatus. This is the second most common class of mutations. These alleles produce receptors whose apparent molecular weights vary from 100-135 kDa. Most have an apparent molecular weight similar to that of the normal precursor (120 kDa). The block in transport caused by Class 2 mutations results from either missence mutations or short in-frame deletions that alter the amino acid sequence of the receptor, leading to complete or partial misfolding. Some mutant receptors contain high

mannose N-linked sugars and the core N-acetylgalactosamine of the O-linked sugars. However, the N-linked sugars are not converted to the complex endoglycosidase H-resistant form nor are the O-linked sugar chains elongated. This mutant receptor does not appear on the surface of the cell but is degraded.

Class 3: defective ligand-binding: Class 3 mutations comprise receptors that are processed and reach the cell surface, but fail to bind LDL normally. In the mature form, these mutant receptors can have a normal apparent molecular weight of 160 kDa. They all undergo normal carbohydrate processing and reach the cell surface, and bind a variety of antibodies directed against the LDLr. However, they have a markedly reduced ability to bind apoB100 or both apoB100 and apoE. These mutations involve amino acid substitution, deletions or duplication in the cysteine-rich LDL binding domain and EGF precursor domain.

Class 4: internalization defective: The receptors reach the cell surface but fail to cluster in coated pits. Electron microscopy reveals that the receptors are distributed diffusely over the surface of the cell rather than being concentrated in coated pits. They therefore cannot carry bound LDL into the cell. Most of the mutations were found to be in the cytoplasmic tail of the receptor.

Class 5: recycling defective: This class of mutations prevent the receptor from recycling back to the surface of the plasma membrane. Davis et al. (1987) discovered that the EGF precursor domain mediates the acid-dependent dissociation of receptor and ligand in the endosome, an essential event for receptor recycling. Several missence mutations have been identified in FH homozygotes within the EGF precursor homology domain. These

mutations produce a phenotype similar to that observed when the entire EGF precursor homology domain is deleted in that the receptor is defective in recycling, and fail to release β-VLDL after acidification (Van der Westhuyzen et al., 1991).

Recently, a new condition has been described, autosomal recessive hypercholesterolemia (ARH), which clinically resembles FH but is not due to mutations in the LDLr gene. Patients with ARH exhibit markedly impaired hepatic LDLr function but normal or only modestly reduced LDLr function in fibroblasts. The molecular basis for ARH has recently been determined (Garcia et al., 2001 and Goldstein and Brown, 2001). Hobbs and colleagues (Garcia et al., 2001) have traced the molecular defect to a gene encoding a cytosolic protein. The cytosolic protein contains a phosphotyrosine-binding domain and is called ARH. Phosphotyrosine-binding proteins interact with the cytoplasmic tails of cell surface receptors that contain an NPXY motif, like the LDLr. It has been postulated that the phosphotyrosine-binding domain of ARH may interact with NPXY motif in the LDLr. This binding may be important for the entry of receptors into coated pits, or in receptor cycling from the cell surface. Alternatively, ARH may be required for trafficking of LDLr to the basolateral surface as seen in polarized epithelial cells. However, the specific role of ARH in the functioning of the LDLr still remains to be defined.

Acquired defects in the LDLr pathway:

A genetic defect in the LDLr pathway is not always the cause for elevated plasma levels of LDL cholesterol. Many FH patients have an acquired suppression of the LDLr pathway in the liver, leading to decreased clearance of LDL. When cells over-accumulate

intracellular cholesterol, the liver suppresses synthesis of LDLr. Since the plasma level of LDL cholesterol exceeds that needed to saturate receptors, the rate of LDL clearance is a function of number of LDLr in the liver. A fat-rich diet can suppress receptor number by overloading the liver with cholesterol. The entry of dietary cholesterol into the liver occurs through another receptor pathway, LRP. This receptor is not sensitive to over-accumulation of cholesterol. The increase in intracellular dietary cholesterol through this pathway suppresses LDLr synthesis and decreases LDL removal, leading to an acquired hypercholesterolemia. Acquired hypercholesterolemia is influenced by genetic and environmental factors.

Rationale and objectives:

The concentration of LDL in the plasma is of critical importance and strongly dependent on regulatory mechanisms that involve the LDLr. High concentrations of LDL lead to the clinical disorder FH. This is in part due to mutations in the LDLr gene. A number of these mutations lead to conformational defects in the mature protein that prevent LDL-LDLr interaction. To date very little is known about structural basis of the binding of the LDLr to its ligands. Although the ligand-binding domain has been characterized, it remains unclear which residues within this domain participate directly in apoE- and apoB- mediated binding. Similarly, the LDLr-binding site has been only incompletely mapped within apoB primary structure. Since the location of specific residues involved in the formation of the LDL-LDLr interaction are not clearly defined

the long-term goal of this study was to produce a soluble and functionally active LDLr in order to identify the LDLr-binding site within apoB.

In the process of producing a recombinant receptor, it became evident that domain-domain interactions within the LDLr and chaperone proteins may be involved in generating a functional receptor. Since mutations within the LDLr lead to FH and some are due to folding defects in the LDLr, an understanding of the folding dynamics of the LDLr may prove insightful to the understanding of the conformational disease, FH. Therefore, our second objective was to study the folding dynamics of the LDLr and to identify specific components that may be required to produce a functional receptor.

Lastly, we characterized the kinetics of binding of LDL to the purified LDLr and defined the physical and chemical properties of LDL that modulate apoB conformation and its ability to mediate binding to the LDLr. To date most of the information on binding kinetics has come from studies using fibroblasts. In these experiments the LDL-LDLr interaction were influenced by cell surface proteoglycans, lipoprotein lipase and receptor clustering within coated pits. In this study we used surface plasmon resonance to study the binding kinetics of LDL-LDLr in the absence of cell interfering components.

Chapter II

Expression and Secretion of a Soluble LDLr

Introduction

The low density lipoprotein receptor is a complex protein both in structure and in functionality. It can serve as a receptor for two ligands, undergo pH-dependent conformational changes and most importantly remove lipoproteins from serum. Our long-term goal was to define specific residues involved in forming the LDLr-LDL interaction and to identify variables that modulate this association. To characterize the LDLr-ligand binding surface and to study the dynamics of binding of lipoproteins to the LDLr an isolated preparation of receptor and ligand was required. Prokaryotic expression systems can be useful for producing recombinant proteins; however, the maturation of LDLr includes specific post-translational modifications such as glycosylation and phosphorylation. Bacteria do not perform these modifications. To resolve these problems, we opted for a eukaryotic system to express a soluble and truncated form of the LDLr. The expression hosts included the methylotrophic yeast, *Pichia pastoris* and Chinese hamster ovary cells.

P.pastoris can use methanol as a sole carbon and energy source (Romanos et al., 1992 and Sreekrishna et al., 1989). The first step in the utilization of methanol is the oxidation of methanol to formaldehyde and hydrogen peroxide that is catalyzed by the enzyme alcohol oxidase (AOX). The AOX promoter is highly inducible and stringently

regulated. AOX is not detectable in *P.pastoris* that is grown on glucose or ethanol. However, when the yeast cells are grown on methanol, AOX can account for thirty-five percent of the total cellular protein (Wegner and Harder, 1987). These properties of the AOX promoter have been exploited for the high level, inducible expression of recombinant proteins in *P.pastoris*. Vectors are commercially available that facilitate the integration of foreign genes onto the AOX locus of the *P.pastoris* genome by homologous recombination and allow the recombinant proteins to be expressed either intracellularly or secreted in the medium (Figure 2-1). Expression levels of foreign proteins as high as 12 g/l have been reported (Wegner and Harder, 1987). A second series of vectors are also commercially available that can target foreign genes to the glyceraldehyde-3-phosphate dehydrogenase (GAPDH) locus of *P.pastoris*. Genes under the control of the GAPDH can be constitutively expressed at high levels in *P.pastoris*. In addition to the presence of a strong promoter that can be used for protein production, *P.pastoris* has a number of other advantages. It is capable of generating post-translational modifications that are similar to those that occur in a mammalian system. Similar to human glycosylation, the proteins produced in *P.pastoris* are not hyperglycosylated (Romanos et al., 1992). The majority of N-linked oligosaccharide chains are high mannose, ~30 residues in length and lack the highly antigenic terminal α–1,3-mannose linkages that are present in proteins expressed in *S. cerevisiae* (Sreekrishna et al., 1988). Nevertheless, the glycosylation in *Pichia* and that in mammals is not identical. Lastly, this strain of yeast grows on a simple mineral media and does not secrete high amounts

Figure 2-1: Features of pPICZαB. The vector pPICZαB contains the following important elements. Sequences to permit integration of insert at the AOX locus of *P. pastoris*, α-factor secretion signal, multiple cloning site with unique restriction sites, carboxy-terminal tags (c-myc & histidine tail) and Zeocin-resistance gene. Other components of the vector include: EM& and TEF1 promoter, CYC1 transcription termination region and ColE1 origin.

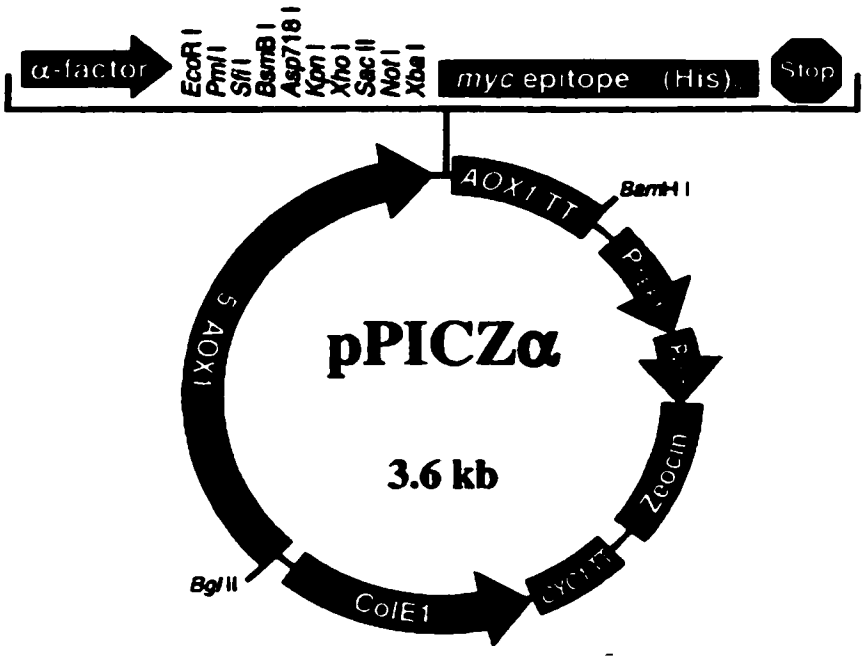
α-factor
EcoR I
Pml I
Sfi I
BamB I
Asp718 I
Kpn I
Xho I
Sac II
Not I
Xba I
myc epitope (His)
Stop
AOX1 TT
BamH I
pPICZα
3.6 kb
5' AOX1
Zeocin
CYC1 TT
ColE1
Bgl II

of endogenous protein, thereby facilitating purification of the heterologous protein (Wegner, 1990).

CHO-K1 are hamster ovary cells that have an epithelial-like morphology. The cell-line was derived as a subclone from a parental CHO cell-line initiated from a biopsy of an ovary of an adult hamster (Bachrati et al., 1999). CHO-K1 cells multiply rapidly and are easy to maintain. Unlike other cells lines such as fibroblasts, COS-7, and Hela cells, CHO-K1 cells can be grown in suspension culture as well as adherent on culture dishes. Products such as microcytodex beads, spinner flasks, and serum-free media are available commercially for facilitating high levels of protein expression in CHO-K1 cells and growth in serum-reduced conditions to assist in recombinant protein purification. Therefore, the cell line has been used extensively for the expression of many recombinant proteins including members of the LDLr gene family.

In the current study a number of constructs containing truncated forms of the LDLr were expressed in both the above described mammalian systems in an attempt to produce an active LDLr.

Materials & Experimental Procedures

Materials: DNA restriction enzymes were purchased from New England Biolabs. Vectors pPICZαB and pGAPZαB were purchased from Invitrogen. Reagents for cell culture were purchased from Gibco BRL Life Technologies, Inc. All chemicals were purchased from Sigma. The expression vector pCMV5 encoding the extracellular domains (amino acid residues 1-692) of the LDLr was a gift from Drs David Russell and Joseph Goldstein. The QuikChange mutagenesis kit was purchased from Stratagene. Immulon II Removawells were purchased from Dynatech Laboratories. Hybridomas, C7 (Beisiegel et al., 1981) and 9E10 (Evan et al., 1985) were purchased from the American Type Culture Collection (ATCC) and were injected into the peritoneal cavity of female BALB/c mice for the generation of ascites (Asai and Wilder, 1993). The anti-oligohistidine monoclonal antibody was purchased from Amersham. Cyanogen bromide-activated sepharose 4B beads were purchased from Pharmacia Biotech. Immuno Pur NHS-LC biotinylation kits were purchased from Boehringer Manneheim.

Expression LDLr ^{331} and LDLr^{692} in methylotrophic yeast Pichia Pastoris:

Vector construction: The plasmid, pCMV5 containing the cDNA encoding the human LDL receptor sequence was used as a template to amplify fragments coding for amino acid residues 1-331 and 1-692 by polymerase chain reaction (PCR). PCR products that had been cleaved with MfeI and XbaI restriction sites were ligated into either vectors pPICZαB (LDLr amino acid residues 1-331) or pGAPZαB (LDLr amino acid residues 1-

692) that had been digested with EcoRI and XbaI. This allowed for in-frame transcription, under the control of either the alcohol oxidase 1 or glyceraldehyde-3-phosphate dehydrogenase promoter of sequences encoding for the α-secretion factor, the insert, the c-myc decapeptide and the oligohistidine tail (Figure 2-1). Vectors containing the insert were propagated in the DH5α strain of *E.coli*; transformants were selected on Luria-Bertani agar (LB) plates containing 25 μg/ml of Zeocin. Transformants were analyzed by restriction mapping and sequencing to confirm in frame fusion of the LDLr with the *S. cerevisiae* α-factor secretion signal and the carboxy-terminal tag. The vector was linearized using SacI and the recombinant plasmid was transformed into *Pichia pastoris* by electroporation, following the manufacturer's protocol (Scorer et al., 1994).

Expression and screening: Recombinant yeast cells were analyzed by PCR to confirm the integration of the LDLr into the *Pichia* genome. The primers that were used annealed to the 5' and 3' sites of the AOX1 promoter. DNA was isolated from yeast cells by sonicating cells in a bath sonifer for one hour and 15 min., followed by vigorous vortexing for 5 min. Positive recombinants that contained the insert were screened for expression of protein after growth on nitrocellulose filters. Briefly, nitrocellulose membranes were moistened and placed on buffered complex glycerol agar plates (BMGY). Yeast colonies were dotted onto the membrane and allowed to grow at 30°C for two days, until large colonies appeared. The blot was transferred onto buffered complex methanol agar plates (BMMY) and protein expression was induced. The plate was incubated at 30°C for 1-3 h. The nitrocellulose filter was removed and washed in

Tris buffered saline (TBS) pH 7.2 to remove yeast colonies. The filter was then treated similarly to an immunoblot and probed with the anti-myc antibody, 9E10.

Scale-up expression: For the vector pPICZαB, a single colony was used to innoculate 25 ml of (BGGY) media in a 250 ml baffled flask. The cells were grown at 28-30°C in a shaking incubator (250-300 rpm) until the culture reached an OD_{600} of 2-6 (16-18 h). The cells were harvested by spinning in a centrifuge at 1500-3000 rpm for 5 min. at room temperature. The supernatant was decanted and the cell pellet was resuspended to an $O.D_{600}$ of 1.0 in buffered complex methanol media to induce expression of protein (100-200 ml). The culture was placed in a 1 liter baffled flask and covered with two layers of sterile gauze. Methanol was added to a final concentration of 0.5% to induce protein expression. A similar protocol was followed for the expression vector pGAPZα, with the exception that the addition of methanol to induce expression was not required, since the cells were constitutively expressing protein.

Purification: The fusion proteins were purified from culture supernatants by nickel chelate affinity chromatography. Culture media containing LDLr were dialyzed overnight in TBS pH 7.2. One quarter of the supernatant was incubated overnight at 4°C with constant inversion, with nickle-triacetic acid (Ni-NTA) resin. The slurry was poured into a 5 ml syringe that had been plugged with glass wool. The resin was washed with 3 ml of ice-cold, EDTA-free phosphate buffered saline (PBS) pH 7.0, followed by progressive washes with 5 ml of ice-cold Ni-NTA wash solution (100 mM citrate/phosphate) of pH 7.0, 6.5, 6.2 and the LDLr was eluted with wash solution adjusted to pH 4.0. Non-retained and eluted fractions were dialyzed in TBS-20 mM

$CaCl_2$ buffer. Samples were run on 10% SDS-PAGE and transferred to nitrocellulose paper for immunodetection using monoclonal antibodies specific to the LDLr (C7), myc epitope (9E10) and the oligohistidine tag (α-His).

Immunoassay for determination of LDL binding activity of LDLr: Immulon II Removawells were coated with 9E10 (5 μg/ml, 5 mM glycine, pH 9.2) overnight and subsequently saturated by incubation for 1 h with 250 μl of 1% bovine serum albumin (BSA) PBS, pH 7.4. Serial dilutions (125 μl) of LDLr were prepared, and 125 μl of 1 μg/ml LDL appropriately diluted in PBS containing 1% BSA and 20 mM $CaCl_2$, was added to the diluted LDLr and allowed to incubate for 4 h at room temperature. Aliquots (200 μl) of the LDL-LDLr mixture were transferred to the 9E10/C7-coated Removawells that had been washed with 1% PBS-BSA. The wells were incubated overnight, washed and counted for bound radioactivity with ^{125}I-1D1, an antibody specific to the amino-terminus of apoB100 on LDL.

Expression of LDLr ^{331}, LDLr$^{331\text{-}His}$, LDLr^{292} & LDLr ^{692} in Chinese Hamster Ovary cells:

Vector constructs:

LDLr $^{331\text{-}His}$: A fragment coding for the signal sequence, ligand-binding domain and the first repeat of the EGF homology domain (residues 1-331) was amplified by PCR. The specific primers introduced restriction sites for the enzymes XbaI and NheI. The PCR product was ligated into pcDNA3.1 with T4 DNA ligase using the XbaI and NheI restriction sites. This allowed for transcription, under the control of the CMV

(cytomegalovirus) promoter, of the sequences encoding the insert, the c-myc decapeptide and the oligohistidine tail.

LDLr^{331}: pcDNA3.1 containing LDLr$^{331\text{-His}}$ was used as a template for inverse PCR to delete the nucleotides that encode the c-myc and oligohisitidine epitope tags. The reverse primer was designed to anneal to nucleotides encoding the carboxy-terminus of EGF repeat one followed by a stop codon (TAA), while the forward primer corresponded to the pcDNA3.1 sequence that immediately followed the nucleotides that encode the oligohistidine tail, thereby excluding the c-myc and oligohistidine epitope tags. The primers contained a BamH1 site in order to facilitate the identification of positive clones. Following PCR, the products were cooled to below 37°C by incubating on ice for two minutes and treated with 1 μL of DpnI and an additional 0.5 μL of Pfu Turbo polymerase. The DpnI endonuclease is specific for methylated and hemimethylated DNA and was used to digest the parental DNA template and to select for mutation-containing DNA. The reaction mixture was incubated further at 37°C for 30 minutes and at 72°C for 30 minutes. The remaining products were incubated overnight at room temperature with 1 μL of T4 DNA ligase and transformed the following day into DH5α bacterial cells.

LDLr^{292}: pcDNA3.1 containing LDLr$^{331\text{-His}}$ was used as a template for deletion of the nucleotides encoding the first EGF repeat by QuikChange mutagenesis. Primers were designed to introduce a stop codon before the first EGF domain. The oligonucleotide primers containing the desired stop codon were complementary to opposite strands of the vector. The primers were extended during PCR by using Pfu Turbo DNA polymerase. Following temperature cycling the product was treated with DpnI. The reaction was

allowed to undergo DpnI digestion for 1 h at 37°C. DpnI-treated DNA (1 μl) from the sample reaction was transformed into DH5α-cells.

Transformation: The various vectors containing the inserts were propagated in DH5α cells and transformants were selected on LB-agar plates that contained 50 μg/ml of Ampicillin. LB plates were incubated at 37°C overnight to allow colony formation. Positive colonies were assessed for the presence of the various inserts by digestion with appropriate endonucleases followed by sequencing. DNA from positive clones was purified using Qiagen plasmid kits or cesium chloride (CsCl) gradient ultra-centrifugation (Griffith, 1991).

Cell culture and transfection: Female Chinese hamster ovary cells (CHO-K1) were cultured using Ham's F12 medium containing 10% fetal bovine serum. For transfection experiments, CHO-K1 cells (100 mm dishes, 10 ml media) were grown to 50-60% confluency and transfected with the expression plasmid encoding various truncated forms of human LDLr (15 μg of DNA) by calcium phosphate precipitation (Chen et al., 1987). Four to five hours after transfection, cells were subjected to glycerol shock and incubated for 24 hours with F12 medium. Stable transfection of 15 μg of expression plasmid was achieved by co-transfection with 0.15 μg of pSV2 neo. Stable transformants were selected using 700 μM G418 and maintained with 500 μM G418. Stable cell lines were produced for $LDLr^{692}$ and $LDLr^{331\text{-}His}$ and $LDLr^{331}$.

Preparation of cell extract and immunoblot analysis: Transfected cells were washed with PBS, resuspended in 200 mM Tris-maleate, pH 6.0, 0.5 mM phenylmethylsulfonyl

fluoride (PMSF), 2.5 uM leupeptin and 1.4% Triton X-100 and incubated on ice for 30 min. Insoluble protein was removed by centrifugation (14000 rpm, 40 min., 4°C) in an Eppendorf microcentrifuge. The media were concentrated ten-fold using centriprep concentrators. The Triton X-100 soluble cell proteins along with the concentrated media were incubated with an equal volume of sample buffer (8 M urea, 2% SDS, 10% glycerol, 10 mM Tris-HCl, pH 8.3) and subjected to gel electrophoresis on a 10% polyacrylamide gel. Proteins were electrophoretically transferred (4 h) onto nitrocellulose membranes for immunoblot analysis. The immunoblots were blocked with 5% fat-free milk in TBS containing 20 mM calcium chloride and probed with antibodies specific to carboxy-terminal tags (9E10, α-His) or to the LDLr (C7). The C7 antibody is specific for the first repeat of the ligand-binding domain and will only react with LDLr that has not been reduced. The binding of C7 to the LDLr is also dependent on calcium. All immunoblot analyses using the C7 antibody after SDS-PAGE under non-reducing conditions were detected with horse-radish peroxidase (HRP) conjugated IgG (1:1000) and developed using enzyme chemiluminescence (ECL) detection.

Scale-up expression of LDLr^{692}: Stable cell-lines were sequentially adapted from serum supplemented medium to complete, serum-free, low protein cell culture medium (CHO-S-SFM II, Gibco). Adapted cells were seeded into twenty, 150 cm^2 flasks containing 50 ml of medium and grown to 60% confluency. The cells were harvested from culture flasks using 0.25% trypsin and seeded into 1 l microcarrier containing 500 ml of CHO-S-SFMII media with 1% fetal calf serum and grown for two weeks. The cells were pelleted

by spinning in a centrifuge at 3000 rpm for 10 min. The media was removed and receptor was purified using affinity chromatography.

Purification of LDLr^{692} from CHO media: The LDLr was purified from CHO media by immunoaffinity chromatography. C7 was immobilized onto cyanogen bromide-activated sepharose 4B beads (Pharmacia, Biotech) by following the manufacturer's instructions. The column was washed with TBS containing 20 mM $CaCl_2$. 500 ml of media from spinner flask culture was passed over the column at a flow rate of 1.5 ml/min. The column was washed with TBS-20 mM $CaCl_2$ and eluted with 0.1 M glycine pH 3. The fractions were dialyzed against TBS-20 mM $CaCl_2$ overnight and stored in liquid nitrogen.

Ligand blot analysis: The purified receptor was subjected to 10% gel electrophoresis under non-reducing conditions and transferred electrophoretically for 4 h using 480 mM Tris Base, 390 mM glycine, to nitrocellulose paper. The transferred proteins were blocked for 1 h with 5% BSA in ligand blot buffer (LBB) (20 mM, 90 mM NaCl, 2 mM $CaCl_2$). Human LDL was biotinylated according to the instructions provided with the Immuno Pur NHS-LC biotinylation kit. The blot was incubated overnight with 20 μg/ml of biotinylated LDL in LBB. The membranes were washed extensively in LBB for 2 h. Blots were probed with HRP conjugated streptavidin (1:1000). Following a 40 min. wash with LBB, the blots were developed using ECL detection.

Competitive ligand-binding assay: Immulon II Removawells were coated with 100 μl of purified LDLr (5 μg/ml in PBS) at room temperature, overnight. Plates were washed with TBS-20 mM $CaCl_2$ and blocked for 1 h with 125 μl of 1% bovine serum albumin in

TBS-20 mM $CaCl_2$. Serial dilutions of native LDL or acetylated LDL in TBS-20 mM $CaCl_2$ were prepared in dilution plates (60 µl). 200 µg/ml of biotinylated LDL (biotinylated according to the instructions provided with the Immuno Pur NHS-LC biotinylation kit) was added to the dilution plates (60 µl). 100 µl of the pre-incubated mixture of either acetylated LDL or native LDL with biotinylated LDL was added to the removawells. The plate was incubated overnight and washed with TBS-20 mM $CaCl_2$. Bound LDL was determined by probing with strepavidin-HRP (1:1000) followed by the addition of terra-methyl-benzidine (TMB) liquid substrate (100 µl, 30 min.). The optical density was read at 655 nm.

Results

Synthesis and secretion of a truncated form of LDLr in the methylotrophic yeast

Cloning of LDLr^{331}: A DNA fragment encoding the ligand-binding domain and the first EGF repeat was successfully amplified and ligated into the vector, pPICZαB to allow expression of the protein under the control of the AOX1 promoter. Figure 2-2A depicts the amplification of a 1 kb fragment corresponding to the LDLr at various annealing temperatures. Annealing temperatures of 54°C and 56°C appear to contain considerably more PCR product, and were subsequently used for cloning into pPICZα. The PCR products digested with Xba1 and Mfe1 were ligated into pPICZαB following digestion with Xba1 and EcoRI. The vector was propagated in *E. coli* and zeocin-resistant colonies were selected. Restriction digest analysis of isolated DNA from recombinant plasmids yielded expected bands of 1 and 3 kb, corresponding to the insert and vector, respectively (Figure 2-2B). DNA sequencing showed the insert to be in-frame with the nucleotides encoding α-secretion factor and carboxy-terminal peptides. The constructs were linearized with the restriction enzyme Sac1 and transformed into KM71 and GS115 strains of *Pichia pastoris* by electroporation. Recombinants were selected for Zeocin resistance and the correct integration of the insert into the *Pichia* genome was confirmed by PCR. Figure 2-3B is a schematic representation of the insertion of LDLr into the *Pichia* genome following homologous recombination at the AOX1 site. The amplification

Figure 2-2: Agarose gel analysis of $LDLr^{331}$. (A) 50 ng of the template pCMV5-$LDLr^{692}$ and 100 ng of each 5' and 3' primer were used to amplify $LDLr^{331}$. The PCR cycle consisted of 5 min. at 95°C, 1 min. each at 95°C, 55-72°C and 72°C for 30 cycles. Lane 1-4; 10 µl of PCR product from annealing temperatures of 54°C, 56°C, 58°C & 60°C respectively. Lane 5; 1 kb ladder. **(B)** Restriction digestion of maxi prep DNA. Lane 1; Maxiprep of $LDLr^{331}$ in pPICZαB digested with Xba1 and Xho1. Lane 2; pPICZαB digested with Xba1. Lane 3; 1 kb ladder.

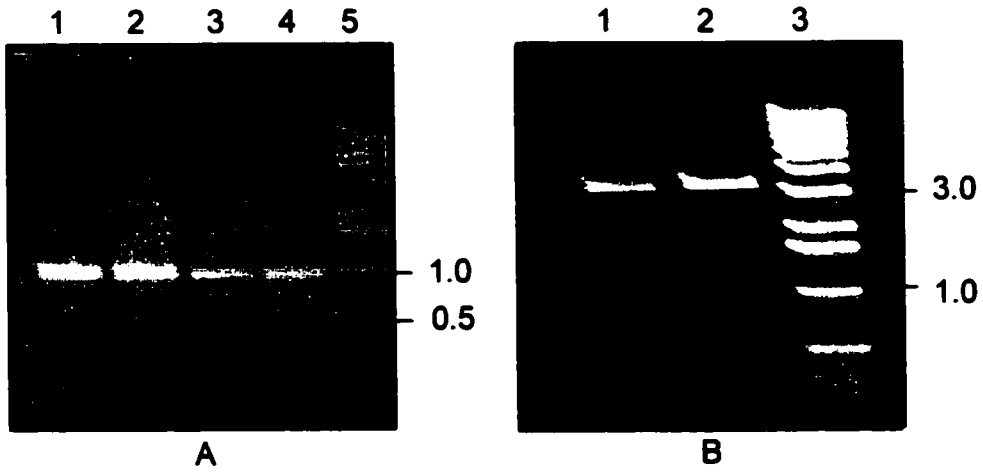
1
2
3
4
5
1.0
0.5
A
1
2
3
3.0
1.0
B

Figure 2-3: PCR analysis of genomic DNA isolated from *Pichia* recombinants using 5' and 3'AOX1 primers. (A) 1 μg of genomic DNA and 500 ng of each 5' and 3' primer were used to amplify $LDLr^{331}$. The PCR cycle consisted of 5 min. at 95°C, 1 min. each at 95°C, 54°C, 72°C and a final 10 min. at 72°C for 30 cycles. 10 μl of PCR product was run on 1% agarose gels. Lane 1 & 2; *Pichia* recombinants. Lane 3; PICZαB alone. Lane 4; 1 kb ladder. **(B)** Schematic diagram depicting the insertion of LDLr in the vector, pPICZαB by homologous recombination at the AOX1 site of the *Pichia* genome.


A.
1
2
3
4
1.0 kb
0.5 kb

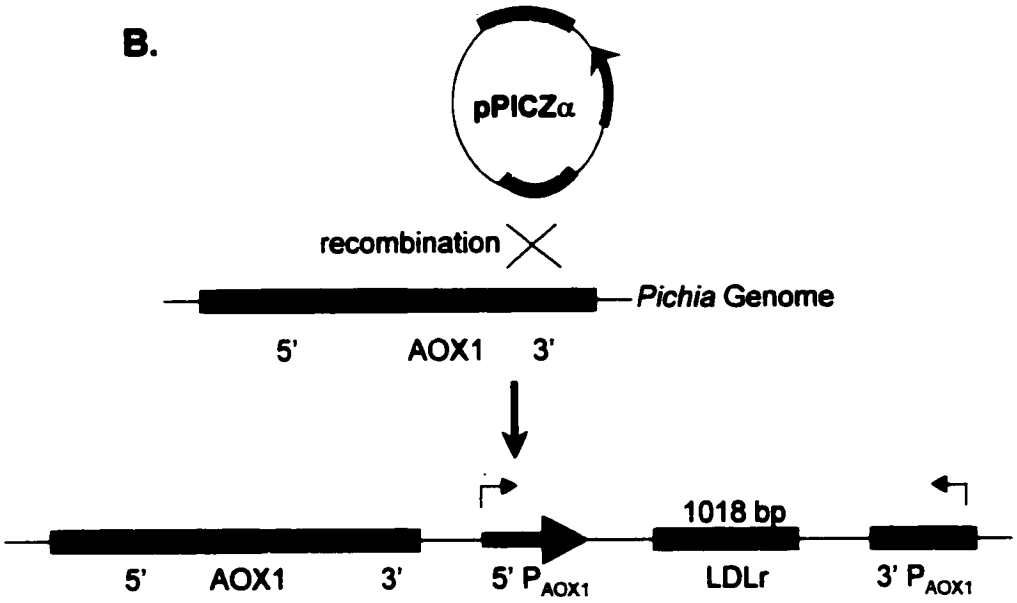
B.
pPICZα
recombination
Pichia Genome
5'
AOX1
3'
1018 bp
5'
AOX1
3'
5' P AOX1
LDLr
3' P AOX1

PCR product of recombinants after electrophoresis on agarose gels is shown in Figure 2-3A. Lane 1 contains a band at 1611 bp corresponding to the insert and AOX1 site, Lane 2 is a negative recombinant and Lane 3 yields a band at 596 kb corresponding to the AOX1 site without the insert. Positive transformants were screened for receptor secretion by colony blotting using a monoclonal antibody against the myc-epitope (9E10). Out of approximately one hundred transformants screened for receptor expression, ten of the most intensely stained colonies were picked and tested for expression in liquid culture.

Characterization of receptor: Cultures of LDLr expressing transformants were grown as described in the Experimental Procedures. The medium was collected and the fusion protein was analyzed by immunoblotting under reducing and non-reducing conditions. Cell culture media were analyzed by immunoblotting following SDS-PAGE using the conformation specific anti-LDLr monoclonal antibody, C7, and the anti-c-myc monoclonal antibody, 9E10. All clones that were screened under non-reducing conditions recognized 9E10. However, the blot showed that the immunoreactive protein was heterogeneous in molecular weight (Figure 2-4). These bands probably represent multiple disulfide-linked receptors, since under reducing conditions most of the bands were abolished except for a doublet, which probably represents different glycosylated forms of the receptor (Figure 2-5). The receptor was not able to bind C7 when tested under non-reducing conditions (data not shown). A lack of reactivity with the conformation-specific antibody C7 is a strong indicator that the LDLr is misfolded. Nonetheless, the receptor was purified from culture supernatants by nickel chelate affinity chromatography and examined for functionality.

Figure 2-4: Immunoblot analysis of LDLr^{331}. 100 µl of cultured media from CHO-K1 LDLr^{331} recombinants (clones A1-A6) were electrophoresed on 10% SDS-PAGE under non-reducing conditions and probed with anti-myc (9E10).

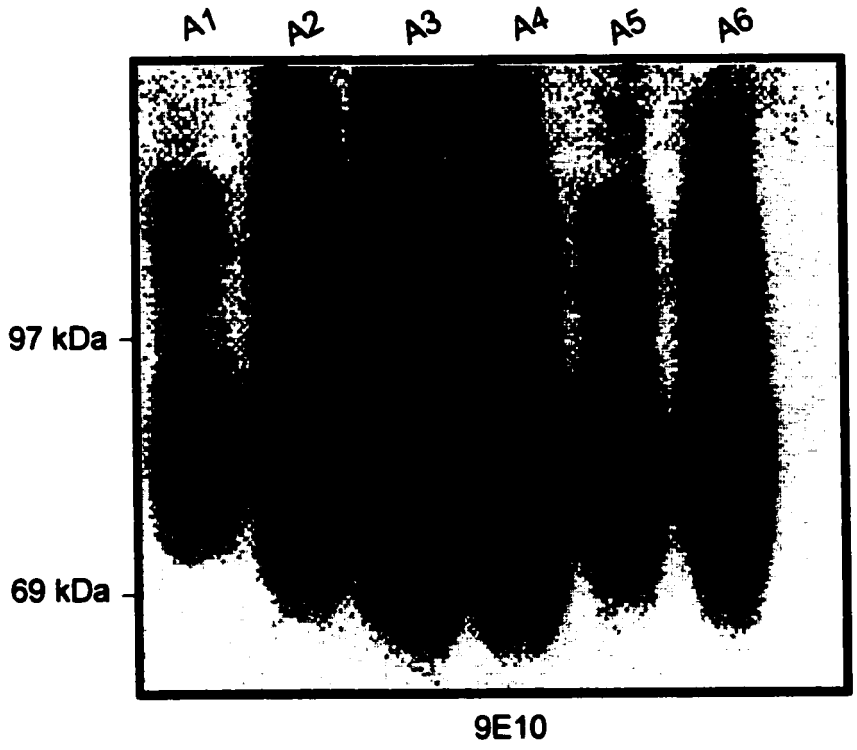
A1
A2
A3
A4
A5
A6
97 kDa
69 kDa
9E10

Figure 2-5: Immunoblot analysis of LDLr^{331}. 100 µl of cultured media from recombinants A1, A2 and A3 were electrophoresed on 10% SDS-PAGE under reducing conditions and probed with anti-myc (9E10).

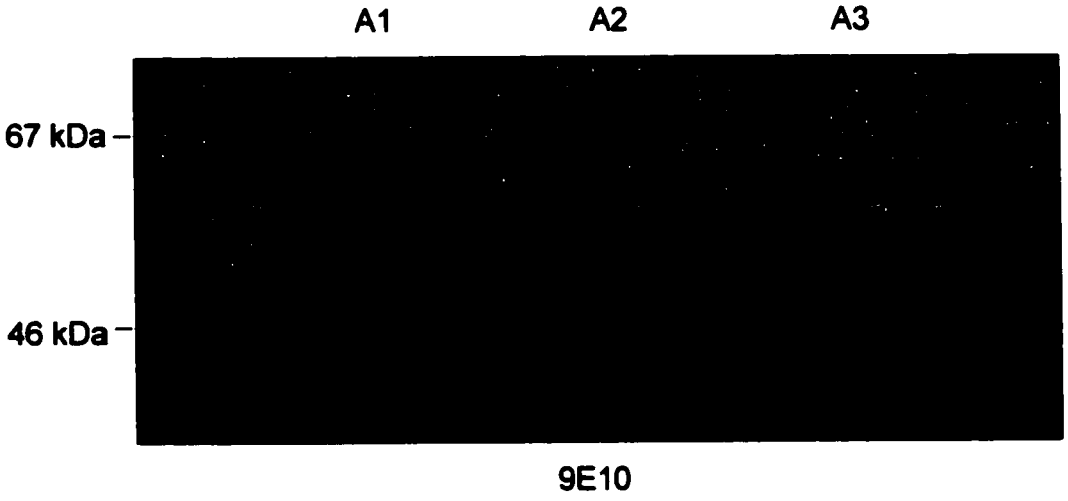
A1
A2
A3
67 kDa
46 kDa
9E10

Fractions isolated after column purification were subjected to electrophoresis and probed with 9E10 and C7. 9E10 reacted with fractions eluted at pH 4.0 to give a heterogeneous population of protein. Again, the purified receptor was not C7-immunoreactive. The ability of the receptor to bind LDL isolated from human plasma was tested by a radioimmunoassay. However, the 9E10-captured receptor was unable to bind LDL and was, therefore, non-functional.

Cloning of LDLr^{692}: The absence of the entire EGF precursor homology domain may have resulted in a non-functional LDLr^{331}. Therefore, we proceeded to clone a cDNA fragment that encoded the ligand-binding domain and the EGF precursor homology domain into the yeast expression vector pGAPZα. This vector was chosen because, unlike pPICZα, protein expression does not have to be induced by methanol. Expression of the recombinant protein is under the control of the GAPDH promoter. GAPDH is constitutively expressed at high levels in many organisms, including *Pichia pastoris*. The level of expression seen with the GAP promoter is normally slightly higher than that obtained with the AOX1 promoter but is dependent on the protein being expressed. The amplified PCR product encoding the first 692 amino acids of the receptor was successfully cloned into pGAPZα. Figure 2-6A shows that the PCR amplification yielded a product of the expected 2.1 kb. The PCR product was digested with the restriction endonucleases Mfe1 / Xba1, and added to EcoRI / Xba1-digested pGAPZαB, incubated with ligase and transformed into DH5α bacterial cells. Purified DNA from positive transformants was digested with Xho1 (digests within the signal sequence of

Figure 2-6: Agarose gel analysis of $LDLr^{692}$. **(A)** 50 ng of the template PCMV5-$LDLr^{692}$ and 100 ng of each 5' and 3' primer were used to amplify $LDLr^{692}$. The PCR cycle consisted of 5 min. at 95°C , 1 min. each at 95°C, 55°C and 72°C for 30 cycles. Lane 1; 10 µl of PCR product. Lane 2; 1 kb ladder. **(B)** Restriction digestion of maxi prep DNA. Lane 1; 1 kb ladder. Lane 2; Maxiprep of $LDLr^{692}$ in pGAPZαB digested with Xba1. Lane 3; Maxiprep of $LDLr^{692}$ in pGAPZαB digested with Xba1 & Xho1.

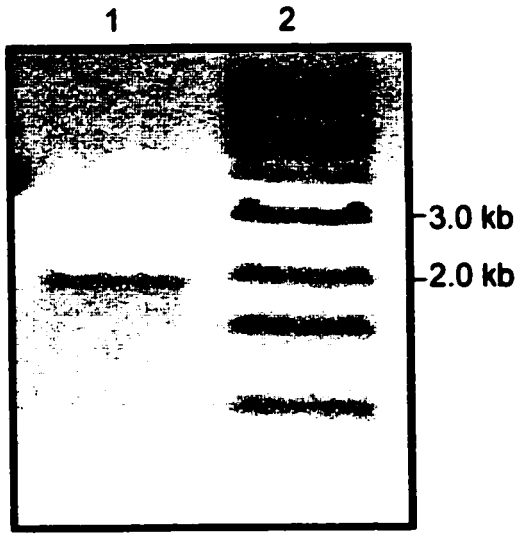

A

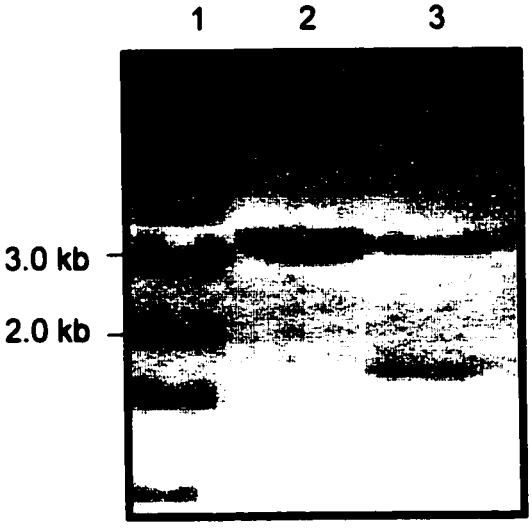

B

vector) and XbaI and yielded bands corresponding to the insert (2.1 kb) and vector (2.9 kb) on agarose gel electrophoresis (Figure 2-6B). Sequencing showed the insert to be in-frame with amino and carboxy-terminal markers. The plasmid was transformed into yeast cells and the insert was shown to be incorporated into the *Pichia* genome by PCR (Figure 2-7). Verified recombinants were grown in yeast peptone dextrose (YPD) media. Supernatants and cells were harvested at various time points and electrophoresed on 10% acrylamide gels and immuno-detected with C7 and an antibody specific to the c-myc epitope (9E10). Figure 2-8 shows the presence of a heterogeneous population of bands between 70-120 kDa in the cells but not in the media when analyzed under reducing conditions. Once again, no reactivity was obtained with the conformation specific anti-LDLr monoclonal antibody, C7 in either cells or media when analyzed under non-reducing conditions (data not shown).

Synthesis and secretion of a truncated and soluble form of the LDLr in CHO-K1 cells

Cloning & expression of $LDLr^{331\text{-}His}$, $LDLr^{331}$ & $LDLr^{292}$: Recombinant plasmids encoding DNA fragments of the LDLr ligand-binding domain in the absence or presence of EGF repeat A and a c-myc/six oligohistidine tag were generated. The PCR amplification reactions are depicted in Figure 2-9. Purified DNA from positive transformants was analyzed by sequencing and restriction enzyme digestion of endonuclease sites that had been incorporated into the primers (Figure 2-10). The recombinant plasmids were used for $CaCl_2$ mediated transfection of CHO-K1 cells. Proteins secreted into the cell culture media, as well as intracellular proteins, were

Figure 2-7: PCR analysis of genomic DNA isolated from *Pichia* recombinants using 5' and 3' AOX1 primers. (A) 1 μg of genomic DNA and 500 ng of each 5' and 3' primer were used to amplify $LDLr^{331}$. The PCR cycle consisted of 5 min. at 95°C, 1 min. each at 95°C, 54°C, 72°C and a final 10 min. at 72°C for 30 cycles. 10 μl of PCR product was run on 1% agarose gels. Lane 1 & 8 positive recombinants. Lane 2-7 & 9-10; negative recombinants. Lane 11; 1 kb ladder. **(B)** Schematic diagram depicting the insertion of LDLr in the vector, pGAPZαB by homologous recombination at the AOX1 site of the *Pichia* genome.

A.

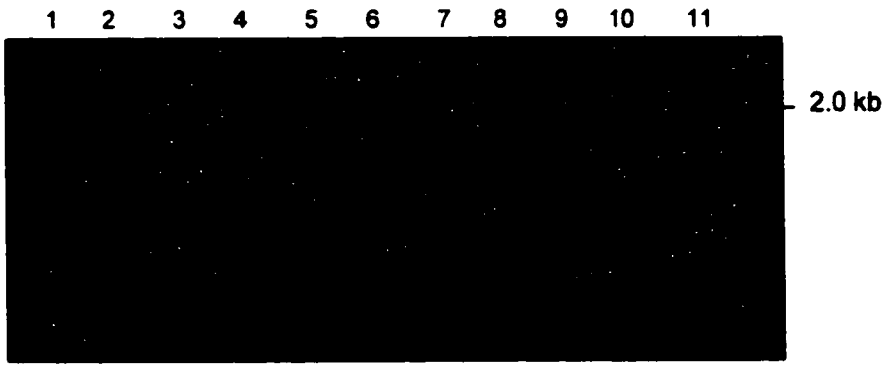
1 2 3 4 5 6 7 8 9 10 11
2.0 kb

B.

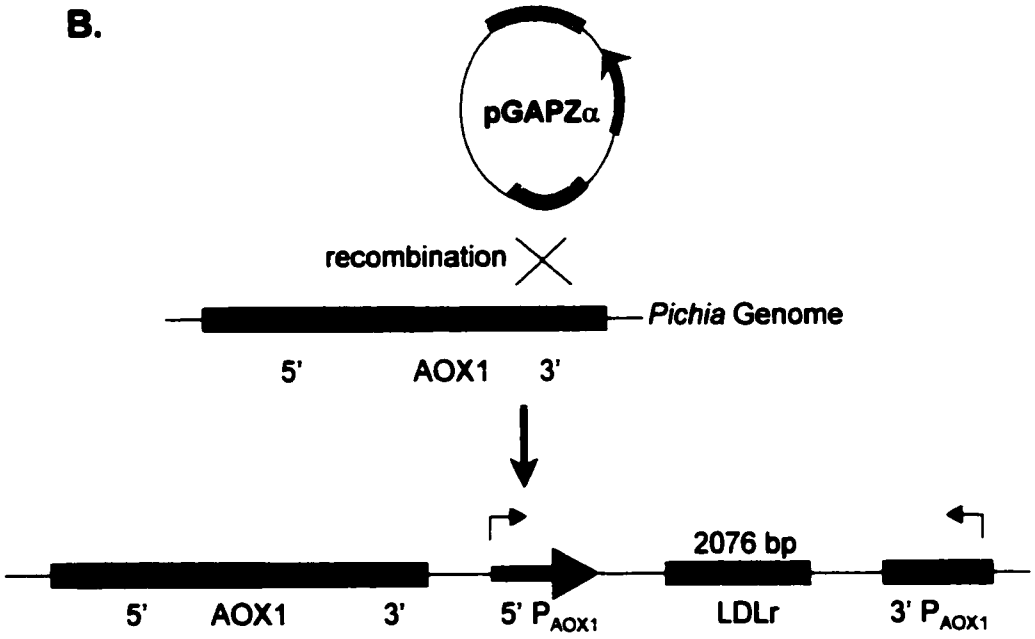
pGAPZα
recombination
Pichia Genome
5' AOX1 3'
2076 bp
5' AOX1 3' 5' P AOX1 LDLr 3' P AOX1

Figure 2-8: Representative immunoblot analysis of LDLr^{692}. 100 μl of cultured media or cell extracts from recombinants, A4 and B3 were electrophoresed on 10% SDS-PAGE under reducing conditions and probed with anti-myc (9E10). Lane 1; positive control (PLTP). Lane 2; Rainbow molecular weight markers. Lane 3; t=0, medium. Lane 4; t=1 day, cells. Lane 5; t=1 day, medium. Lane 6; t= 2 days, cells. Lane 7; t=2 days, medium. Lane 8; t=3 days, cells. Lane 9; t=3 days, medium. Lane 10; t=4 days, cells. Lane 11; t= 4 days, medium.

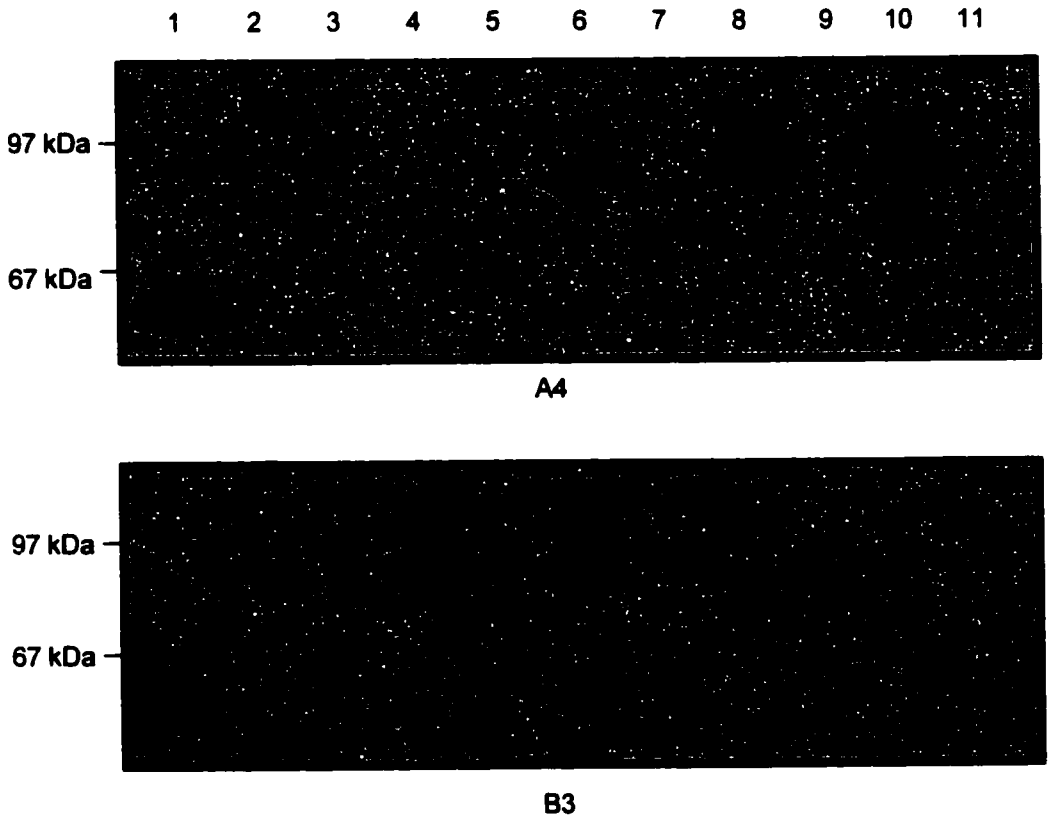
1
2
3
4
5
6
7
8
9
10
11
97 kDa
67 kDa
A4
97 kDa
67 kDa
B3

Figure 2-9: Agarose gel analysis of $LDLr^{331\text{-}His}$, $LDLr^{331}$ & $LDLr^{292}$ 50 ng of the template pCMV5-$LDLr^{692}$ and 100 ng of each 5' and 3' primer were used to amplify $LDLr^{331}$. The PCR cycle consisted of 5 min. at 95°C, 1 min. each at 95°C, 55-72°C, 72°C and an additional 72°C for 30 cycles. *For* $LDLr^{331\text{-}His}$: Lane 1; 1 kb ladder. Lanes 2 - 6; PCR amplification using annealing temperatures ranging from 54°C - 62°C (every 2 degrees) respectively. *For* $LDLr^{292}$: Lane 1-5; PCR amplification using annealing temperatures ranging from 62°C-68°C (every 2 degrees) respectively. Lane 6; 1 kb ladder. *For* $LDLr^{331}$: Lane 1-9; PCR amplification using annealing temperatures ranging from 55°C - 71°C (every 2 degrees) respectively. Lane 10; 1 kb ladder.

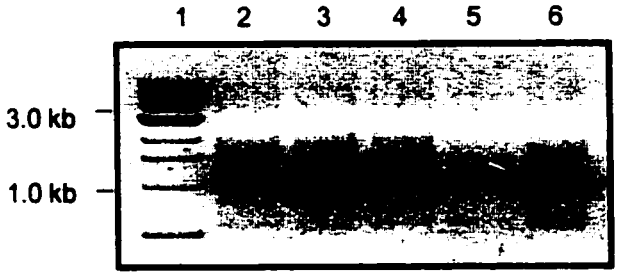

$LDLr^{331\text{-}His}$

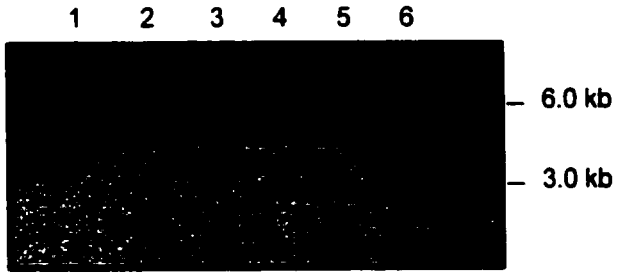

$LDLr^{292}$

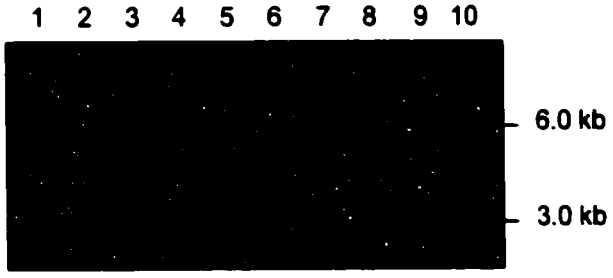

$LDLr^{331}$

analyzed by immunoblotting with monoclonal antibody, C7, and antibodies specific to the carboxy-terminal tags (α-His & 9E10). Figure 2-11 is a representative immunoblot of samples obtained from $LDLr^{331\text{-}His}$ transfected cells. The receptor was detected in both the cell culture media and within the cells. The secreted form of the receptor had a higher molecular weight (40 kDa) than the intracellular form of the protein (30 kDa). The increase in apparent molecular weight is probably due to post-translational modifications, most likely glycosylation at asparagine and serine residues in the ligand-binding domain (Dirlam et al., 1996). Further analysis using the conformation specific antibody, C7, revealed that the ligand-binding domain was improperly folded since the antibody did not bind. Interestingly, expression of LDLr without the carboxy-terminal epitope tags yielded a protein that was recognized by C7 on an immunoblot (Figure 2-12). However, the protein appeared to be aggregated and did not migrate at the correct molecular weight. Similar results were obtained for the construct that contained only the ligand-binding domain of the receptor. Transfection of $LDLr^{292}$ into CHO-K1 cells resulted in a protein that was secreted and detectable by C7. However, once again, most of the proteins migrated as a smear or as badly resolved bands, indicating substantial heterogeneity, aggregation and partial misfolding (Figure 2-12).

Expression of $LDLr^{692}$ in CHO-K1 cells: The expression plasmid encoding the extracellular domain of the LDLr, kindly provided by Drs Russell & Goldstein was transiently transfected into CHO-K1 cells. Proteins secreted into the cell culture media, as well as intracellular proteins were subjected to immunoblot analysis by using the anti-LDLr monoclonal antibody, C7. C7 recognized the receptor in the medium as a single

Figure 2-10: Agarose gel analysis of purified DNA from positive $LDLr^{331\text{-}His}$, $LDLr^{331}$ & $LDLr^{292}$ transformants. *For $LDLr^{331\text{-}His}$*: Lane 1; 1 kb ladder. Lane 2 & 3; Isolated DNA from two clones double-digested with XbaI and NheI to yield the insert (1.0 kb) and vector (5.5 kb). *For $LDLr^{331}$*: Lane 1 & 2; Isolated DNA from two clones digested with BamH1, a unique restriction site incorporated into the primers to identify positive transformants (yields a 6.7 kb fragment corresponding to the insert and vector). Lane 3; 1 kb ladder. *For $LDLr^{292}$*: Lane 1; Double digest with Xba1 and Nhe1 to yield the insert (1.0 kb) and the vector (5.5 kb); Lane 2; Vector without insert digested with Xba1. Lane 3; Vector with insert digested with Sal1, a unique restriction site incorporated into the primers to identify positive transformants. Lane 4; Vector alone cut with Sal1. Lane 5; 1 kb ladder. Lane 6; 100 kb ladder.

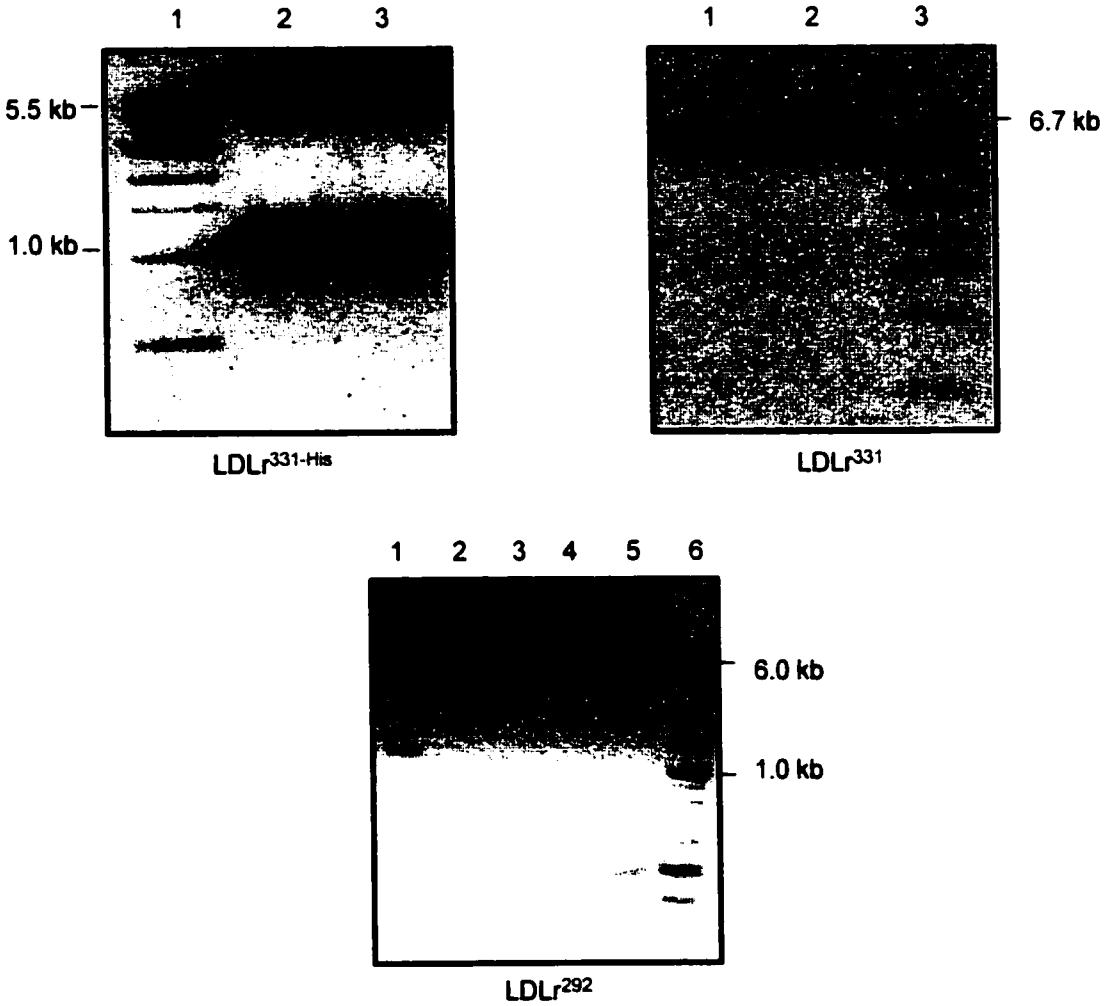
1 2 3
5.5 kb
1.0 kb
LDLr331-His
1 2 3
6.7 kb
LDLr331
1 2 3 4 5 6
6.0 kb
1.0 kb
LDLr292

Figure 2-11: Immunoblot analysis of media and cells from LDLr$^{331\text{-His}}$ transfected CHO-K1 cells. Samples were electrophoresed on 10% polyacrylamide gels under reducing conditions and detected using the anti-His antibody (specific for the oligohistidine epitope tag) and 9E10 (specific for the carboxy-terminal c-myc epitope). Samples were also run under non-reducing conditions and detected using the conformation specific anti-LDLr monoclonal antibody, C7. Lanes 1-5; correspond to cellular LDLr$^{331\text{-His}}$, empty vector in cells (negative control), His-PLTP (positive control), secreted LDLr$^{331\text{-His}}$ and empty vector in media (negative control) respectively. Lanes 6-7; correspond to cellular and secreted LDLr. Lane 8-9; correspond to secreted LDLr and medium from cells LDLr^{692}.

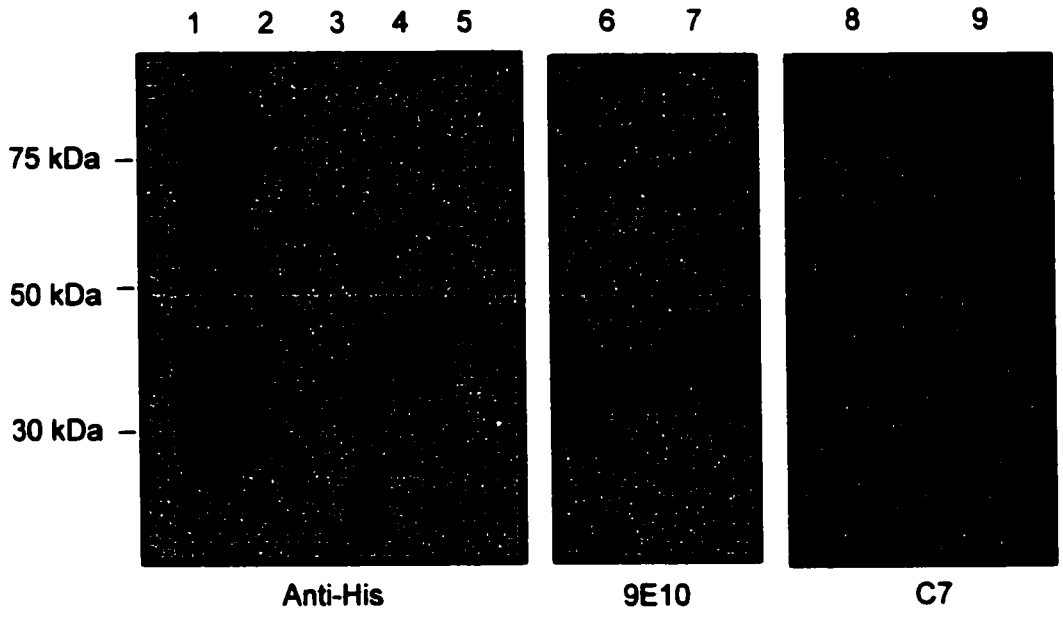
1
2
3
4
5
6
7
8
9
75 kDa
50 kDa
30 kDa
Anti-His
9E10
C7

Figure 2-12: Immunoblot analysis of media from $LDLr^{331}$ & $LDLr^{292}$ transfected CHO-K1 cells. Samples were electrophoresed on 10% polyacrylamide gels under non-reducing conditions and detected using the conformation specific anti-LDLr monoclonal antibody, C7. Lane 1; mock transfected. Lane 2; $LDLr^{292}$. Lane 3; $LDLr^{331}$.

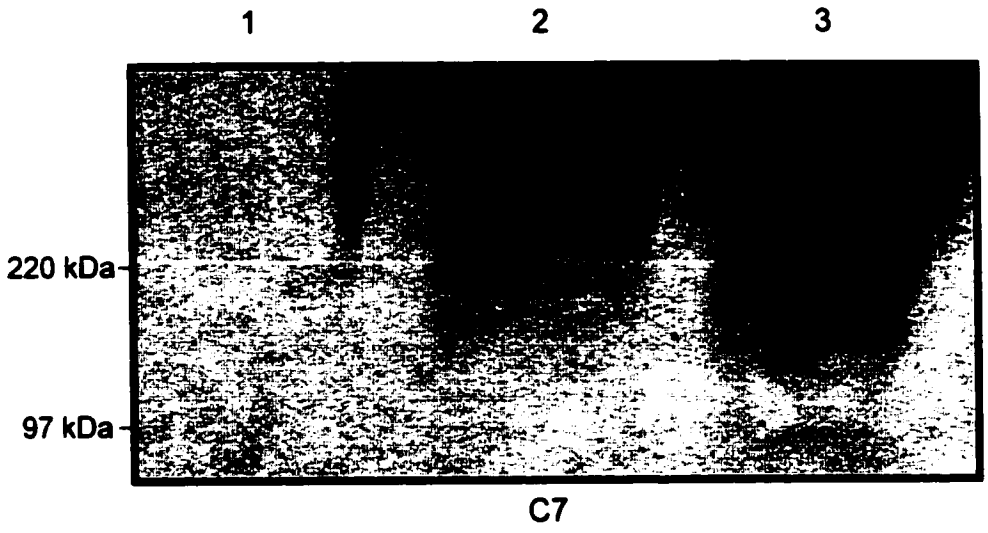
1
2
3
220 kDa
97 kDa
C7

Figure 2-13: Immunoblot analysis of LDLr^{692}. Media from cultured cells were electrophoresed on 10% SDS-PAGE, transferred onto nitrocellulose membranes and incubated with the anti-LDLr monoclonal antibody, C7. Positive immunoreactivity was obtained for clones V4, V8, V9, V14 and V25. Clone V14 was used in all subsequent studies.

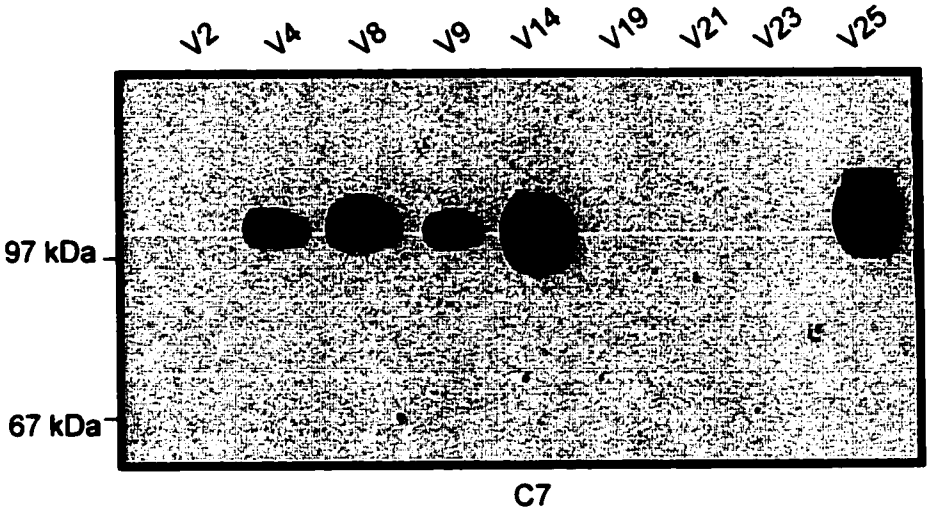
V2
V4
V8
V9
V14
V19
V21
V23
V25
97 kDa
67 kDa
C7

discrete band at the correct molecular weight of 97 kDa (data not shown). Following these positive results, we proceeded to produce stable $LDLr^{692}$ expressing cell lines. Stable transfection was achieved by co-transfection of LDLr with pSV2neo, a vector that confers neomycin resistance. Stable transformants were selected by using the antibiotic, G418. From the 46 colonies that were screened for expression of the receptor, only 20 appeared to be positive. Figure 2-13 is an immunoblot analysis of the screening results for some of these transformants. The positive transformants V14, V8, V10 and V13 were expanded, frozen and used for functional assays.

Adaptation of cells to serum-free media: CHO cells expressing $LDLr^{692}$ were initially grown in Ham's F12 media supplemented with fetal calf serum. Fetal calf serum contains proteins that interfere with purification and downstream processing of the expressed product. To facilitate the purification of the receptor, cells were adapted to media that was supplemented with nutrients and amino acids and therefore did not require serum to maintain cell viability. The media was also designed for the growth of cells in suspension culture. The adaptation procedure was slow and was achieved by a gradual substitution of serum supplemented medium for serum-free media. However, even after one month, the $LDLr^{692}$ cells were unable to grow in the absence of serum, the cells appeared to require a minimum of 1% serum to maintain cell viability. An immunoblot analysis of clones V14, V8 and V25 after adaptation to serum-free media is shown in Figure 2-14.

Scale-up expression and purification of $LDLr^{692}$: The antibody C7 binds specifically to the first repeat of the ligand-binding domain of the LDLr and was used to prepare an

Figure 2-14: Western blot analysis of media from stably transfected LDLr^{692} cells after adaptation to serum-free media containing 1% serum. Clones V14, V8 and V25 were adapted to CHO-SKI media over a period of two weeks. The clones were screened for LDLr^{692} expression by immunoblot analysis using the anti-LDLr monoclonal antibody, C7.

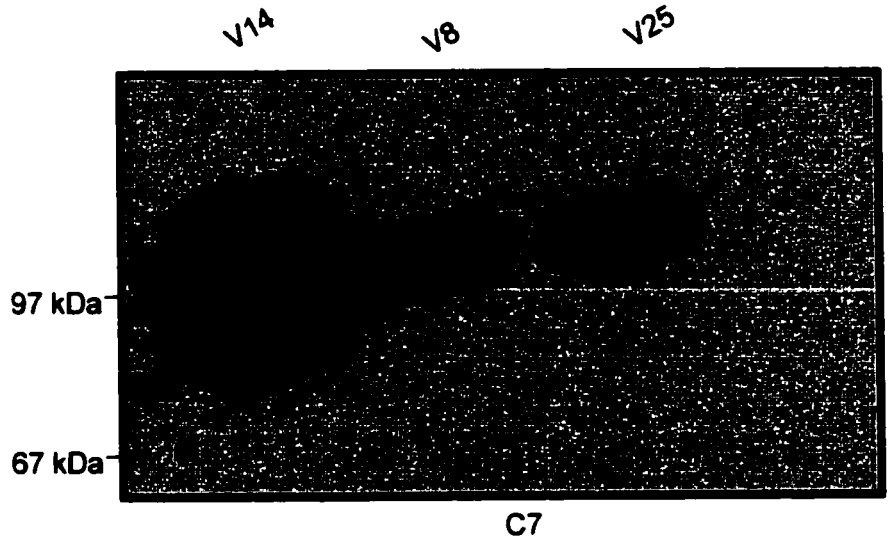
V14
V8
V25
97 kDa
67 kDa
C7

Figure 2-15: Analysis of purified LDLr^{692}. Medium from CHO-K1 cells was passed over a C7 immunoaffinity column and eluted with 0.1 M glycine, pH 3.0. The flowthrough (FT), and elutant were collected and subjected to immunoblot analysis using the conformation specific anti-LDLr monoclonal antibody, C7. LDLr functionality was determined by ligand blot analysis using biotinylated LDL. LDLr purity was determined by Coomassie blue stain. MWM, standard rainbow molecular weight markers.

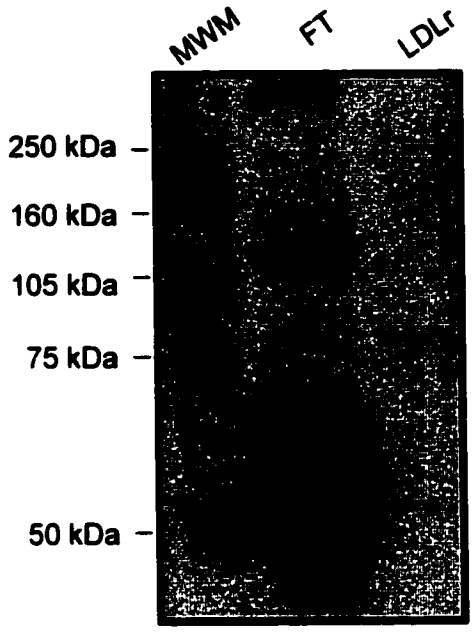

Commassie Blue

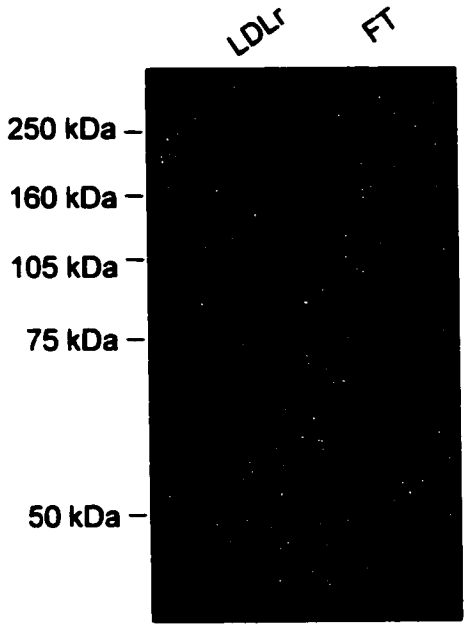

Immunoblot C7

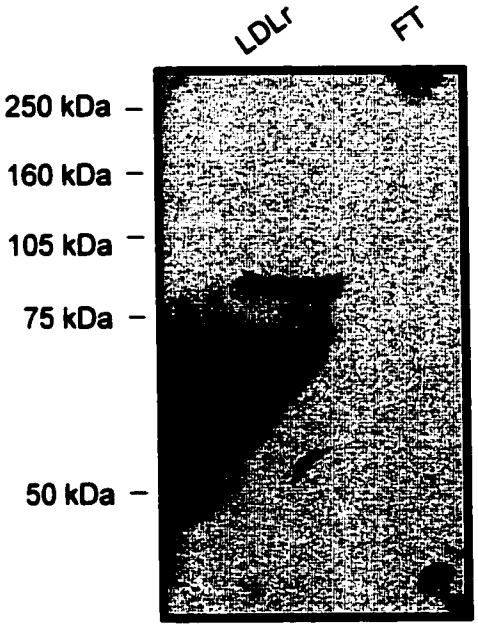

Ligand Blot *LDL

Figure 2-16: Competitive enzyme-linked immunoassay. 5 μg/ml of purified $LDLr^{692}$ was coated on microtiter wells. Serial dilutions of either 50 μg/ml of unlabeled native LDL or acetylated LDL with 200 μg/ml of biotinylated LDL were added to LDLr-coated wells. Bound LDL was detected by the addition of strepavidin-HRP followed by TMB liquid substrate. Binding is expressed as a ratio of strepavidin-HRP bound in the presence of native LDL or acetylated LDL (B), to strepavidin-HRP bound in the absence of competitors (Bo).

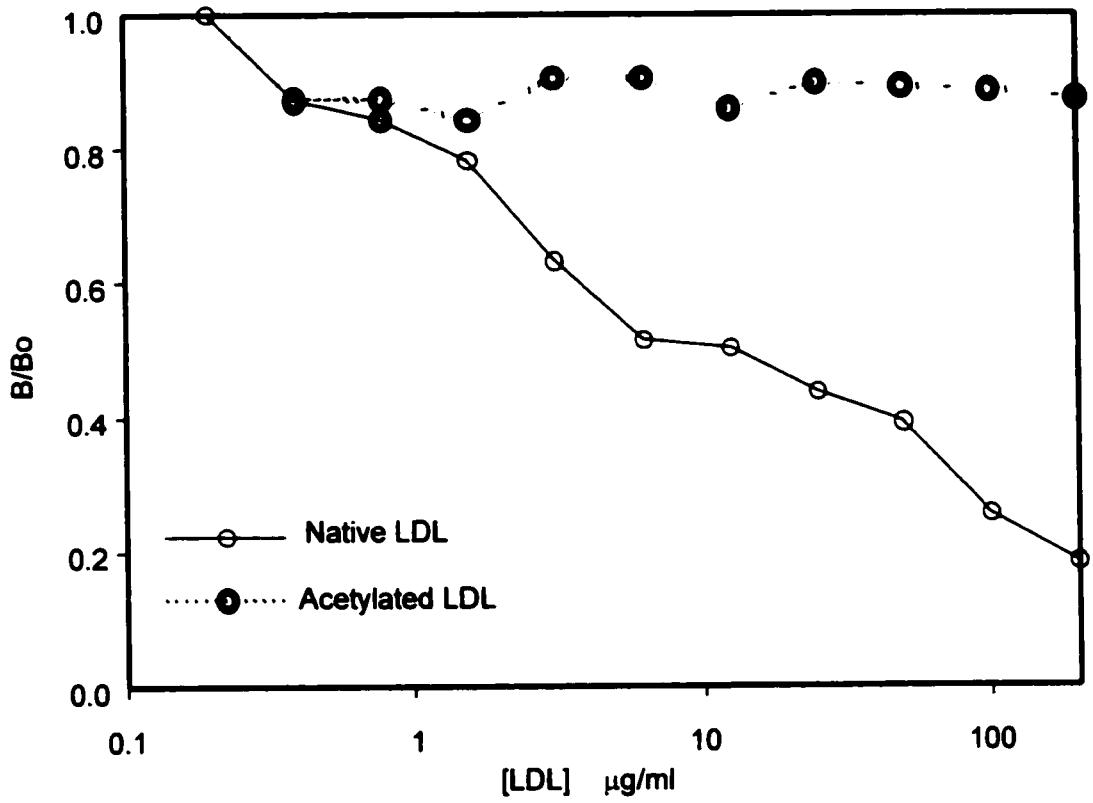
1.0
0.8
0.6
0.4
0.2
0.0
B/Bo
Native LDL
Acetylated LDL
0.1
1
10
100
[LDL] µg/ml

immunoaffinity column. One liter of cultured cells stably transfected with $LDLr^{692}$ were grown in suspension culture over a period of two weeks in media containing 1% serum. After two weeks, the cells were pelleted by centrifugation and the media was passed over a C7 immunoaffinity column. Receptor that was retained on the column was eluted with an acidic buffer and dialyzed overnight in TBS containing 20 mM $CaCl_2$. Aliquots of unpurified media, flow-through and eluted fractions were subjected to SDS-PAGE and immunoblot analysis. A portion of the resultant gel was stained with Coomassie Blue R-250. Figure 2-15 shows that the purified receptor migrated as single species of correct molecular weight (97 kDa), providing strong evidence that it comprises a structurally homogenous population and reacts with the conformation specific anti-LDLr antibody, C7.

Functional analysis of purified $LDLr^{692}$: To assure that a homogenous, correctly folded and fully active receptor was produced; functionality assays were performed. One characteristic of the native LDLr is that it has high affinity binding to LDL. Ligand blot analysis was performed, in order to test the purified receptor's ability to bind LDL. The receptor was subjected to SDS gel electrophoresis under non-reducing conditions and the proteins were transferred electrophoretically to nitrocellulose membrane. The membrane was incubated with biotinylated human LDL, and subsequently incubated with horse radish peroxidase conjugated streptavidin. Figure 2-15 shows that after electrophoresis in the absence of reducing agents and presence of calcium, the purified recombinant receptor bound LDL. The receptor's ability to bind LDL was further tested on a

competitive enzyme linked immunoassay (ELISA). Figure 2-16 shows that normal LDL but not acetylated LDL, could complete with biotinylated LDL for binding to immobolized $LDLr^{692}$. Therefore, $LDLr^{692}$ shows the same specificity as the cell-surface LDLr.

Discussion

The multidomain structure of the LDLr and its central role in cholesterol homeostasis has made it a target protein for experimental studies. In the late seventies, the group of Brown and Goldstein successfully purified the receptor from membranes of bovine adrenal cortex and cultured human cells by using a nonionic detergent (Schneider et al., 1981). The purified protein maintained its ability to bind LDL. Since the introduction of genetic engineering, several investigators have made an effort to produce a recombinant protein in either prokaryotic or eukaryotic systems. Dirlam et al., (1996) produced a truncated LDLr that contained the seven cysteine-rich repeats that comprise the ligand-binding domain, as well as repeat one of the EGF-like domain. Upon expression in a baculovirus system, the protein was secreted from cells and formed multimers on non-reducing SDS-PAGE. The majority of the receptor migrated as an aggregated complex, and no receptor was found at the correct molecular weight. Nonetheless, the purified receptor was able to compete with cell surface receptor present on fibroblasts for the binding of LDL. Simmons et al. in 1997 produced in *Escherichia coli* a soluble fragment of the LDLr containing the ligand-binding domain as a thrombin-cleavable fusion protein. The expression levels of protein were in modest amounts and only 10% of the protein could be folded to a functional conformation. After non-reducing SDS-PAGE of the purified LDLr fragment, the majority of the protein appeared to be aggregated (results not shown).

In this study, several strategies were used in an attempt to produce a soluble, truncated and active receptor. A eukaryotic system was chosen over a bacterial expression system for the following reason. Eukaryotic expression provides a number of modifications that may occur at the post-translational stage, after protein synthesis is complete such as acetylation, phosphorylation and glycosylation. Glycosylation is a post-translational modification that endows a protein with stability and, in some instances, its distinctive properties. We were encouraged by reports of successful expression of proteins in the yeast expression system (Sreekrishna et al. 1989 and 1988). For example, it was shown that human serum albumin could be expressed and secreted from *P. pastoris* and that the recombinant protein exhibited the same 17 disufilde bonds that are present in human serum albumin that is isolated from plasma (Kobayashi et al., 1998). Similarly, cholesterol ester transfer protein, a protein involved in lipoprotein metabolism was also expressed and purified in an active form (Kotake et al., 1996).

Therefore, we proceeded to transform truncated forms of the low density lipoprotein receptor into *P. pastoris*. The vectors that were used contained either the highly inducible alcohol oxidase promoter or the constitutively expressing glyceraldehyde-3-phosphate dehydrogenase promoter, which would guarantee high levels of protein expression. The receptor constructs containing either LDLr amino acid residues 1-331 or 1-692 (Figure 2-17A) were successfully transformed into the *Pichia* genome.

Figure 2-17: Schematic of constructs. A schematic representation of the LDLr with its multidomain structure comprised of the ligand-binding domain, EGF precursor homology domain containing the β-propeller, O-linked sugars, a transmembrane domain and cytoplasmic tail. The various constructs that were expressed in **(A)** *Pichia pastoris* and **(B)** CHO-K1 cells are also shown. The carboxy-terminal tags include an oligohistidine tail (6his) and a c-myc epitope (cmyc).

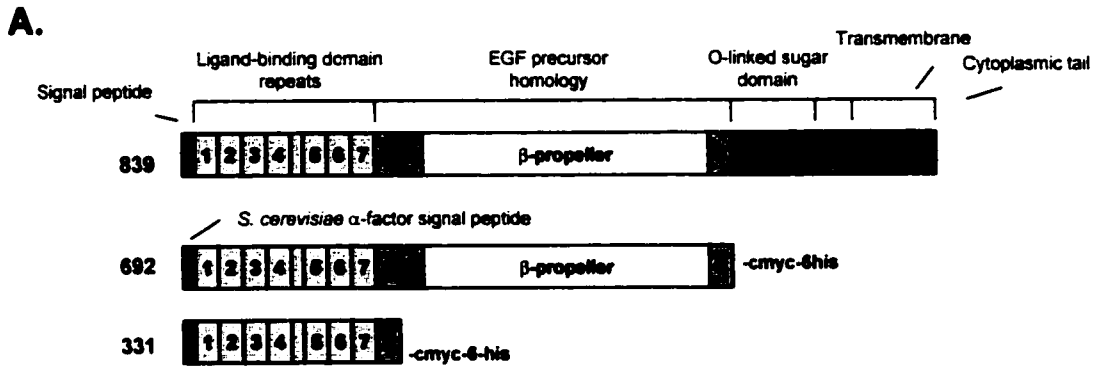
A.
Signal peptide
Ligand-binding domain repeats
EGF precursor homology
O-linked sugar domain
Transmembrane
Cytoplasmic tail
839
β-propeller
S. cerevisiae α-factor signal peptide
692
β-propeller
-cmyc-6his
331
-cmyc-6-his

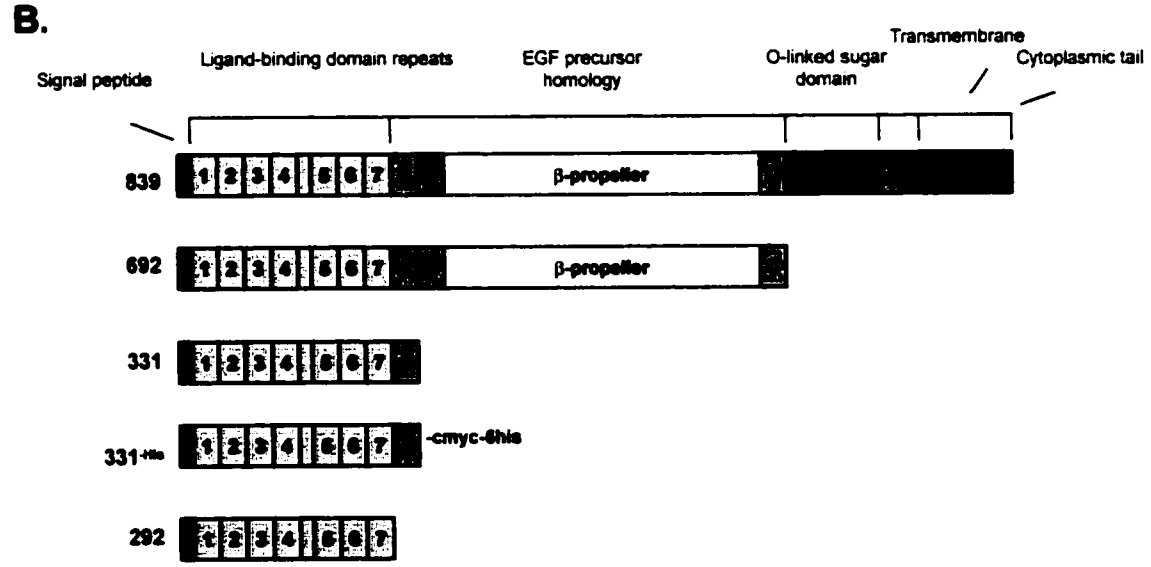
B.
Signal peptide
Ligand-binding domain repeats
EGF precursor homology
O-linked sugar domain
Transmembrane
Cytoplasmic tail
839
β-propeller
692
β-propeller
331
331-His
-cmyc-6his
292

$LDLr^{331}$ appeared to be secreted in high quantities into culture media, unlike $LDLr^{692}$, which was retained in the cells. Most importantly, neither LDLr fragment was recognized by the conformation specific anti-LDLr monoclonal antibody, C7 nor was able to bind LDL. The inability of yeast cells to secrete the more complex of the two receptor constructs, $LDLr^{692}$, implies that it does not contain the cellular environment to fold, process and secrete a functional receptor. There have been examples cited of foreign proteins (e.g. HIV-1 gp120) that are inefficiently secreted from yeast cells due to the complexity of their structure (Romanos et al., 1992). Although numerous proteins have been successfully expressed in *P. pastoris*, not all target proteins produced by this yeast species are functional. Simmons et al. (1997) also were not successful in expressing $LDLr^{292}$ in *P. pastoris*. The ability of *P.pastoris* to express correctly folded foreign proteins appears to be dependant on features inherent in the individual protein.

Following the very limited success with protein expression in the yeast, *Pichia pastoris*, we focused on expression in a mammalian cell line, Chinese hamster ovary cells. This cell line was chosen because many recombinant proteins have been successfully expressed in CHO-K1 cells at high expression levels and also due to the inability of C7 to recognize hamster LDLr. The constructs that were transfected into CHO-K1 cells are summarized in Figure 2-17B. The recombinant $LDLr^{331}$ and $LDLr^{292}$ proteins were found to be extensively heterogeneous in size, forming higher order multimers. Nevertheless, at least some of the aggregates escaped the quality control mechanisms of the cell were secreted. These multimers were able to recognize C7 but were not able to bind LDL. The heterogeneity of the secreted proteins is likely due to the

formation of disulfide-linked homo- and hetero-oligomers. NMR studies have revealed that for repeat one of the ligand-binding domain, only one arrangement of the disulfide bridges appear to be thermodynamically favored over alternatives (Daly et al., 1995 and Djordjevic et al., 1996). The LDLr comprises seven cysteine-rich repeats that have been highly conserved through evolution (Esser et al., 1988). Therefore, disruption in the thermodynamic stability of any one of these repeats would probably result in a nonfunctional protein.

Analysis of $LDLr^{331}$ containing the carboxy-terminal tags, c-myc and oligohistidine tail showed that, unlike the previous two constructs, this one was not able to recognize C7. The epitope tags appear to interfere with the conformation of the ligand-binding domain and create an improperly folded protein. The oligohistidine tag consists of highly charged histidine residues that may chelate calcium ions, causing improper disulfide bond formation. Calcium is also required for the maintenance of the native conformation of the repeats in the ligand-binding domain of the receptor (Van Driel et al., 1987). Studies have shown that each repeat contains a calcium binding site where a single calcium ion is trapped in a octahedral cage formed by four conserved acidic residues and two carbonyl oxygens (Blacklow et al., 1996). Competition for calcium between the receptor ligand-binding domain and the histidine tag could eventually result in a disrupted receptor. Alternatively the carboxy-terminal tags may mask the C7 epitope or possibly interfere with its folding. The histidine tail could intercalate between repeats in the ligand-binding domain and cause misalignment of disulfide bonds or prevent

cysteine residues from forming disulfide bonds, thereby disrupting the overall conformation of the receptor.

Analysis of $LDLr^{692}$ by non-reducing SDS-PAGE revealed a high electrophoretic purity and homogeneity. Unlike any of the other constructs, this purified receptor reflected the behavior of the physiological LDLr of intact cells and membranes in that the LDL binding activity of the receptor required the divalent cation, calcium and was abolished when lysine residues of the LDL were modified by acetylation. The improper folding of receptors that lack the EGF precursor homology domain suggests the necessity of this domain for the production of a fully functional protein. It is possible that the EGF precursor homology domain may assist in the folding of the domain through inter-domain interactions. Even though the first repeat of this domain was expressed in $LDLr^{331}$, it seems that the entire EGF precursor homology domain is required to achieve proper folding of the ligand-binding domain. It is known that domains such as the EGF precursor homology domain that adopt a β-propeller structure are frequently involved in protein-protein interactions (Springer, 1998). Examples of this are also found in the very low density lipoprotein receptor, LDLr-related proteins and nidogen (Springer, 1998). In the case of the LDLr, the predicted β-propeller structure could either mediate interaction with chaperone proteins or directly aid in the folding of the ligand-binding domain. A large number of naturally occurring point mutation in the EGF precursor homology domain have been identified as being responsible for retention of nascent LDLr in the endoplasmic reticulum (Springer, 1998). Furthermore, it is thought that the EGF precursor homology domain participates in the pH-mediated dissociation of lipoprotein-

LDLr complex that occurs following endocytosis (Davis et al., 1987). This indicates functionally important interactions between the ligand-binding domain and EGF precursor homology domains.

In the current study, we successfully produced in CHO-K1 cells, sufficiently high quantities of a functional receptor containing the ligand-binding and EGF precursor homology domains. The soluble receptor can now be used as a tool to examine factors that influence LDL-LDLr interaction.

Chapter III

Components Required for the Proper Folding of the LDLr

Introduction

Protein misfolding is implicated in the pathogenesis of many genetic diseases (Feldman et al., 2000). Most diseases caused by missense mutations and small in-frame deletions affect the conformation of the protein and result in its degradation or aggregation (Jorgensen et al., 2000). Almost fifty percent of the characterized mutations in the LDLr gene lead to mutant proteins that are partially or totally retained in the ER (Jorgensen et al., 2000). However, the specific factors and mechanisms are not known. Unraveling the folding dynamics of the LDLr, a protein with potential complex secondary structure and a high disulfide bond content, should prove insightful in understanding the pathogenesis of conformational diseases such as FH.

Molecular chaperone proteins such as receptor associated protein (RAP) have been implicated in the folding of many members of the LDLr gene family, specifically the VLDLr and LRP. It is a universal antagonist for all ligands that bind to the VLDLr and LRP (Obermoeller et al., 1998 and Sarti et al., 2000). It consists of three homologous domains of which domain one consists of a three-helix bundle. RAP domains 1 and 3 are both receptor-binding but only domain 3 is sufficient to mimic the chaperone-like functions of RAP in cells. RAP domain 2 is a substrate for cAMP-dependent protein kinase but has only low affinity for LRP compared with RAP domains 1 and 3 (Medved et al., 1999). Although RAP has been shown to have very low affinity

for the full length LDLr, it may nonetheless be involved in the folding of truncated forms of the LDL receptor.

Preliminary results in this study suggest that the LDLr may contain domains that facilitate its folding. There are many examples of proteins that undergo domain-assisted folding. Human nerve growth factor (NGF) and members of the neurotrophin family are examples of such proteins (Rattenholl et al., 2001). The ligand-binding repeats of the LDLr and NGF share characteristically similar disulfide-bonding pattern between cysteine residues. NGF is synthesized as pre-pro-protein. The pre-sequences mediate secretion, while the pro-sequence acts as a folding enhancer by promoting folding of the mature protein. This is not unique to the NGF as for a series of proteins, pro-sequences have been demonstrated to stimulate folding of the mature protein. The best known example for pro-sequence-facilitated folding is insulin. Other examples include serine proteases such as α-lytic protease, subtilism, or carboxypeptidase Y (Baker et al., 1992, Eder et al., 1993 and Sohl et al., 1998). These proteins fold very poorly in the absence of their pro-sequences. *In vitro* folding studies of pro-α-lytic protease and pro-subtilisim suggested that the pro-sequences thermodynamically stabilize folding intermediates. In some instances the pro-sequence may act as a scaffold and direct folding intermediates towards the native conformation. Mutations in pro-sequences have led to a structurally altered mature protein by promoting misaligned disulfide bond formation. The role of prosequences as separate polypeptides from the native protein has been studied for the transforming growth factor (TGF) –β1 protein, NGF and activin A (Gray et al., 1990). It

has been shown that TGF-β1 and activin A can be refolded *in vivo* by their pro-peptides *in trans* but yields were significantly reduced compared to renaturation *in cis*.

In this study we independently examined how the molecular chaperone protein, RAP and inter-domain interactions may be involved in producing a homogeneous population of soluble LDLr that is functional and conformationally stable.

Materials & Experimental Procedures

Materials: pCDNA3.1-RAP and anti-RAP polyclonal antibody was kindly provided by Rita Kohen Avramoglu and Dr Zemin Yao, University of Ottawa Heart Institute. Lipofectamine was purchased from Gibco Life Technology. DNA restriction enzymes were purchased from New England Biolabs. Pfu turbo DNA polymerase, QuikChange mutatgenesis kit and T4 DNA ligase were purchased from Stratagene. GST-RAP was provided by Dr. Gerard Vassiliou, University of Ottawa Heart Institute. $LDLr^{692}$ with an oligohisitidine tail was provided kindly by Ann Ngyuen, University of Ottawa Heart Institute. Chicken anti-LDLr polyclonal antibody was purchased from Progen, Heidelberg, Germany.

Vector Constructs:

***$LDLr^{292}$ & $LDLr^{331}$*:** These constructs were described in detail in Chapter II, Materials and Procedures.

W556S mutant: The vector, pCMV5 encoding $LDLr^{692}$ with a oligohistidine tail was used as template to mutate the linker region between repeat two and repeat three of the LDLr EGF precursor homology domain by QuikChange mutagenesis. Two complimentary oligonucleotides with the mutation flanked by unmodified nucleotide sequences were synthesized. The mutagenic primers converted LDLr amino acid residue 556, which encodes for a tryptophan (TGG) into a serine (TCG). The QuikChange site-directed mutagenesis method was performed using PfuTurbo DNA polymerase and a temperature cycler. PfuTurbo DNA polymerase replicates both plasmid strands with

high fidelity and without displacing the mutant oligonucleotide primers. The oligonucleotide primers containing the mutation were extended by temperature cycling following manufacturer's instructions. The PCR products were treated with Dpn1 endonuclease. The nicked vector DNA incorporating the desired mutation was transformed into DH5α competent cells as described previously. Positive colonies were analyzed for the presence of the mutation by restriction digest and sequencing.

LDLr$^{EGF\pm His}$: The vector, pCMV5 encoding the cDNA sequences of the ligand-binding domain and EGF precursor homology domain of the LDLr with and without the six carboxy-terminal histidine residues was used as a template to delete the segment of DNA encoding the ligand-binding domain by inverse polymerase chain reaction (inverse PCR). The reverse and forward primers annealed to the nucleotides encoding the carboxy-terminus of the signal sequence and amino-terminus of the first EGF repeat, respectively. The forward primer included a SalI restriction site, which facilitated the identification of positive transformants. Following PCR cycling, the products were cooled to below 37°C by incubation on ice for two minutes and were treated with 1 μl of DpnI and an additional 0.5 μl of Pfu Turbo polymerase. The reaction mixture was incubated further at 37°C for 30 minutes and at 72°C for 30 minutes. The remaining products were incubated overnight at room temperature with 1 μl of T4 DNA ligase and transformed the following day into DH5α strain of bacterial cells. Positive transformants were analyzed for the absence of the ligand-binding domain by restriction digest and DNA sequencing.

Cell culture:

Transfection: CHO-K1 cells were cultured using Ham's F12 medium containing 10% fetal bovine serum (growth media). For transfection experiments, CHO-K1 cells (100 mm dishes, 10 ml media) were grown to 50-60% confluency and transiently transfected with the expression plasmid encoding human $LDLr^{292}$ or W556S mutant (1-5 μg of DNA) and the expression plasmid containing either human RAP or $LDLr^{EGF+His}$ (1-5 μg). Similar experiments were also conducted using cell lines that were stably expressing $LDLr^{331}$. The transfections were performed using a liposome-DNA delivery method. A DNA solution was incubated with a liposome formulation of polycationic lipids (Lipofectamine) for thirty minutes at room temperature. The DNA-liposome complexes were added to cells and incubated for 4-5 h. After the incubation period, the cells were washed with F12 media without serum (starvation media) and incubated overnight with growth media. The cells were then incubated for two days in starvation media. The cells were lysed as described previously in Chapter II and the media was concentrated 20 fold. The samples were analyzed by immunoblotting, followed by ECL detection.

In some experiments, following transfection of $LDLr^{292}$ by lipofectamine, cells were incubated with starvation media containing 10 μg/ml of purified GST-RAP.

β-propeller antibody: BALB/C female mice were immunized intraperitonealy with 50-100 μg of antigen (a synthetic peptide corresponding to residues 593-608 of LDLr coupled to keyhole limpet hemocyanin) in 100 μl of PBS emulsified in 100 μl of complete Freund's adjuvant. At intervals of at least three weeks, four intraperitoneal boosts were given with antigen emulsified in incomplete Freund's adjuvant. Four weeks

after the last boost the mice were exsanguinated under anesthesia, blood samples were tested for antibody production by ELISA. Microtitre wells were coated with 10 μg/ml of antigen, overnight in PBS. The wells were washed three times with PBS containing 0.025% Tween 20 (v/v) and unoccupied binding sites on the plastic were blocked by a thirty minute incubation with PBS containing 1% bovine serum albumin (BSA). Serial dilutions of sera were added to wells and incubated for 2 h. The wells were washed and bound antibody was detected using anti-mouse IgG-HRP followed by TMB detection.

Results

Role of RAP in protein folding: Receptor-associated protein is a 39 kDa, ER resident protein. It has been identified as assisting in the biosynthesis and intracellular transport of members of the LDLr gene family (Bu, 1998 and Savonen et al., 1999). To examine the potential role of RAP in the proper folding of the ligand-binding domain, we analyzed LDLr expression and secretion in the absence and presence of RAP co-expression. CHO-K1 cells were transiently transfected with cDNA for $LDLr^{292}$ with co-transfection of cDNA for RAP. After two days in starvation media, cells were lysed, and the media was concentrated and analyzed by immunoblotting using the conformation specific anti-LDLr monoclonal-antibody, C7 and a polyclonal-antibody against an epitope within the first three repeats of the ligand-binding domain (IgY). The polyclonal IgY is an antibody that can be analyzed by immunoblotting under reducing conditions while C7 must be analyzed under non-reducing conditions. Figure 3-1B shows an analysis of both the cells and media. Under non-reducing conditions, the soluble LDLr in the absence of RAP is secreted as high molecular weight aggregates, corresponding to trimers and multimers. The aggregates are not dependent on the amount of DNA transfected since even at lower DNA concentrations, the receptor remains secreted as a misfolded protein (Figure 3-2). Under reducing conditions, the multimers disappeared and a distinct band was prevalent at the correct molecular weight of the protein (Figure 3-4, Lane 10). This implies that

Figure 3-1: Immunoblot analysis of media and cells of RAP transfected $LDLr^{292}$ & $LDLr^{331}$ cells. Samples were electrophoresed on 10% polyacrylamide gels under non-reducing conditions and detected using the conformation specific anti-LDLr monoclonal antibody, C7. **(A)** RAP transfection into stable $LDLr^{331}$ cell lines. Lanes 1-4; correspond to media from cells transfected with 15 μg RAP, 9 μg RAP, 15 μg pCMV5 (negative control), 0 μg DNA respectively. Lanes 6-9 correspond to extracts of cells transfected with 15 μg RAP, 9 μg RAP, 15 μg pCMV5 (negative control), 0 μg DNA respectively. **(B)** RAP co-transfection with $LDLr^{292}$. Lanes 1-4; correspond to media from cells transfected with 6 μg RAP, 6 μg RAP & 3 μg $LDLr^{292}$, 3 μg $LDLr^{292}$, 6 μg pCMV5 & 3 μg $LDLr^{292}$ respectively. Lanes 6-9 correspond to extracts of cells transfected with 6 μg RAP, 6 μg RAP & 3 μg $LDLr^{292}$, 3 μg $LDLr^{292}$, 6 μg pCMV5 & 3 μg $LDLr^{292}$ respectively.

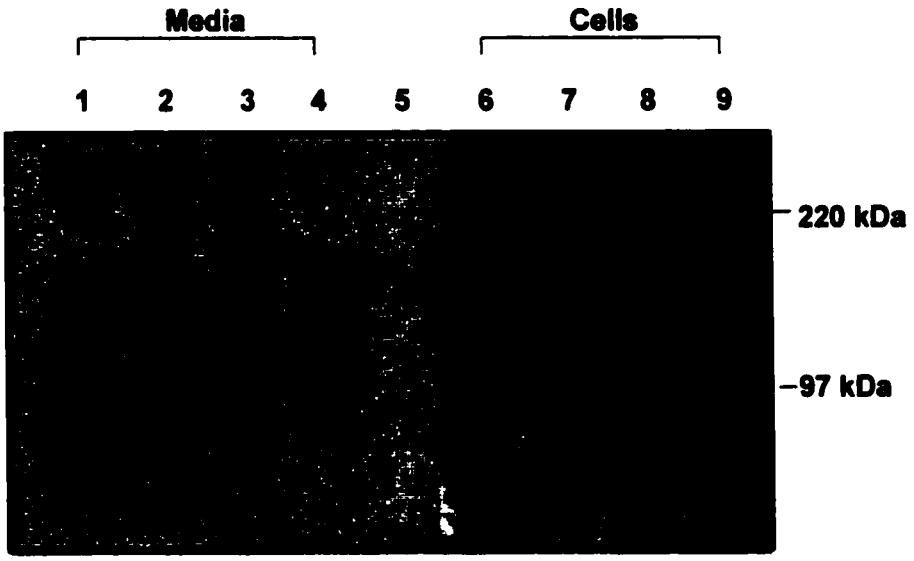

(A) LDLr^{331}

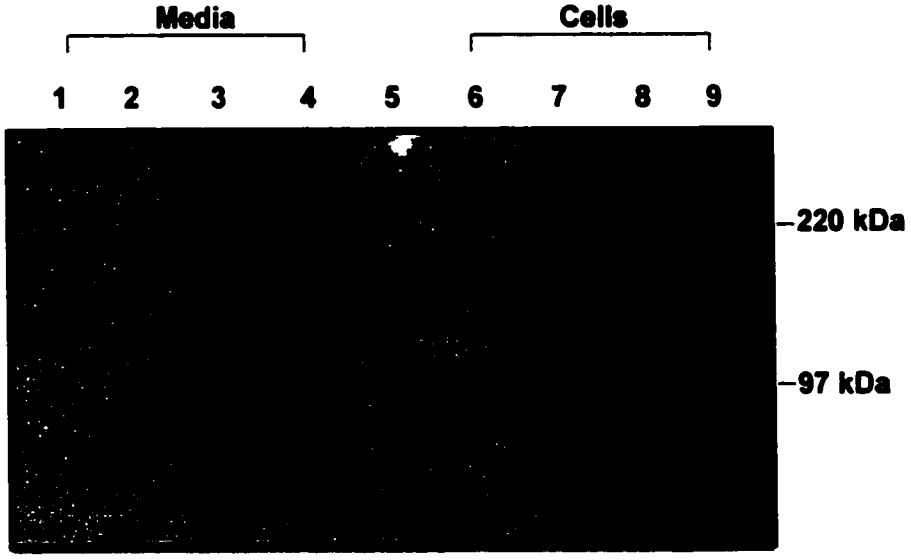

(B) LDLr^{292}

Figure 3-2: Immunoblot analysis of media from LDLr^{292} transfected cells at different DNA concentrations. Samples were electrophoresed on 10% polyacrylamide gels under non-reducing conditions and detected using the conformation specific anti-LDLr monoclonal antibody, C7. Lanes 1-7; correspond to media from cells transfected with 3 μg pCMV5 (negative control), 0 μg DNA, 6 μg LDLr^{292}, 4 μg LDLr^{292}, 2 μg LDLr^{292}, 0.5 μg LDLr^{292}, respectively. Lane 8; Rainbow molecular weight markers.

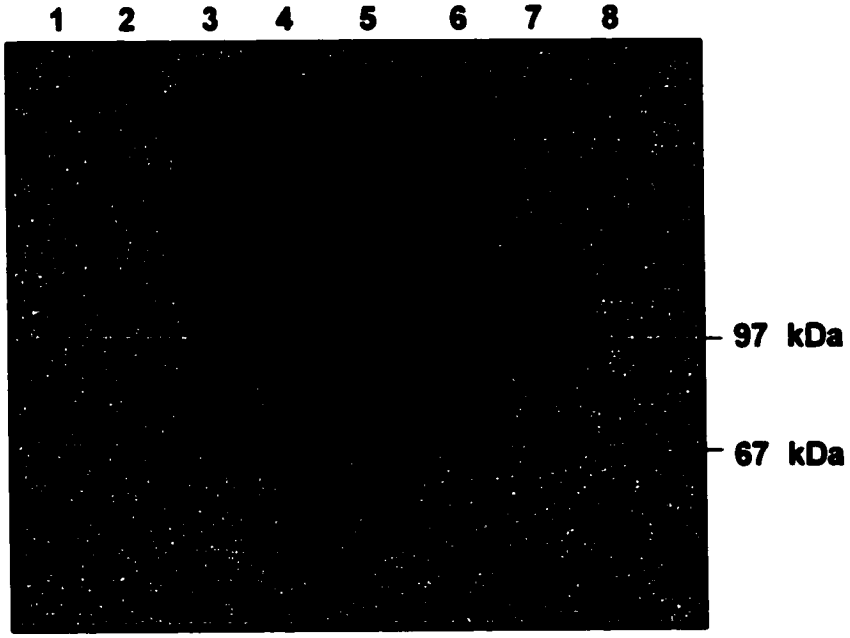

LDLr^{292}

Figure 3-3: Immunoblot analysis of media from RAP & LDLr$^{692/292}$ transfected cells. Samples were electrophoresed on 10% polyacrylamide gels under non-reducing conditions and detected using the conformation specific anti-LDLr monoclonal antibody, C7.

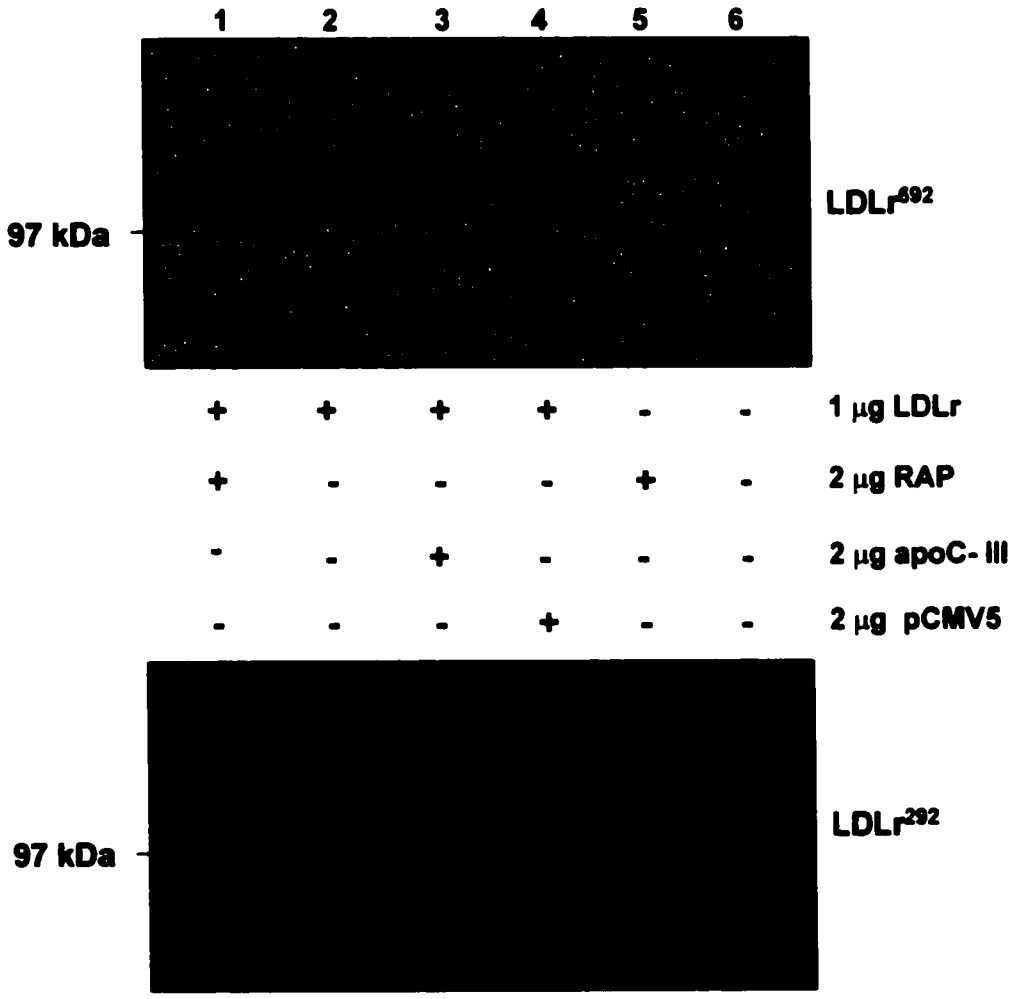
1 2 3 4 5 6
97 kDa
LDLr492
+ + + + - - 1 µg LDLr
+ - - - + - 2 µg RAP
- - + - - - 2 µg apoC-III
- - - + - - 2 µg pCMV5
97 kDa
LDLr292

most of the protein aggregation was due to the presence of molecular disulfide bonds between misfolded receptors or between misfolded receptors and other proteins. In the presence of RAP, these multimers were significantly reduced to yield a predominant band at 92 kDa, both intracellularly and extracellulary. However, no band was present at the correct molecular weight of the receptor (32 kDa) (Figure 3-1B, Lane 2). Moreover, the 92 kDa band did not bind biotinylated LDL on a ligand blot (data not shown). Therefore, RAP may allow the secretion of a more homogeneous population of receptor. To ensure that the effects of RAP could not be mimicked by an unrelated protein, the transfection was repeated with constructs encoding apolipoprotein CIII and $LDLr^{692}$. RAP did not alter the secretion of $LDLr^{692}$ and, more importantly, apolipoprotein CIII did not reduce aggregation of $LDLr^{292}$, implying that the effect of RAP was specific (Figure 3-3). To test this further, we examined the influence of RAP on stably expressing $LDLr^{331}$ cell lines. Similar to the $LDLr^{292}$, these cell lines secrete a heterogeneous population of receptor, which appear to be aggregated and misfolded. Transient transfection of RAP at various concentrations, however, did not appear to reduce the aggregates (Figure 3-1A), even though, in all experiments, RAP expression was confirmed by detection using an anti-RAP polyclonal antibody (data not shown). Although RAP contains a sequence for retention in the endoplasmic reticulum, when overexpressed, RAP can be secreted. To determine if RAP prevents aggregation of $LDLr^{292}$ after the two molecules are secreted, purified RAP protein was added directly to media of $LDLr^{292}$-transfected cells. However, no reduction in aggregated protein was observed (data not shown). Therefore, RAP does not appear to induce its effects extracellularly.

Figure 3-4: Immunoblot analysis of media from LDLr^{292} transfected cells. Samples were electrophoresed on 10% polyacrylamide gels under reducing conditions and detected using an anti-chicken LDLr polyclonal antibody.

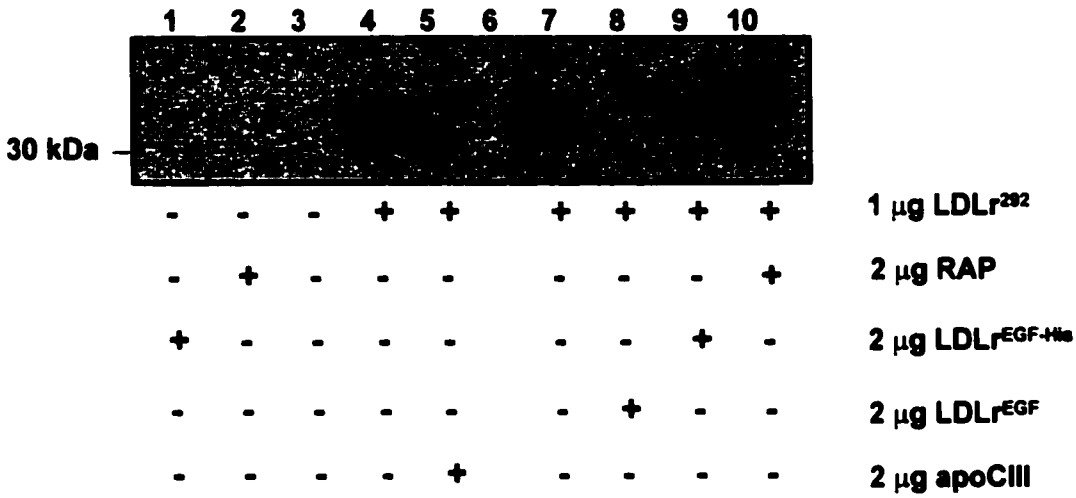
1 2 3 4 5 6 7 8 9 10
30 kDa
- - - + + + + + +
- + - - - - - - +
+ - - - - - - + -
- - - - - - + - -
- - - - + - - - -
1 µg LDLr292
2 µg RAP
2 µg LDLrEGF-His
2 µg LDLrEGF
2 µg apoCIII

Figure 3-5: Agarose gel analysis of PCR amplification product and restriction digest of positive LDLr$^{EGF-His}$ and W556S transformants. **(A)** PCR amplification product of LDLr^{EGF}; Lane 1-12; annealing temperatures 55-77°C (every two degrees), respectively. Lane 14; 1 kb ladder. **(B)** PCR amplification product of W556S mutant. Lane 1-10; annealing temperatures 55-73°C (every two degrees), respectively. Lane 11; 1 kb ladder. **(C)** Restriction digest analysis of purified DNA from positive transformants. Lane 1; uncut. Lane 2: digested with SalI. Lane 3; digested with SmaI. Lane 7; uncut. Lane 8; digested with SalI. Lane 9; digested with SmaI. Lane 10; 1 kb ladder.

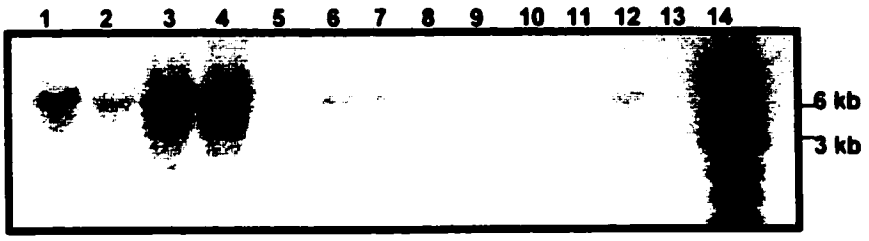

(A) LDLr^{EGF}

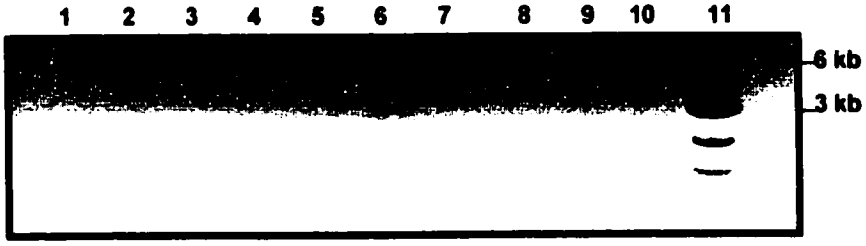

(B) W556S Mutant

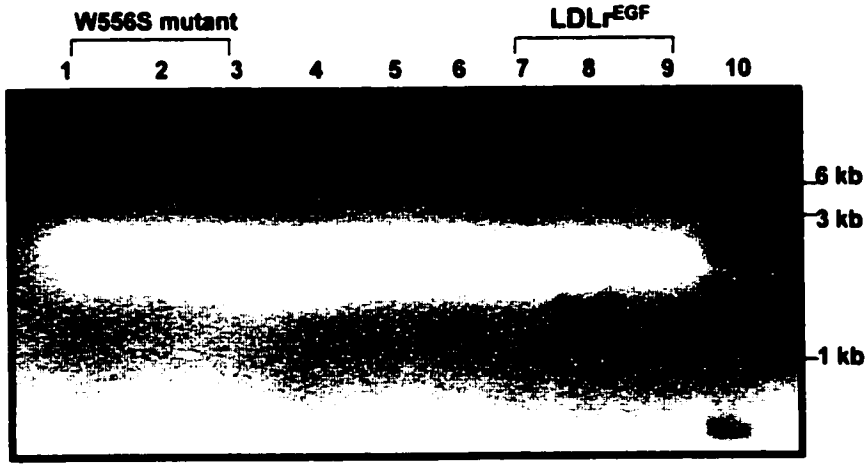

(C) Restriction Digest Analysis

Role of RAP on mutant receptor: We have previously shown that a receptor comprised of the ligand-binding and EGF homology domains is secreted as a properly folded protein that is functional and homogeneous in composition. To further test the role of RAP in the folding of the LDLr, we introduced a mutation into the $LDLr^{692}$ cDNA to convert tryptophan 556 to serine. This corresponds to a natural mutation of the LDLr that results in familial hypercholesterolemia due to retention of the newly synthesized receptor in the endoplasmic reticulum. Figure 3-5B shows an agarose gel analysis of amplified PCR product corresponding to the vector and insert (6.7 kb). Purified DNA from transformants was digested with Sal1 and a restriction site that was removed from the template DNA (Sma1). Sal1 digestion yielded an expected band at 6.7 kb while Sma1 did not digest the DNA (Figure 3-5C, Lanes 1-3). Positive transformants were confirmed to contain the point mutation by DNA sequencing. The mutant was transiently transfected into CHO-K1 cells; cells were lysed and media was collected and analyzed by immunoblotting using C7. However, unlike $LDLr^{692}$, the mutant was retained in the cells as an aggregated protein (Figure 3-6) and was not secreted into the media. Furthermore, a transient co-expression with RAP and the W556S mutant did not induce receptor secretion or reduce intracellular aggregates (data not shown).

Role of the EGF precursor homology domain in folding of the LDLr: Inter-domain interactions may be required for the proper folding of the ligand-binding domain. In order to test this we proceeded to delete the segment of cDNA encoding the ligand-binding domain of $LDLr^{692}$ by inverse PCR. Two primer were synthesized complementary to the nucleotides encoding the carboxy-terminus of the signal sequence

Figure 3-6: Immunoblot analysis of media & cells from W556S mutant transfected cells. Samples were electrophoresed on 10% polyacrylamide gels under non-reducing conditions and detected using the conformation specific anti-LDLr monoclonal antibody, C7. Lanes 1-4; correspond to media from cells transfected with 3 μg W556S, 5 μg W556S, 5 μg pCMV5 (negative control), 0 μg DNA, respectively. Lanes 6-9; correspond to cells transfected with 0 μg DNA, 5 μg pCMV5 (negative control), 5 μg W556S, 3 μg W556S, respectively. Lane 5 & 10; Rainbow molecular weight markers.

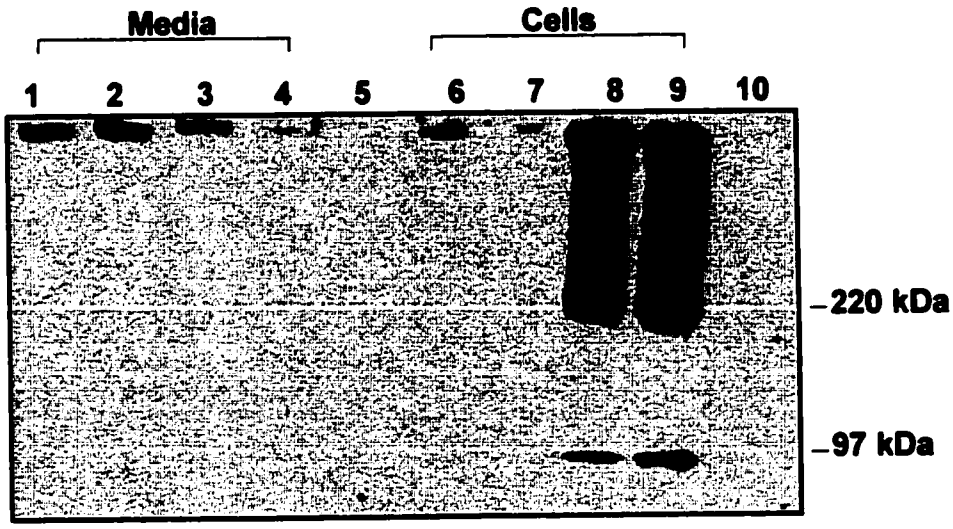

W556S Mutant

and the amino-terminus of the EGF precursor homology repeat one, respectively. The primers contained a restriction site that would allow for the identification of positive transformants (SalI site). The DNA template that was used for the PCR reaction was PCMV5 containing $LDLr^{692}$ with and without an oligohistidine tail. Figure 3-5B shows an amplification product of 6.7 kb after PCR cycling. Figure 3-5C (Lanes 7-9) shows restriction digest analysis of positive transformants using SalI and SmaI. SalI digests the plasmid at two sites while SmaI only digests the plasmid at one unique site. Purified DNA from positive transformants was sequenced to ensure that the sequences encoding the signal peptide were in-frame with those encoding the EGF precursor homology domains. The cDNA of the EGF homology domain was co-transfected with $LDLr^{292}$ into CHO-K1 cells in order to determine if it could act *in trans* as a molecular chaperone protein and assist the proper folding and secretion of the ligand-binding domain. Cells and media were subjected to SDS-PAGE under non-reducing and reducing conditions. Following electrophoresis, the proteins were transferred to nitrocellulose, and immunoblotted with C7, a polyclonal antibody against an epitope within the β-propeller region of the EGF homology precursor domain and an anti-LDLr polyclonal antibody (IgY). The effect of the EGF precursor domain on the secretion of $LDLr^{692}$ was also assessed. Unexpectedly, Figure 3-7 shows that the EGF precursor homology domain containing the β-propeller module, inhibit the secretion of both $LDLr^{692}$ and $LDLr^{292}$. Similarly, transient transfection of $LDLr^{EGF=His}$ into stable cell lines expressing $LDLr^{331}$ also caused an inhibition in the expression of receptor, although not so dramatically (data not shown). However, this inhibition was not specific to the LDLr since co-transfection

of the EGF precursor homology repeats with an unrelated protein, CETP, also caused inhibition in its secretion (Figure 3-8, Lane 4). While this does not exclude a role for the EGF precursor homology domain in domain-assisted folding of the LDLr, it does show that the EGF precursor homology domain as a separate polypeptide, cannot act *in trans* to chaperone the proper folding of the ligand-binding domain. However, it is also plausible that the EGF-precursor domain itself was aggregated within the cells or proteolytically cleaved and therefore could not interact with the ligand-binding domain.

Figure 3-7: Immunoblot analysis of media from $LDLr^{EGF}$ & $LDLr^{692/292}$ transfected cells. Samples were electrophoresed on 10% polyacrylamide gels under non-reducing conditions and detected using the conformation specific anti-LDLr monoclonal antibody, C7.

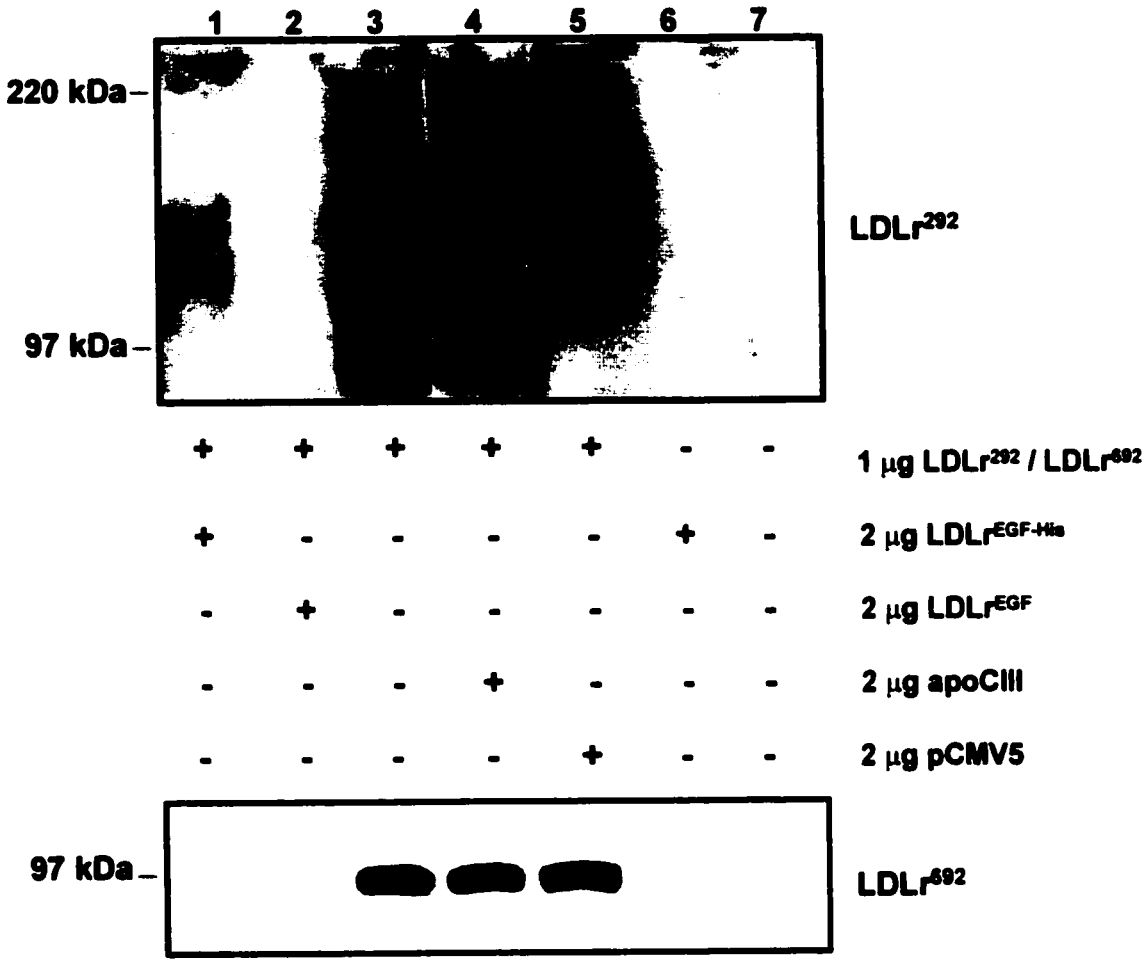
1 2 3 4 5 6 7
220 kDa
97 kDa
LDLr292
+ + + + + - -
1 µg LDLr292 / LDLr692
+ - - - - + -
2 µg LDLrEGF-His
- + - - - - -
2 µg LDLrEGF
- - - + - - -
2 µg apoCIII
- - - - + - -
2 µg pCMV5
97 kDa
LDLr692

Figure 3-8: Immunoblot analysis of media from CETP, LDLr$^{EGF\text{-}His}$ & LDLr$^{292/692}$ transfected cells. Samples were electrophoresed on 10% polyacrylamide gels under reducing conditions and detected using anti-CETP monoclonal antibody, TP2.

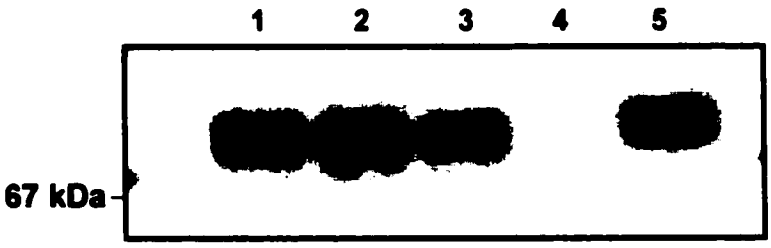

0	0	0	0	2	pCMV5 (μg)
0	0	0	2	0	$LDLr^{EGF-His}$ (μg)
2	2	1	1	1	CETP (μg)
0	1	0	0	0	$LDLr^{692}$ (μg)
1	0	2	0	0	$LDLr^{292}$ (μg)

Discussion

Similar to other proteins destined for the plasma membrane, the LDLr probably folds within the lumen of the endoplasmic reticulum (ER) (Ellis and Hartl, 2000 and Netzer and Hartl., 1998). The ER plays an important role at the start of translation. The intralumenal milieu contains a specialized environment, replete with a variety of folding catalysts. A glutathione redox buffer holds the redox state of the ER more oxidizing than that of the cytosol to allow disulfides to form and rearrange (Frydman et al., 1994). Folding catalysts such as protein disulfide isomerase (PDI) accelerate slow chemical steps and catalyze disulfide formation and rearrangement (Gilbert et al., 1998). Molecular chaperone proteins such as glucose regulated stress protein (Grp78) also known as heavy chain binding protein (BiP) prevent proteins from aggregating (Gething, 1999). For most proteins the existence of this quality control system ensures that only correctly folded proteins exit the ER. Those that are retained are normally degraded or acted upon by proteins that aid in their attaining conformational stability. Many *in vitro* folding studies indicate that the tendency of polypeptides chains to misfold increases significantly with their complexity, whereas spontaneous folding is usually efficient for small single domain polypeptides (Netzer and Hartl, 1997). The folding and maturation of newly synthesized LDLr is most likely a dynamic process that involves a constant trial and error, especially in the formation of correct disulfide bonds. Rearrangement of disulfide bonds during the normal folding process is suggested by the observation that misfolded low density lipoprotein receptor related protein containing extensive

intermolecular disulfide bonds can be refolded into functional monomeric LRP (Obermoeller et al., 1998). These results suggest that the ER possesses all the factors and machinery necessary to convert LRP molecules from misfolded states to correctly folded states.

Amongst these factors are chaperone proteins, such as RAP. RAP interacts with high affinity to certain members of the LDLr-like receptors including LRP and VLDL receptor (Obermoeller et al., 1998, Sato et al., 1999 and Mikhailenko et al., 1999). The role of RAP in preventing protein aggregation and misfolding has been studied extensively in LRP and VLDLr. Studies with truncated forms of LRP showed that within the ER, RAP associates with LRP upon receptor synthesis and assists in folding and trafficking (Obermoeller et al., 1998). In addition to promoting folding, RAP also regulates ligand-binding to LRP as a means of preventing premature ligand interactions with the receptor within the early secretory pathway. The role of RAP in the maturation and trafficking of LRP is also supported by gene knockout studies, which demonstrate that cells lacking RAP exhibit ER-retention of aggregated LRP and a 75% reduction in functional LRP (Willnow et al., 1995 and Willnow et al., 1996). Studies in RAP knockout mice have indicated that RAP may play a role in the biogenesis of the VLDL receptor, since VLDL receptor transport to the cell surface was completely blocked in heart muscle cells of RAP knockout mice. Savonen et al., (1999) showed using intracellular crosslinking techniques that RAP was associated with newly synthesized VLDL receptor. In the absence of RAP co-expression, newly synthesized VLDL

receptor exhibited slower trafficking along the early secretory pathways, most likely due to misfolding of the receptor.

In contrast it has been shown that binding of RAP to the LDLr is much weaker (Mikhailenko et al., 1999). However, no investigators, to date, have examined the role of RAP on truncated forms of the LDLr. Our interest in the function of RAP in LDLr folding was sparked by Obermoeller et al., (1998) who showed that minireceptors of LRP in the absence or RAP co-expression yielded high molecular weight aggregates of misfolded LRP when examined under non-reducing SDS-PAGE. These observations were similar to the aggregation that was seen in this study with $LDLr^{331}$ and $LDLr^{292}$. In the absence of RAP, the receptor migrated as aggregated multimers that were not able to bind LDL. However, co-transfection of $LDLr^{292}$ with RAP appeared to limit aggregation of the protein. A single band was prevalent at 92 kDa on non-reducing SDS-PAGE that was immunoreactive with C7 but was not able to bind LDL. The 92 kDa band was reduced to monomers when analyzed on SDS-PAGE with β-meracaptoethanol, which implies that the aggregation was due to the formation of intermolecular disulfide bonds between misfolded receptors or between misfolded receptors and other proteins. Co-transfection of RAP into stable cell lines expressing $LDLr^{331}$ did not reduce aggregation of the protein. Two possible explanations are that EGF repeat one within $LDLr^{331}$ could inhibit binding of RAP to the receptor or that stable cell lines have higher expression of aggregated receptor.

To further examine the role of RAP in LDLr trafficking, we proceeded to create a naturally occurring mutant receptor. The mutant receptor contained a missense mutation

that caused a tryptophan to serine substitution at amino acid position 556 (W556S) in the receptor protein. About 12% of FH in Denmark is caused by this W556S mutation (Jorgensen et al., 2000). Unlike $LDLr^{692}$, which was secreted, non-aggregated and functional, the W556S mutant was retained within the cells, aggregated and not functional. It has been shown for many proteins that mutations, which disrupt folding often result in receptor molecules that are retained in the ER or are transported slowly to the Golgi complex and the cell surface (Carrell and Lomas, 1997). The mechanism responsible is not well understood, but it is thought to involve a quality-control step that only permits proteins recognized as being properly folded to proceed to the Golgi complex, while misfolded proteins are retained and ultimately degraded (Beissinger and Buchner, 1998). Since the W556S mutant was retained in the ER we proceeded to test whether RAP could assist in the trafficking of the mutant by co-transfecting RAP and the W556S mutant into CHO-K1 cells. However, the mutant still remained aggregated and retained within the cells. Therefore, this study was not clearly able to delineate the exact role of RAP in LDLr trafficking. Further studies that involve the monitoring of the kinetics of aggregate formation by metabolic labeling and immunoprecipatation are needed to verify the exact role of RAP in LDLr folding. However, due to the lack of an antibody that could successfully immunoprecipatate the aggregates, we were unable to perform these experiments.

One commonality between the mutant W556S and the aggregated receptors ($LDLr^{331}$ & $LDLr^{292}$) is that each lack or contain an altered EGF precursor homology domain. The W556S mutant contains an amino acid substitution in one of the conserved

YWTD repeats of the β-propeller while $LDLr^{292}$ / $LDLr^{331}$ do not contain the β-propeller domain. Deletion experiments suggest that the β-propeller and/or EGF repeats are important for proper exposure of LDL binding sites (Springer, 1998). The β-propeller is thought to allow the EGF precursor homology domain to adopt a more compact, three-dimensional structure thereby causing amino-terminal and carboxy-terminal module neighbors to come into close proximity (Springer, 1998). It may also facilitate folding of the ligand-binding repeats through inter-domain interactions. To address this question, we proceeded to clone and co-express the entire EGF precursor homology domain with $LDLr^{292}$ in CHO-K1 cells. The rationale was that the EGF domain as a separate polypeptide would act as a chaperone protein and assist in the formation of correct disulfide bonds, thereby producing a homogeneous population of functional receptors. However, unexpectedly the EGF domain entirely inhibited the secretion of the receptor. The receptor was not C7-immunoreactive within the cell or extracellularly. It was also not detected with the chicken polyclonal anti-LDLr antibody, IgY (Figure 3-4, Lanes 8 & 9). Co-expression of $LDLr^{EGF}$ with either $LDLr^{692}$ or $LDLr^{331}$ also inhibited protein secretion. The effects of the $LDLr^{EGF}$ were not specific to the LDLr since this domain also inhibited the secretion of an unrelated protein, CETP. Therefore, the EGF homology domain as a separate polypeptide does not facilitate the folding of the ligand-binding domain but may, nevertheless, exert its affects when affixed to the ligand-binding domain. These results parallel the prosequence of human nerve growth factor, which promotes the folding of the mature protein only *in cis* (Rattenhol et al., 2001). Experiments investigating the *in trans* refolding of NGF were unsuccessful. The

investigators concluded that the propeptide was either proteolytically degraded or highly aggregated. However, it should be noted that the prosequence in NGF precedes the mature protein whereas, in the LDLr the EGF precursor homology domain follows the ligand-binding domain. At present, more studies are being performed to further elucidate the mechanism by which the EGF precursor domain stimulates folding of the ligand-binding domain.

In this study, we broached the subject of receptor folding in relation to chaperone proteins and inter-domain interactions. Although we were not able to completely elucidate the roles of RAP and inter-domain interactions in the proper folding of the LDLr, we did show that RAP could promote the secretion of a more homogeneous population of $LDLr^{292}$ proteins. Moreover, while the EGF precursor homology domain does appear to facilitate the folding of the LDLr ligand-binding domain, it cannot act *in trans*.

Chapter IV

The Kinetics of LDL-LDLr Interaction

Introduction

The affinities and kinetics of lipoprotein interaction with the LDLr have been determined from studies of binding of LDL to the *in situ* receptor. However, these results could be influenced by lattice effects, caused by clustering of LDL receptors in coated pits (Chappell el al., 1991). A number of other factors can also influence LDL-LDLr interactions including ligand conformation, cell surface proteoglycans and other unknown cellular proteins. To examine the LDL-LDLr interaction in an isolated system without the influence of steric hindrance and other cell components, a recombinant human LDLr was used to determine the kinetics of binding by surface plasmon resonance (SPR).

SPR is an optical technology that detects refractive index changes at the surface of a sensor chip, which is lined with a thin gold film on the flat surface of a prism (Jonsson et al., 1992, Schuck, 1997 and Edwards et al., 1995). Plane polarized light passed through the prism at a critical angle will be totally internally reflected (TIR) and no light will pass through. Although no light passes out of the prism in TIR, the electric field at TIR penetrates the gold and can interact with free electron constellations in the gold surface. The incident light photons are converted (absorbed) into surface plasmons. Light and electron densities have wave and particle properties; "plasmon" is the particle name for the electron density waves, just as "photon" is the particle name for light waves.

Plasmons have a characteristic momentum determined by factors that include the nature of the conducting film and the properties of the medium on either side of the film. Resonance (i.e. transformation of photons into plasmons) occurs only when the wave momentum of the light in the plane of the sensor surface matches that of the surface plasmon. The resonance causes an energy loss in the reflected light, which is visible as a sharp minimum in the angle-dependent reflectance. Plasmons in the surface film create an electric field called the evanescent field that extends into the medium on either side of the film. The velocities of the plasmons change with the properties of the medium on either side of the conducting film. When the analyte concentration at the sensor surface changes, the velocity of the surface plasmons is altered, and the incident light angle at which resonance occurs shifts. It is this shift that is experimentally the primary recorded quantity and eventually leads to a typical sensorgram.

SPR has several intrinsic features that allow for label-free, real-time monitoring of interactions (Fivash et al., 1998 and Fisher and Fivash, 1994). The basic experimental protocol for examining the binding interaction between lipoprotein and LDLr can be summarized as a four step process: (a) capture the receptor (b) inject the ligand, and record a real-time interaction curve; (c) perform step (b) using a series of concentrations of the ligand; and (d) choose the appropriate kinetic model and fit the raw data to extract rate-constant estimates. There are a number of factors that can influence the validity of kinetic measurements (Fisher and Fivash, 1994). The list of factors include: purity and homogeneity of analyte and ligand, non-specific binding, formation of specific multimers, the valency of the interaction, limitation on mass transfer of analyte to and

from the surface, efficiency of regeneration of the surface after each analysis cycle and matrix effects. In this study, all these parameters were considered and by varying experimental conditions we were able to control for them independently.

Materials & Experimental Procedure

Materials: All chemicals were purchased from Sigma and were of analytical grade. All enzymatic kits were purchased from Boehringer Mannheim. Paragon lipoprotein electrophoretic kit was supplied by Beckman. Pre- cast 3-8% Novex gels were purchased from Invitrogen. Molecular weight calibration kit was purchased from Pharmacia. Sensor chips were purchased from Biacore Inc.. BIAevaluation 2.0 software was provided by Biacore, Inc..

Cell culture & transfection: The vector pCMV5 containing the extracellular domain of the LDL receptor ($LDLr^{692}$) was transfected into CHO-K1 cells and stable cell lines were produced as described in Chapter II, Materials and Experimental Procedures. The LDLr was purified from CHO media by immunoaffinity chromatography as described previously.

Isolation of LDL: LDL were isolated from fresh plasma of fasting normolipidemic or hypertriglyceridemic donors by sequential centrifugation ($1.019<d<1.063$ g/ml) (Havel et al., 1955). A mixture of preservatives was added to the freshly drawn blood; final concentrations were 0.05% EDTA, 0.05% NaN_3 and 0.2 mM PMSF. The plasma was centrifuged at 8°C, 40 000 rpm for 28 h using a 55.2 Ti rotor. The top layer of VLDL was removed, while the bottom infranatant solutions were pooled and adjusted to a density of 1.019 g/ml using dry KBr. The tubes were spun in a centrifuge at 8°C, 40 000 rpm for 28 h to float IDL. The IDL was removed and the bottom infranatant solutions were adjusted to a density of 1.063 g/ml using dry KBr and spun again at 8°C, 40 000

rpm for 28 h to isolate LDL. The LDL was dialyzed in PBS containing 0.05% EDTA, 0.05% NaN_3 and 0.2 mM PMSF and filtered using a 0.45 μm filter.

LDL characterization: *Composition.* Total cholesterol, free cholesterol, triglycerides and phospholipids were determined enzymatically using Boehringer Mannheim kits and manufacturer's suggested procedures. LDL protein was measured according to Markwell et al. (1978). *Charge & Mobility.* Electrophoretic mobilities were determined by electrophoresis on precast 0.05% agarose gels. Samples (6 μg protein) were electrophoresed at 100 Volts for 30 min. at 25°C in a barbital buffer, pH 8.6. After electrophoresis, the gels were fixed in a solution of ethanol-acetic acid-water (60:10:30) (v/v/v), oven dried (80°C for 1 h) and stained (5 min) with Sudan Black B lipid stain. *Particle Size.* The homogeneity and hydrodynamic diameters of the particles were estimated by non-denaturing gradient gel electrophoresis using precast 3-8% gels followed by Coomassie Blue staining. The sizes were compared to reference globular proteins (17.0 nm; thyroglobulin, 12.2 nm; ferritin, 10.4 nm; catalase, 8.2 nm; lactate dehydrogenase, and 7.1 nm; albumin).

Apolipoprotein E-dimyristoylphosphatidylcholine (DMPC) complexes: ApoE-DMPC complexes were a kind gift from Dr Karl Weisgraber at the Gladstone Institute of Cardiovascular Disease.

Surface plasmon resonance: All measurements were performed using a BIACORE 1000 biosensor system. Purified $LDLr^{692}$ at a concentration of 10 μg/ml in 10 mM sodium acetate pH 4.5 was immobilized on a research grade F1 sensor chip using the amine coupling kit supplied by the manufacturer. Approximately 100 resonance units

(RU) of LDLr were immobilized under these conditions, where 1 RU corresponds to an immobilized protein concentration of approximately 1 pg/mm^2 (Stenberg et al., 1991). Unreacted moieties were blocked with ethanolamine. All measurements were carried out in HEPES-buffered saline, which contained 10 mM HEPES, pH 7.4, 150 mM NaCl, 1.5 mM $CaCl_2$ 0.005% P-20. Analysis was performed at 25°C and at a flow rate of 5 µl/min for the determination of on-rates and off-rates.

Surface plasmon resonance data analysis: Association and dissociation rate constants were calculated by non-linear fitting of the sensorgram using the BIAevaluation 2.0 software. Fitting experimental data to models in BIAevaluation relies on two mathematical steps. The first is to generate rate equations for the model used, the second is to find values for parameters in the rate equation that best fit the experimental data (curve fitting). Curve fitting in BIAevaluation relies on the Marquardt-Levenberg algorithm (O'Shannessy et al., 1993), which optimizes parameter values by minimizing the sum of the squared residuals. The residuals are the difference between the calculated and experimental curve at each point. The algorithm is an iterative process that begins with an initial value for each parameter in the equation. These parameters are defined in the conformational model, either as constants or as values at defined points on the experimental curve (eg. Ymax, Xmin). The fitted curve is generated for each iteration of the fitting algorithm by calculation from the rate equations for the model using the current set of parameter values. In kinetic systems, rate equations are fundamentally differential equations (the rate is the differential of response with respect to time dR/dt). For a number of models, the differential rate equations can be integrated to give

equations from which the response against time can be calculated directly. Analytical integration is used in BIAevaluation for models where the rate equations can readily be integrated, to give rapid fitting of the data. Described below are the rate equations for the conformational change model.

Conformational change model: $\mathbf{A + B \rightleftharpoons AB \rightleftharpoons ABx}$

A = analyte (injected)

B = ligand (immobilized on sensor chip)

AB = complex formed by binding A to B

ABx = complex formed by conformational change from AB

RI = bulk refractive index contribution (RU)

$\mathbf{k_{a1}}$ = association rate constant for A+B→AB ($M^{-1}s^{-1}$)

$\mathbf{k_{d1}}$ = dissociation rate constant for AB←A+B (s^{-1})

$\mathbf{k_{a2}}$ = forward rate constant for AB→ABx (s^{-1})

$\mathbf{k_{d2}}$ = backward rate constant for AB←ABx (s^{-1})

Rate equations for conformational change model:

A = Concentration

B(0) = Rmax

$dB/dt = -(k_{a1}*A*B \times k_{d1}*AB)$

AB[0] = 0

$dAB/dt = (k_{a1}*A*B \times k_{d1}*AB) \times (k_{a2}*AB \times k_{d2}*ABx)$

ABx(0) = 0

$dABx/dt = (k_{a2}*AB \times k_{d2}*ABx)$

Total response:

AB + ABx + RI

Evaluation of the goodness of fit: For each set of residual, three statistical values were calculated: standard deviation of the residual, X^2 and standard error.

Results

Characterization of the LDL: The total lipid composition (cholesterol, triglyceride and phospholipids) of the LDL isolated from normolipidemic and hypertriglyceridemic patients is presented in Table 4-1. Compared to normal LDL, HTG-LDL was relatively enriched in triglycerides and depleted in both free and esterified cholesterol. HTG particles were also smaller in size as seen by the greater mobility on non-denaturing 3-8%-PAGE (Figure 4-1). The overall exposed surface charge of LDL isolated from normolipidemic patients relative to HTG patients was assessed by agarose gel electrophoresis as illustrated in Figure 4-2. On agarose gel electrophoresis, HTG-LDL exhibited a faster mobility relative to normal LDL. This faster mobility implies an increase in exposed net negative charge on surface of the particles. Overall, the HTG-LDL exhibited properties similar to what has been observed by other investigators (Marcoux et al., 1998, Dachet et al., 1995 and Redgrave and Carlson, 1979).

Kinetic analysis of LDL-LDLr interaction by surface plasmon resonance:

Conditions for binding: To perform binding studies using the purified receptor, it was necessary to covalently bind the receptor to a derivatized gold surface suitable for use in the optical biosensor. A number of sensor surfaces are available from BIACORE, each with different surface properties. The coupling chemistry involved activating the sensor surface carboxyl groups with N-hydroxysuccinimide (NHS) / N-ethyl-N'-(3-dimethylaminopropyl) carbodiimide hydrochloride (EDC). The most frequently used sensor chip (CM5) contains ~100 nm dextran hydrogel derivatized with carboxyl groups.

Figure 4-1: Non denaturing gradient gel electrophoresis. LDL isolated from hypertriglyceridemic patients and normolipidemic patients were subjected to electrophoresis on 3-8% precast Novex gels. Samples were stained with Coomassie Blue, protein stain. Lanes 1; normolipidemic LDL. Lane 2; HTG- LDL. Lane 3; Size standards.

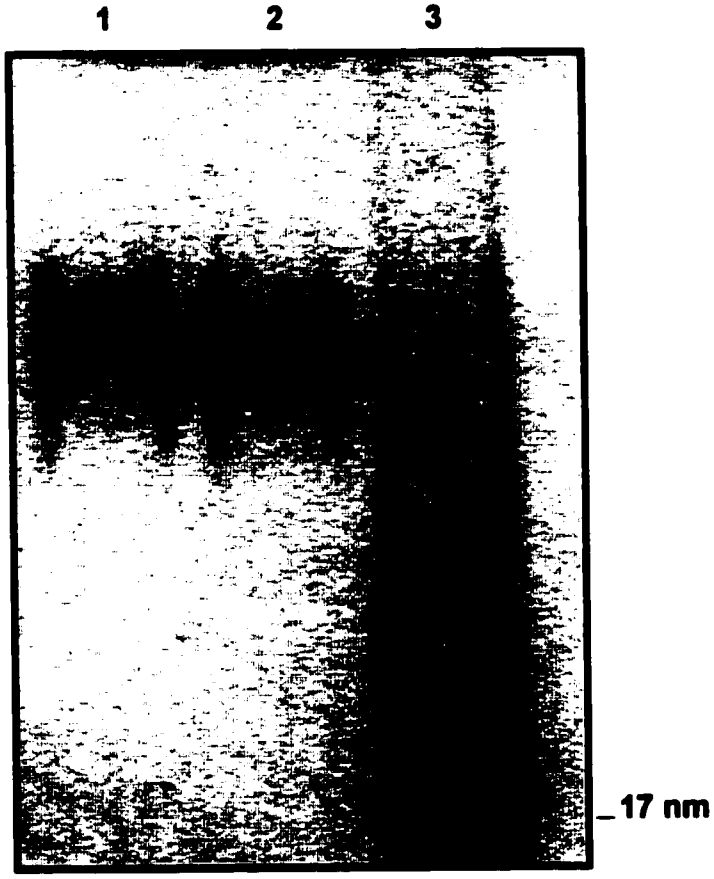
1
2
3
17 nm

Figure 4-2: Agarose gel analysis. LDL isolated from hypertriglyceridemic patients and normolipidemic patients were subjected to electrophoresis on 0.5% agarose gels. Samples were electrophoresed at 100 Volts for 30 min. and stained with Sudan Black B lipid stain. Lanes 1-3; HTG- LDL. Lane 4; normolipidemic LDL.

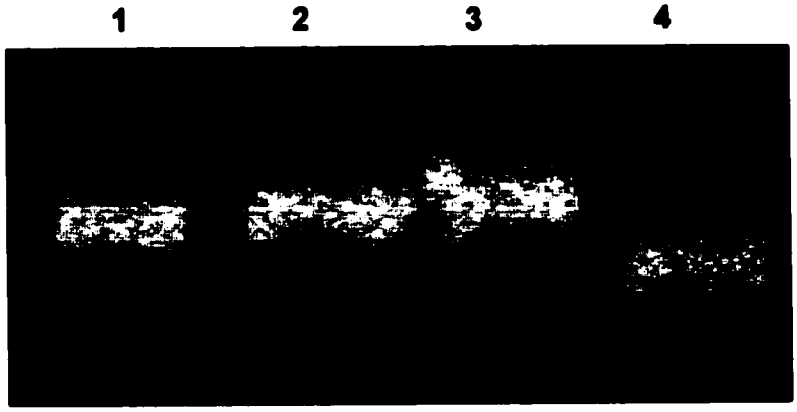

origin

Table 4-1: Mass percentage composition of LDL and HTG-LDL. TG; triglyceride. FC; free cholesterol. CE; cholesteryl ester.

	n	TG	FC	CE	PL	ApoB
LDL	3	11.2±1.9	2.6±0.3	35.2±2.3	24.0±1.4	27.0±1.9
HTG-LDL	3	21.1±0.9	5.0±1.1	25.2±1.3	21.2±2.1	24.7±1.5

However for our studies, the CM5 chip showed unacceptable non-specific binding and was not suitable. The absence of any non-specific binding was observed when a short dextran sensor chip (F1) was used with a minimum of 100 RU of receptor coupled and with 12 minutes of EDC/NHS activation. An analysis cycle normally consists of LDLr capture, LDL binding to the receptor and surface regeneration. The LDLr surface was typically stable for at least 3-4 regenerations using a 0.05% SDS, 350 mM EDTA mixture. To ensure restoration of the LDLr conformation and surface capacity, every injection of SDS/EDTA was followed by a six-minute injection with 20 mM $CaCl_2$ in running buffer.

Reference surface: A reference surface can dramatically improve the quality of the binding data by correcting for artifacts such as bulk refractive index changes, matrix effects, nonspecific binding, injection noise and baseline drift. In this study, two reference surfaces were used, the first surface was simply blocked with ethanolamine and the second surface had immobilized IgG (Figure 4-3). Both surfaces were treated with the same immobilization conditions used for the active surface in order to ensure similar dextran activation in all flow cells. Figure 4-3 shows that there was negligible binding of ligand to either of the reference surfaces.

LDLr binding specificity: LDL isolated from a normolipidemic patient was passed over the LDLr surface at a flow rate of 10 µl/min. The LDL bound to the receptor giving a response of ~100 RU at 150 seconds (Figure 4-4). It is believed that particles may

Figure 4-3: Non-specific and specific binding of LDL to F1 sensor chip. 50 nM of LDL was injected over F1 sensor chip coupled to purified LDLr, ethanolamine or Se155-4 IgG.

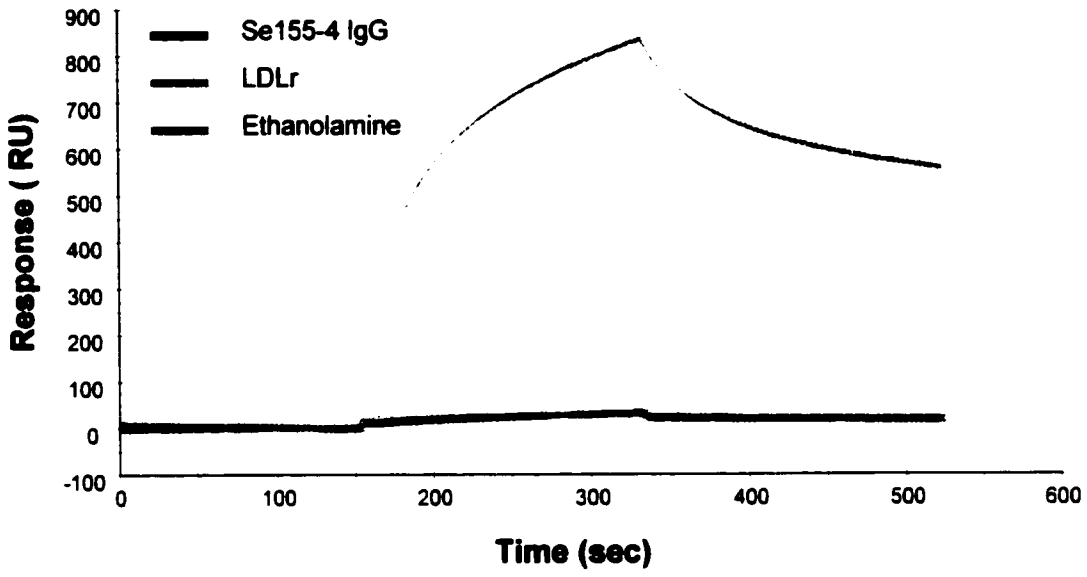
Se155-4 IgG
LDLr
Ethanolamine
Response (RU)
900
800
700
600
500
400
300
200
100
0
-100
0
100
200
300
400
500
600
Time (sec)

Figure 4-4: Sensorgram for binding of acetylated LDL and normal LDL to LDLr. LDLr was coupled to a sensor chip. Either 20 nM LDL or 20 nM acetylated LDL was passed over the chip at a flowrate of 5 µl/min using HEPES running buffer. The sensor chip was regenerated using 0.01% SDS and cleaned with 0.01% SDS and 100 mM HCl.

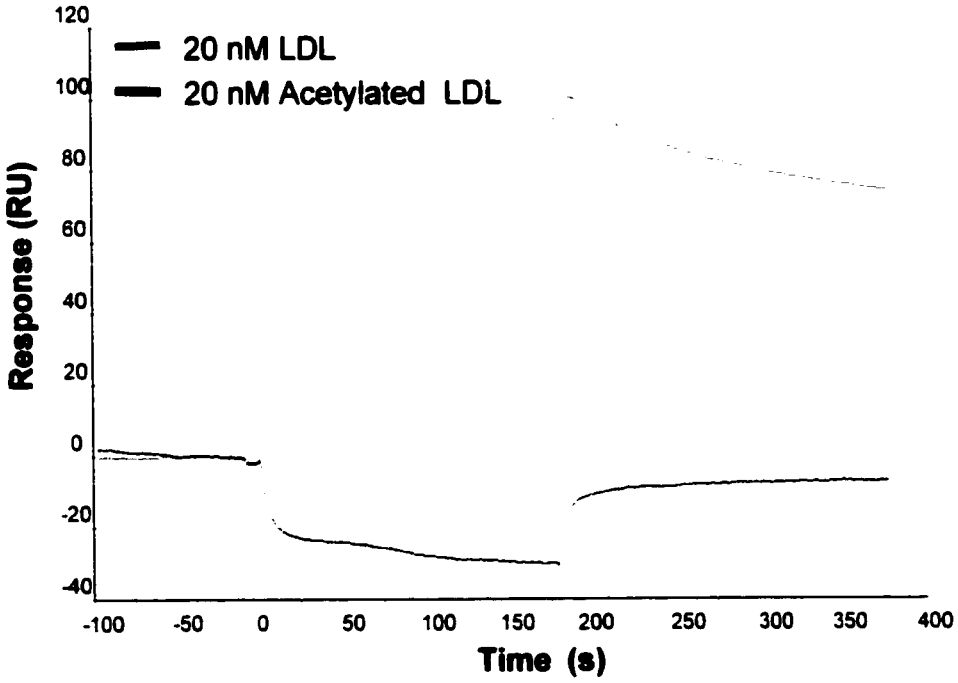
20 nM LDL
20 nM Acetylated LDL
Response (RU)
120
100
80
60
40
20
0
-20
-40
-100
-50
0
50
100
150
200
250
300
350
400
Time (s)

interact through an ionic association between acidic residues present on the LDLr surface and basic charges present on apoB100 of LDL. Abolition of the positive charges of apoB100 on LDL by acetylation of lysine residues renders the particles unable to associate with the LDLr on cultured fibroblasts (Pitas et al., 1992). Acetylated LDL passed over the LDLr surface on the sensor chip was unable to bind the receptor, which confirms the physiological specificity of the interaction (Figure 4-4).

Model fitting: The association and dissociation data contained in BIACORE sensorgrams can be fitted to various interaction models for the derivation of rate and affinity constants. Careful experimental design is crucial for the accurate determination of these constants. The data were fitted to a number of models. The simplest of these models, the one to one model, implies a 1:1 (Figure 4-5) interaction between ligand and immobilized receptor. For this model to fit accurately, the injected component or analyte should be homogeneous with respect to its binding affinity for the immobilized reactant. The bivalent model (Figure 4-6) describes the binding of a bivalent ligand to immobilized receptor, where one ligand can bind to one or two receptor molecules. The heterogeneous analyte model (Figure 4-7) is intended for analysis of the kinetics of the interaction of a mixture of ligands that are heterogeneous in terms of their affinities for the immobilized receptor. The binding kinetics for the LDL-LDLr interaction do not appear to fit any of the above models. The kinetic model that best fits the experimental results is a two-state conformational change model (Figure 4-8 and 4-9). In the conformational change model, a 1:1 binding of ligand to immobilized receptor is

Figure 4-5: Curve fitting using 1:1 Langmuir model. Sensorgram of LDL binding to the LDLr immobilized on a F1 sensor chip, curve fitted with equations for 1:1 Langmuire model. Black line represents actual data, while the red line represents curve fitted data. For this graph and all subsequent graphs A: represents ligand. B: represents receptor.

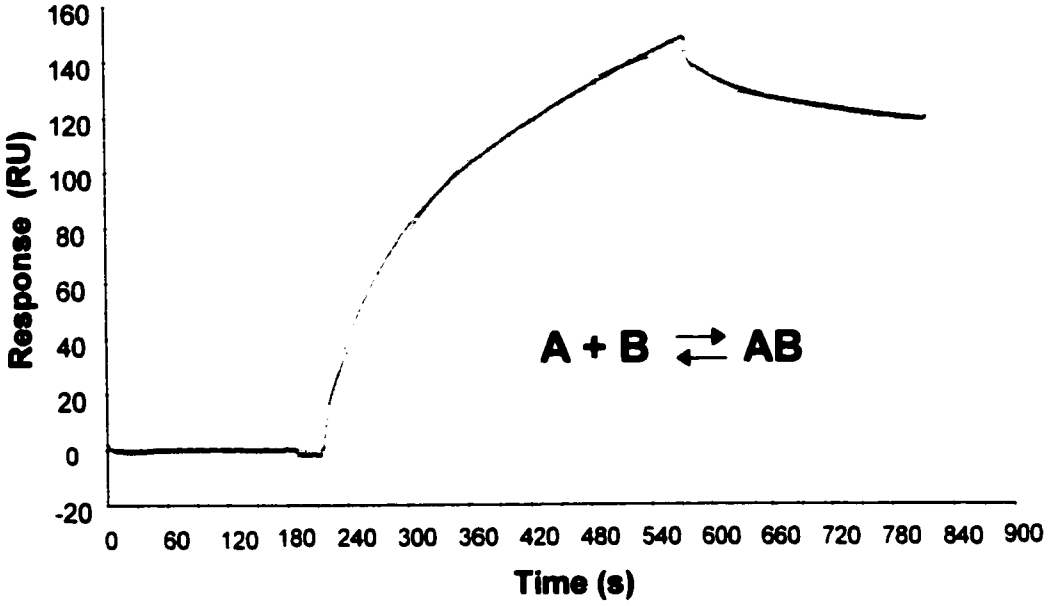
160
140
120
100
80
60
40
20
0
-20
Response (RU)
0
60
120
180
240
300
360
420
480
540
600
660
720
780
840
900
Time (s)
A + B ⇄ AB

Figure 4-6: Curve fitting using bivalent model. Sensorgram of LDL binding to the LDLr surface (F1 chip) and curve fitting with equations for bivalent analyte model. Black line represents actual data, while the red line represents fitted curve.

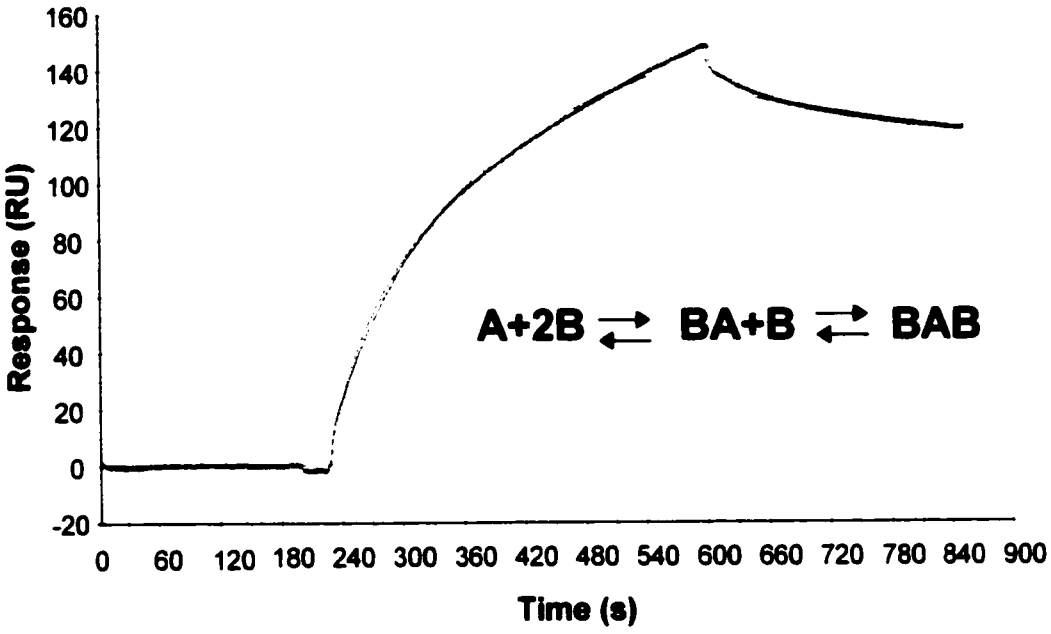
160
140
120
100
80
60
40
20
0
-20
Response (RU)
0
60
120
180
240
300
360
420
480
540
600
660
720
780
840
900
Time (s)
A+2B ⇄ BA+B ⇄ BAB

Figure 4-7: Curve fitting using heterogeneous ligand model. Sensorgram of LDL binding to the LDLr surface (F1 chip) and curve fitting with equations for heterogeneous ligand model. Black line represents actual data, while the red line represents fitted curve.

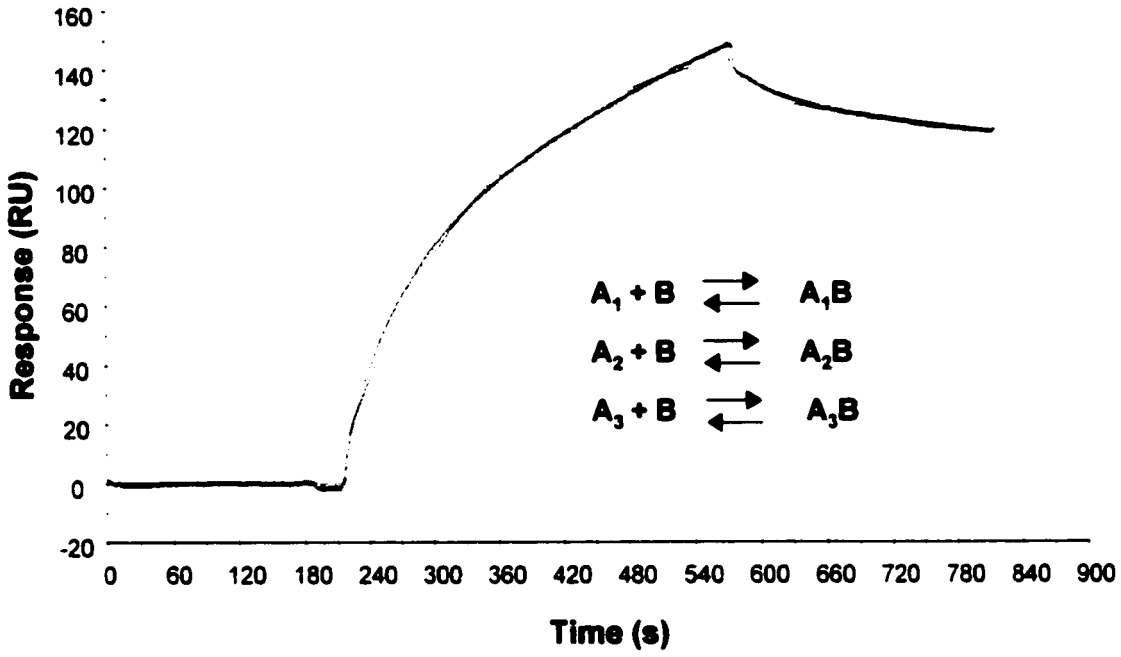
160
140
120
100
80
60
40
20
0
-20
Response (RU)
0
60
120
180
240
300
360
420
480
540
600
660
720
780
840
900
Time (s)
A1 + B
A1B
A2 + B
A2B
A3 + B
A3B

Figure 4-8: Curve fitting using conformational change model. Sensorgram of LDL binding to the LDLr surface (F1 chip) and curve fitting with equations for conformational change model. Black line represents actual data, while the red line represents fitted curve.

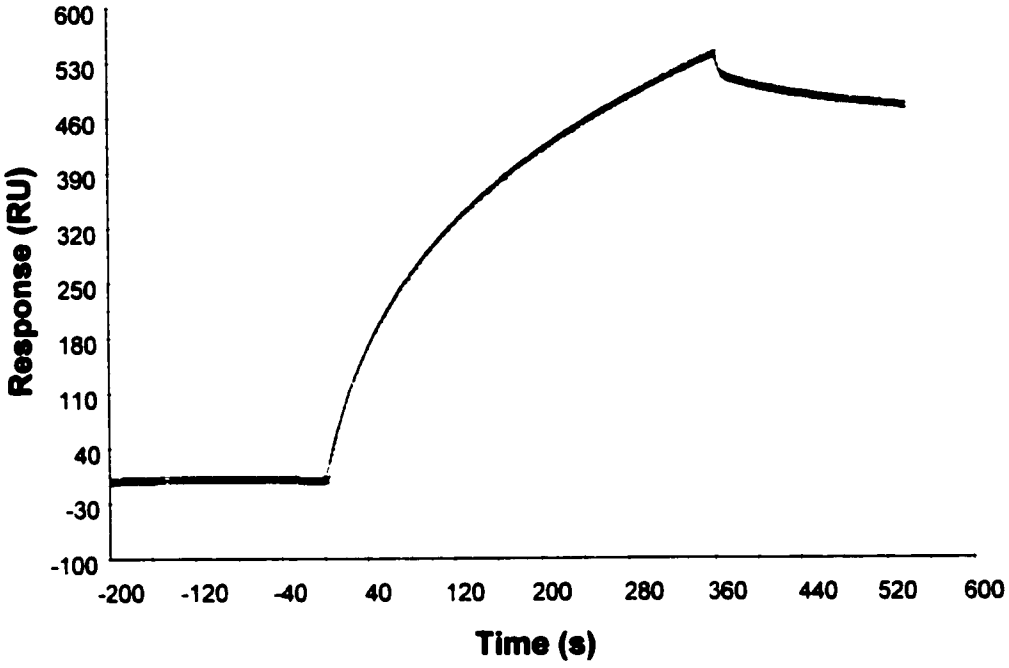
600
530
460
390
320
250
180
110
40
-30
-100
Response (RU)
-200
-120
-40
40
120
200
280
360
440
520
600
Time (s)

Figure 4-9: Components of conformational change model. A typical LDL-LDLr interaction sensorgram was fitted to a conformational change model. The components of the binding are shown: A represents ligand, B represents receptor, AB represents a low affinity interaction and ABx represents a high affinity interaction.

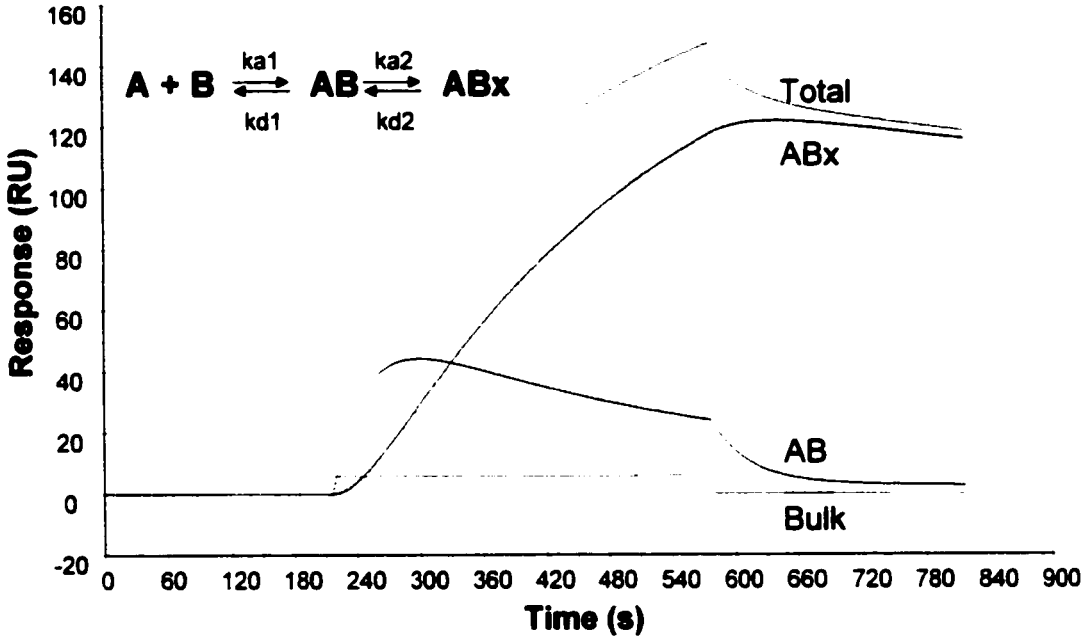
A + B
ka1
kd1
AB
ka2
kd2
ABx
Total
ABx
AB
Bulk
Response (RU)
Time (s)
160
140
120
100
80
60
40
20
0
-20
0
60
120
180
240
300
360
420
480
540
600
660
720
780
840
900

Figure 4-10: LDL-LDLr interaction as a function of injection time. LDLr was coupled to a F1 sensor chip. Sensorgrams were obtained for LDL injected for of 5.0, 3.7 and 0.5 mins. Longer injection times yielded slower dissociation rates.

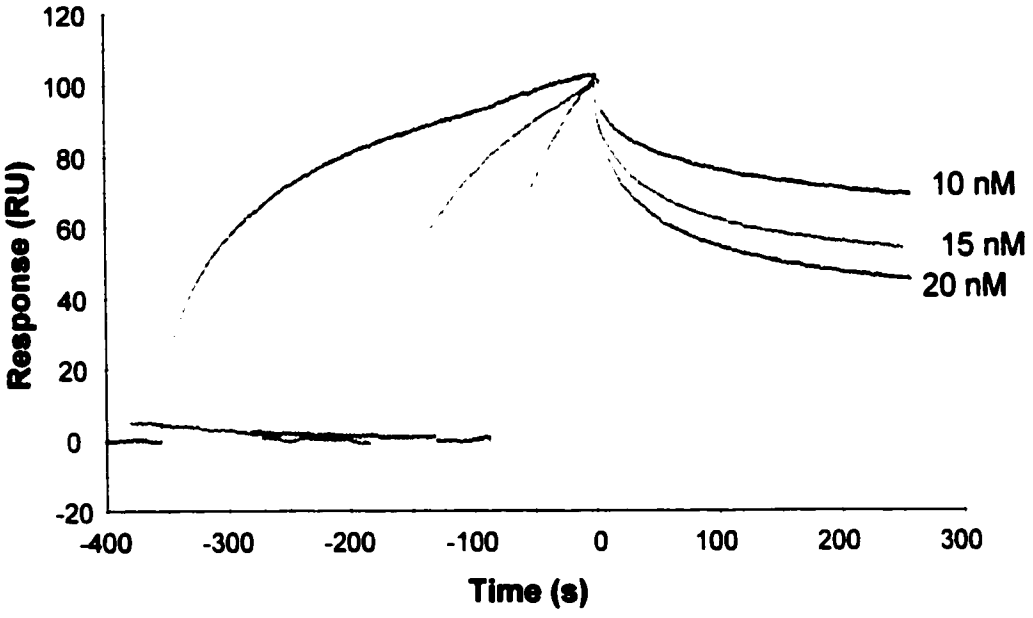
120
100
80
60
40
20
0
-20
Response (RU)
-400
-300
-200
-100
0
100
200
300
Time (s)
10 nM
15 nM
20 nM

followed by a conformational change in the complex. Alternatively, an initial low affinity site is converted with time to a high affinity site. Chappell et al. (1992) proposed a similar model for the interaction of LDL with the LDLr based on the binding of ^{125}I-LDL to the LDLr on the surface of cultured fibroblasts. The authors referred to this process as an isomerization of the LDL-LDLr complex. The isomerization model predicts that the initial receptor-ligand complex should dissociate relatively rapidly, whereas the complex formed by isomerization should dissociate more slowly. To test this, LDL was injected over the LDLr surfaces for various time periods. If the conformational change model were correct then a longer injection time should result in a slower dissociation rate due to the formation of the higher affinity complexes. As can be seen in Figure 4-10, the dissociation rate of the complex decreases when injection times are increased from 0.5 to 5 minutes. LDL from 3 subjects was tested and in each case isomerization was observed.

Effects of LDL concentration & receptor density on binding kinetics: The characteristically large size of LDL particles relative to the LDLr poses a special problem for ligand-receptor binding. A single LDL particle is more than twenty times larger than LDLr (Chappell et al., 1991). Ligand size plays an important role in receptor interaction because 70-80% of receptors are clustered in clathrin-coated pits (Orci et al., 1978). The presence of many LDL particles, within a single coated pit has been seen by electron microscopy using colloidal gold-conjugated LDL (Mommaas-Kienhuis et al., 1985). Therefore, receptor-bound LDL is large enough to sterically hinder binding to nearby receptors, consequently resulting in binding kinetics that may deviate from the conformational change model. In order to test this, we injected different concentrations

of analyte over the LDLr surface in order to determine if, at higher LDL concentrations, steric hindrance would affect binding kinetics. However, the kinetics of binding appeared to be independent of analyte concentration (Figure 4-11). This implies that at the ligand concentrations tested, lattice effects were not important contributors to the LDL-LDLr interaction. To further test the effects of steric hindrance and the possible role of receptor dimerization on binding kinetics, we immobilized the LDLr at a higher surface density. Van Driel et al. (1987b) showed that up to 20% of the LDLr on the cell surface could be cross-linked by a cross-linking reagent and concluded that many LDL receptors existed as noncovalently associated dimers or higher order aggregates. In this study, the isomerization was independent of receptor density (data not shown). Therefore, analyte-binding to the LDL receptor probably occurs by independent interactions between single particles and single receptors. Even if the particles are in close proximity to neighbouring receptors, they may not experience steric hindrance or negative cooperativity. Further, even if receptor dimerization occurs, the kinetics of LDL-LDLr binding still fit a conformational change model.

Temperature effects: To date, most of our knowledge of the affinities and kinetics of binding of lipoproteins to the LDLr has come from experiments using cultured fibroblasts at 4°C and not at a physiological temperature of 37°C (Chen et al., 1994). Kinetic analysis of ligand/receptor interaction performed at 37°C on cultured fibroblast would not be accurate since equilibrium cannot be achieved due to the continuous internalization of LDL. However, at 4°C the cells are not able to internalize lipoproteins and therefore direct binding to cell surface receptors can be monitored at non-physiological conditions.

Figure 4-11: LDL-LDLr interaction as a function of [LDL]. Sensorgrams for LDL-LDLr interaction at different LDL concentrations. Curves were fitted to a conformational change model. Black line represents actual data, while colored line represents fitted curve.

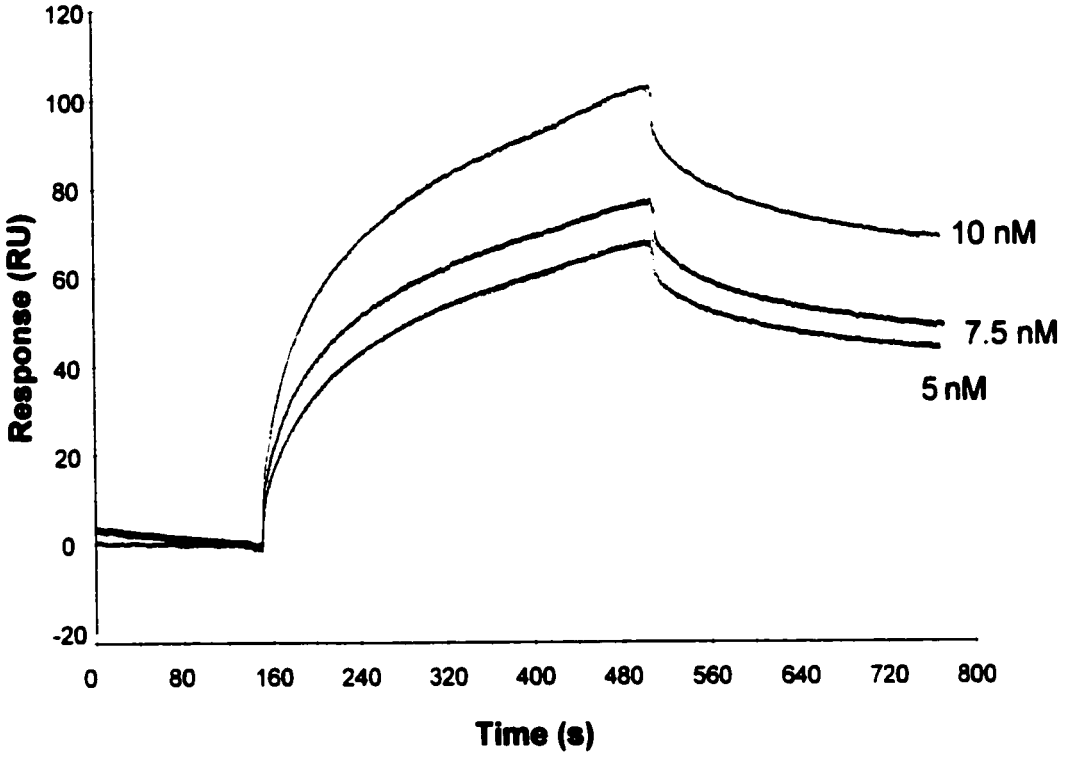
120
100
80
60
40
20
0
-20
Response (RU)
0
80
160
240
320
400
480
560
640
720
800
Time (s)
10 nM
7.5 nM
5 nM

In this study, SPR was used for kinetic analysis of binding at 37°C and was found to mimic those observed at 25°C. The LDL initially forms a complex with the LDLr that has a high dissociation rate but, with time, converts to a much more stable complex (Figure 4-12). Van Driel et al., (1989) had previously shown that LDLr in a solid-phase assay displayed the same affinity for LDL at 4°C and 37°C.

Hypertriglyceridemic LDL: The potential physiological consequences of the apparent isomerization of the LDL-LDLr complex was determined using HTG-LDL samples that have low affinity binding to cell surface LDLr relative to native LDL. Specifically, we tested the hypothesis that the lack of isomerization is responsible for the low affinity binding of small, dense LDL found in the plasma of hypertriglyceridemic patients. The binding kinetics for LDL isolated from a hypertriglyceridemic patient can be seen in Figure 4-13, a summary of the association and dissociation rate constants derived from Figure 4-13 is presented in Table 4-2. The table illustrates that HTG-LDL binds to the LDLr with conformational change kinetics that are similar to those of normal LDL. As well, similar to native LDL, longer injection of ligand results in isomerization to a higher affinity site and a slower dissociation rate of the complex (Figure 4-14). HTG-LDL from 3 subjects were tested and in each case isomerization was observed.

Apolipoprotein E binding: Apolipoprotein E serves as ligand to a number of receptors, including the LDLr. Therefore, we were interested in determining whether apoE and apoB bind by different mechanisms. Like most exchangeable apolipoproteins, the N-terminal domain of apoE is capable of transforming multilamellar vesicles of dimyristoylphosphatidylcholine (DMPC) into uniform-size bilayer disc complexes

(Raussens et al., 1998). ApoE complexed with DMPC was passed over the LDLr surface at a flow rate of 5 μl/min until a maximum response was obtained. However, the apoE-DMPC vesicles showed non-specific interactions with the ethanolamine blocked surface. Free apoE not complexed to lipids may be inconsistently interacting with the surface of the chip. Eventually, the particles clogged the biosensor, making it impossible to continue any further experimental studies.

Figure 4-12: LDL-LDLr interaction as a function temperature. LDLr was coupled to a F1 sensor chip. A sensorgram was obtained for LDL injected at a temperature of 37°C. The data were fitted to a conformational change model.

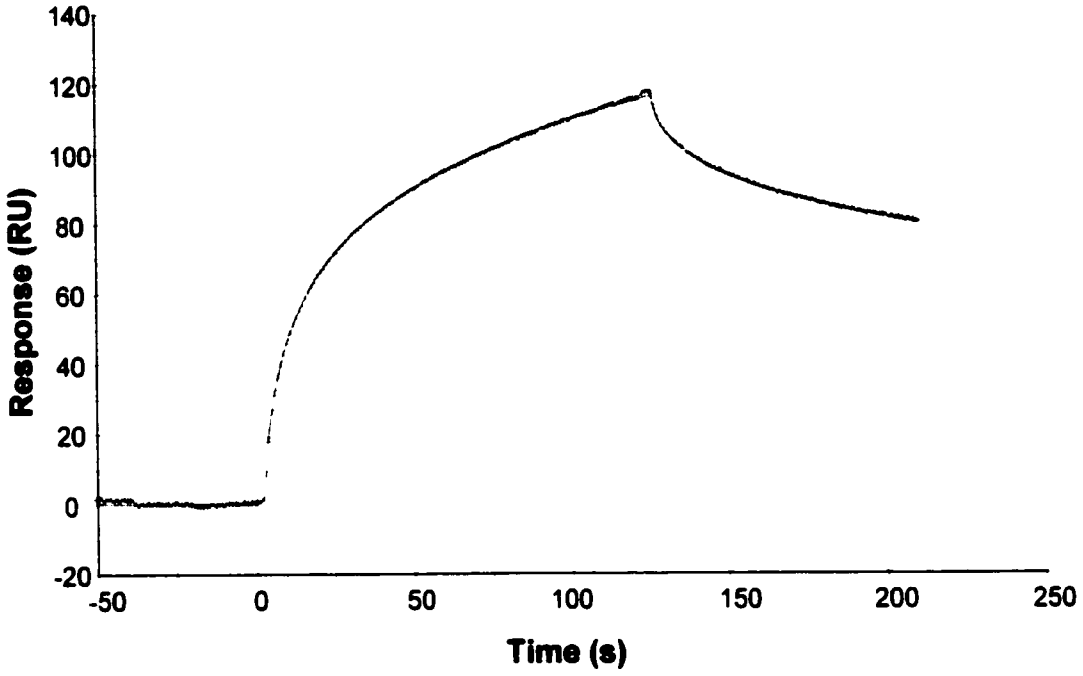
140
120
100
80
60
40
20
0
-20
Response (RU)
-50
0
50
100
150
200
250
Time (s)

Figure 4-13: Curve fitting at different [HTG-LDL]. Sensorgrams for HTG-LDL & LDLr interaction at different HTG-LDL concentrations. Curves were fitted to a conformational change model.

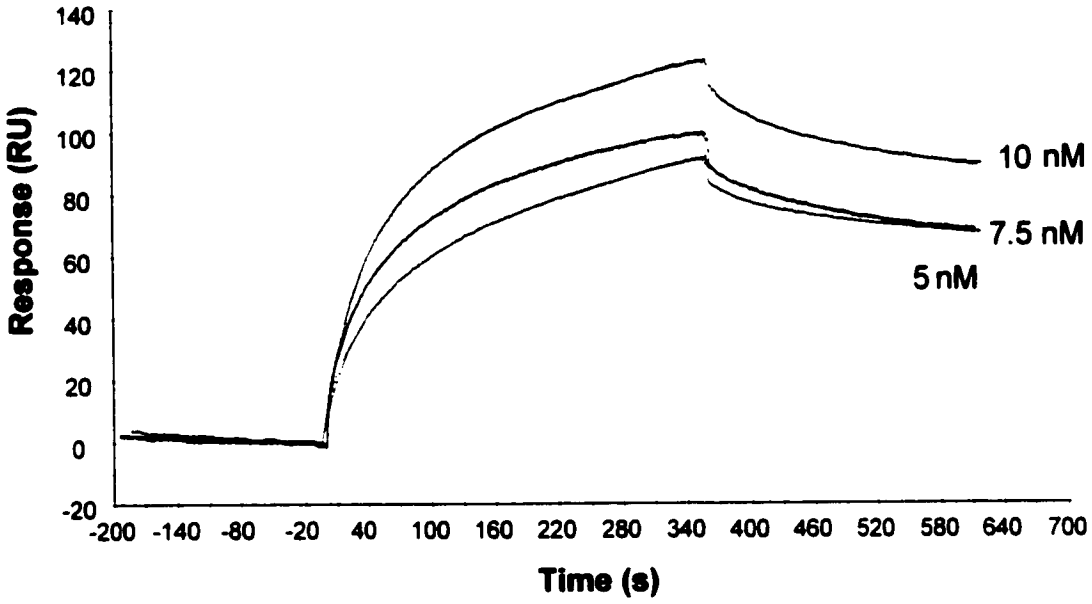
140
120
100
80
60
40
20
0
-20
Response (RU)
-200 -140 -80 -20 40 100 160 220 280 340 400 460 520 580 640 700
Time (s)
10 nM
7.5 nM
5 nM

Figure 4-14: HTG-LDL & LDLr interaction as a function of injection time. LDLr was coupled to an F1 sensor chip. A sensorgram was obtained for HTG-LDL injected at time points of 4.7, 3.5 and 0.5 mins.

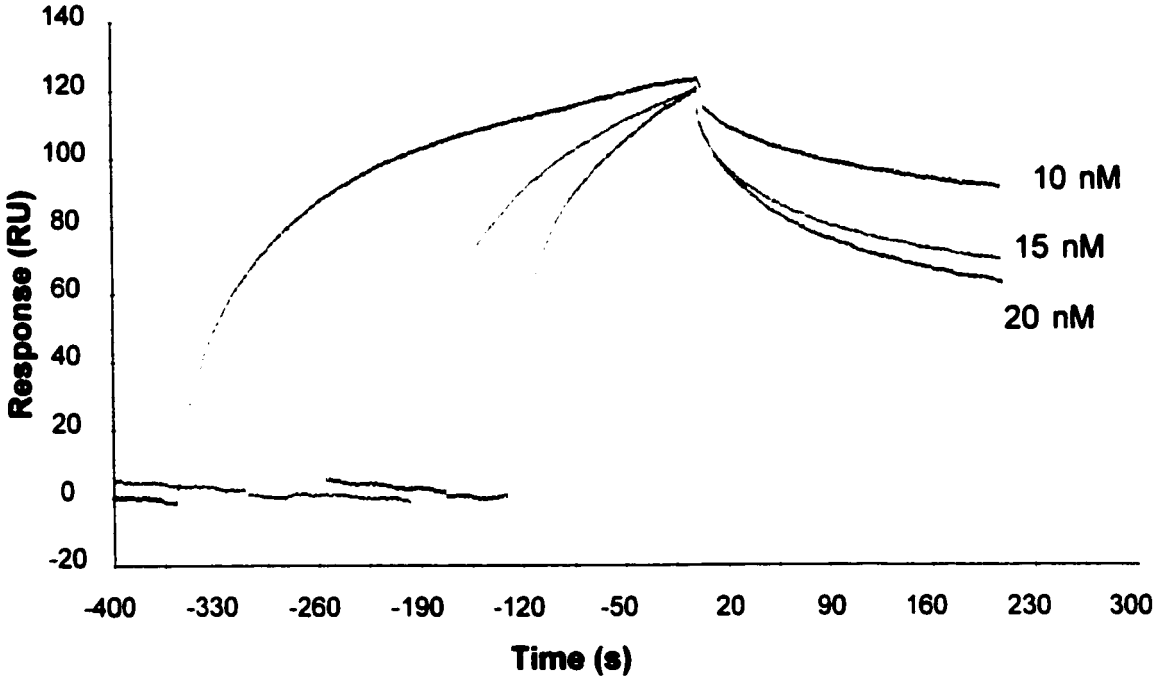
140
120
100
80
60
40
20
0
-20
Response (RU)
10 nM
15 nM
20 nM
-400
-330
-260
-190
-120
-50
20
90
160
230
300
Time (s)

Table 4-2: Rate constants. Summary of the association and dissociation rate constants for normal LDL at 25°C and 37°C and HTG-LDL at 25°C.

$$A + B \underset{k_{d1}}{\overset{k_{a1}}{\rightleftharpoons}} AB \underset{k_{d2}}{\overset{k_{a2}}{\rightleftharpoons}} ABx$$

	Normal LDL$^{25°C}$	HTG LDL$^{25°C}$	Normal LDL $^{37°C}$
k_{a1} (1/Ms)	1.6 ±0.2 X 10^{6}	2.1 ± 0.6 X 10^{6}	1.6 X 10^{6}
k_{d1} (1/s)	1.7 ± 0.3 X 10^{-2}	1.6 ± 0.3 X 10^{-2}	6.0 X 10^{-2}
k_{a2} (1/s)	8.5 ±0.8 X 10^{-3}	9.2 ±0.9 X 10^{-3}	2.4 X 10^{-3}
k_{d2} (1/s)	0.9 ±0.1 X 10^{-3}	1.0 ± 0.2 X 10^{-3}	3.3 X 10^{-3}
K_D (1/M)	0.8 ±0.2 X 10^{9}	1.5 ±0.5 X 10^{9}	0.2 X 10^{9}

Discussion

The present investigation represents the first effort to examine the kinetics of LDL-LDLr interactions in the absence of other interfering cellular components. A receptor, containing the ligand-binding domain and EGF precursor homology domain was successfully expressed and purified from Chinese Hamster Ovary cells in sufficiently high quantities. The purified LDLr was immobilized onto the surface of a biosensor chip and real-time binding kinetics of ligand-receptor interaction were monitored. Our preliminary kinetic analysis revealed that, as observed for many systems studied with BIACORE technology, the LDL-LDLr interaction failed to be represented as a simple bimolecular interaction. Deviations from the first order kinetics may be explained by phenomena inherent to the design of the BIAcore technology or the experiment itself. These artifacts include heterogeneity of the immobilized ligand and rebinding effects. On the other hand, it is also possible that a more complex kinetic model is required to explain the biological interaction between LDL-LDLr. After optimizing experimental conditions by the use of a reference surface and still observing a deviation from the simple model, we tested more complex biological interaction models. Among all the models tested, the one describing a conformational change in the receptor-ligand complex after initial binding yielded the best fit. Evidence for this model has also been reported by Chappell et al., (1992) who examined the binding kinetics of human LDL interacting with receptors on cultured human fibroblasts at 4°C. The investigators proposed that LDL-LDLr pattern of interaction was through an isomerization mechanism.

In our study, examination of the binding kinetics of LDL isolated from normolipidemic patients showed results that were comparable to the studies from cultured fibroblasts (Chappell et al., 1992). The binding was found to be rapid and with high affinity (K_d = 1 nM) and fit to a model in which an initial low affinity site converted with time to a high affinity site. The interaction was also specific to LDL, since acetylated LDL did not bind to the immobilized receptor. Temperature or lattice affects did not affect this interaction. The conformation model was further confirmed when longer injection times of ligand, resulted in slower dissociation rates.

There exist numerous examples of receptor/ligand complexes that undergo conformational changes. Through crystallographic evidence and *in vivo* protein interaction assay, it was shown for the erythropoeitin receptor/ligand system that the activation of the complex requires a change in its conformation after ligand-binding (Livnah et al., 1999 and Remy et al., 1999). Real-time kinetic studies on the interaction of transforming growth factor α with the epidermal growth factor receptor extracellular domain revealed a conformational change model (De Crescenzo et al., 2000). There is considerable evidence in the literature to show that both the LDLr and LDL can undergo conformational changes independently. Recently, it has been shown that the LDLr is capable of undergoing conformational changes upon binding calcium to a more ordered solvent-inaccessible structure (Blacklow et al., 1986 and Dirlam-Schatz et al,. 1998). A pH-dependent conformational change in EGF-like repeats A and B has been proposed to mediate acid-dependent ligand release (Davis et al., 1987). Similarly, the lipid composition and size of LDL particles have conformational effects on apoB100 (Lund-

Katz et al., 1998). It has been reported that modification of the triglyceride content of LDL by *in vitro* lipid exchange reactions alters reactivity of the particles with cell surface receptors and monoclonal antibodies as well as apoB100 conformation as measured by ^{13}C-NMR (Lund-Katz et al., 1998). A change in the conformation of the carboxy-terminus of apoB has been proposed to be necessary for exposure of the LDLr-binding site as VLDL is converted to LDL (Borén et al., 1998).

In order to examine how the physical and chemical properties of native LDL influence the kinetics of binding to the LDLr, we isolated LDL from hypertriglyceridemic patients. The LDL of these patients was characterized by an over-representation of small, dense, lipid-poor particles when compared to the LDL of normal subjects. There is a general agreement in the literature that small, dense LDL has higher susceptibility to oxidation suggesting that these particles may have elevated atherogenic potential. Kleinman et al. (1985) demonstrated that small, dense, cholesteryl-ester depleted LDL in patients with endogenous hypertriglyceridemia, have decreased affinity for the LDLr on cultured fibroblasts. Lund-Katz et al., (1998) concluded that the lower number of exposed lysine residue in apoB100 in small dense LDL relative to normal LDL is the cause for the reduction in the binding of small, dense LDL to the cellular receptor. However, a study by Galeano et al., (1998) showed that compared to normal LDL, small dense LDL have decreased binding to the LDLr but increased cell binding to LDL receptor-independent sites and that cell surface proteoglycans play a significant role in LDL cell binding at physiological LDL concentrations. Previous studies did not account for these LDLr-independent pathways, which are influenced by cell surface

proteoglycans. In this study, we were able to examine the LDL-LDLr binding kinetics in isolation in the absence of interfering factors such as other receptor pathways and cell components. Contrary, to the above results, our studies using SPR have shown that small, dense LDL isolated from HTG patients, exhibits the same binding kinetics as normal LDL. The affinity constants are not altered and neither is the model for binding. The small dense lipoproteins are able to promote a conformational change from a low affinity state to a high affinity state upon receptor-binding. However, we cannot exclude the possibility of other cell surface components such as proteoglycans being involved in inhibiting binding to the receptor, which may explain the low affinity binding of small dense LDL particles that has been observed by other investigators. As well the possibility that LDL-associated apoE may contribute to the binding of LDL to the LDLr cannot be overlooked. To test this possibility, samples of HTG-LDL can first be immunodepleted of apoE by using anti-apoE (1D7) immuno-affinity chromatography and then re-tested for binding to the LDLr.

The exact mechanistic changes that occur upon LDL-LDLr interaction have yet to be examined. However, they could involve conformational changes in the ligand-binding repeats of the receptor and/or the receptor-binding site of the apoB100 on LDL particles (Figure 4-15). Mutational analysis has shown that repeats 2-7 and repeat one of the EGF precursor homology domain of the LDLr are required for maximal binding of LDL (Esser et al., 1988). Each of the seven adjacent LDL repeats are connected by a four residue linker of variable primary sequence, except for repeats four and five, which are connected by a 12-residue linker. Recent NMR studies of a fragment of the ligand-binding domain

of the LDLr composed of repeats 4 and 5 support the conclusion that the linkers, which separates the modules are highly flexible and impose no rotational constraints on adjacent repeats (Beglova et al., 2001). The four residue linker, although, short is capable of separating two modules by up to 15Å. Such flexibility in the linker region connecting modules may be a mechanism for ligand-binding repeats to undergo conformational changes upon ligand-binding. As an example, initial binding of repeats 2 & 3 on LDLr ligand-binding domain may induce a conformational reorganization of the modules upon binding LDL that exposes the higher affinity repeats 5 & 6. Alternatively, it is known that the interaction of tryptophan 4369 of apoB100 with arginine 3500 dramatically increases the receptor-binding affinity, possibly by causing a conformational change in the receptor-binding site (Borén et al., 2001). Therefore, the isomerization of the LDL-LDLr complex to a high affinity form may involve the carboxy-terminus of apoB100. The initial binding of the receptor to a low affinity site (Site A or Site B) on apoB100 may with time, cause a conformational change in Sites A and B to form a higher affinity site by causing tryptophan 4369 of apoB100 to interact with arginine 3500. However, more studies are needed to elucidate the exact mechanisms for the conformational change.

Figure 4-15: Schematic of the conformational change model. A schematic representation of LDL (A) binding to the LDLr (B) to initially, form a low affinity complex (AB) that with time is converted to a high affinity complex (AB*). In Panel 1 the LDLr is shown to undergo a conformational change, while in Panel 2 the LDL-apoB is shown to undergo a conformational change.

1.

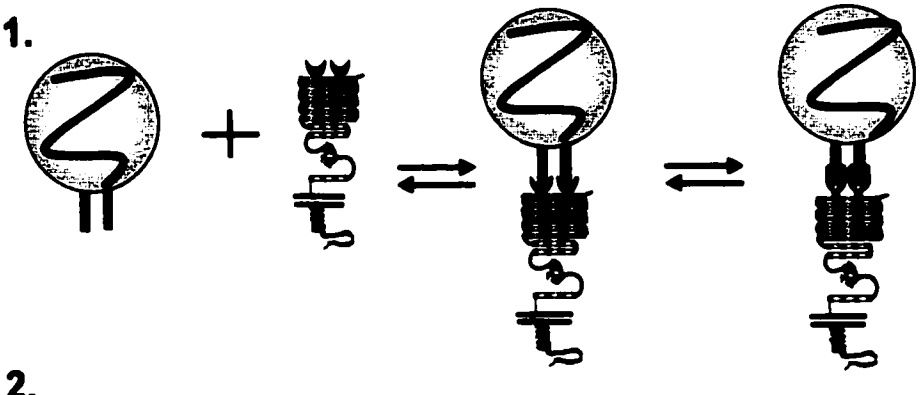

2.

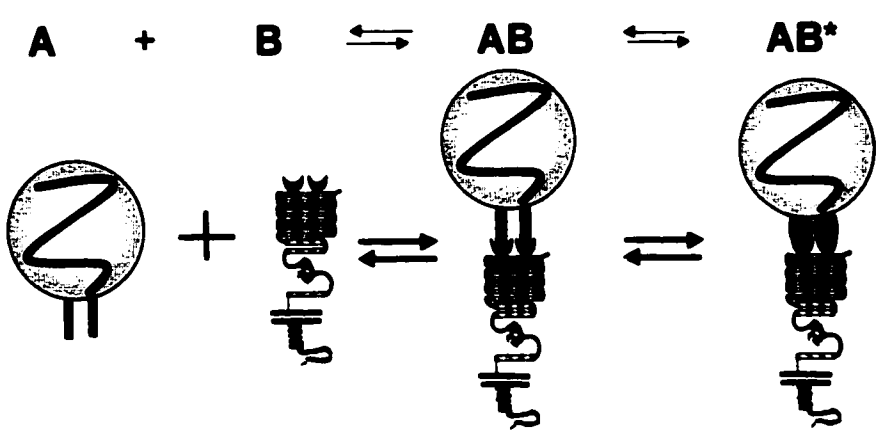

Chapter V

Future Perspectives

Atherosclerosis is a major cause of mortality in Western society. Amongst the contributing factors in the pathogenesis of this disease are elevated plasma cholesterol levels. The loss of regulatory mechanisms that are involved in the maintenance of cholesterol homeostasis within cells can arise through many mechanisms including cell surface receptors that specifically bind lipoproteins, the transporters of cholesterol in the plasma. The LDLr, found on the surface of most cells is an example of one such receptor. Individuals with familial hypercholesterolemia exhibit extremely high blood cholesterol concentrations and are known to have inherited defects in the LDLr gene, and without treatment, suffer severe premature coronary artery disease.

Due to the pioneering efforts of Drs Brown and Goldstein, the cellular and molecular biology of the LDLr pathway has been clearly elucidated (Goldstein et al., 1985b). However, our understanding of factors that influence binding and folding of the LDL receptor to its ligands is incomplete. The goals of the present project were, first, to produce a functional preparation of the extracellular domains of the LDLr. Secondly, we set out to identify factors that participate in the proper folding of the ligand-binding domain. Lastly, we aimed to characterize the kinetics of the LDL-LDLr interaction and define the physical properties of LDL that modulate binding to the LDLr.

Our initial attempts to produce an active preparation of LDLr were unsuccessful. The methyltrophic yeast, *Pichia pastoris* expressed a secreted form of the truncated receptor. However, the LDLr was not active and the majority of the receptor was

aggregated. *P. pastoris* may not provide a suitable environment or the specific chaperone proteins that are necessary for the correct folding of the LDLr. One important difference in the folding mechanisms between yeast system and mammalian cells is in the absence of the glycosylation protein, glycosidase II (Ziak et al., 2001). This enzyme is involved in the calnexin/calreticulin cycle and plays a role in determining the glucosylated state of a glycoprotein, which in turn determines their interactions with calnexin/calreticulin. We also considered the possibility that the C-terminal epitope tags interfere with the normal folding of the LDLr fragments. This is unlikely, at least in the case of the $LDLr^{692}$ fragment. $LDLr^{692}$ with a C-terminal oligo-histidine tail is expressed and secreted in a functional form in CHO-K1 cells but is aggregated and not secreted in yeast (data not shown).

Following the limited success with *P. pastoris*, we proceeded to another expression system, CHO-K1 cells. A number of truncated LDLrs depicted in Figure 2-17 were transfected into CHO-K1 cells, however only the $LDLr^{692}$ protein was secreted as a monomeric functional protein. LDLr fragments that lacked an intact EGF precursor homology domain were secreted as high-ordered multimers and were non-functional. Thus, the EGF precursor homology domain may facilitate the folding of the LDLr ligand-binding domain. Within this domain is a specialized module that forms a structural motif referred to as the β-propeller. The β-propeller domain has an important role in the function of a diverse array of proteins (Springer, 1998). Many mutations that cause FH have been mapped to specific regions within this domain in the LDLr (Figure 5-1). LDL receptors that lack the β-propeller domain and flanking EGF repeats bind β-VLDL but

not LDL, are defective in recycling and fail to release β-VLDL after acidification (Springer, 1998). Numerous studies have shown that this module exerts its effects by bringing domains into close proximity, thereby allowing for inter-protein and inter-domain interactions (Springer, 1998).

Due to the unique properties of the β-propeller, we proceeded to clone it along with the surrounding EGF repeats, in an attempt to determine if it was able to assist in the proper folding of the ligand-binding domain. However unexpectedly, the EGF precursor homology domain as a separate polypeptide completely inhibited the secretion of the ligand-binding domain. This inhibition was not specific to the LDLr, since it also affected CETP secretion. We initially hypothesized that, when expressed as a fragment the EGF precursor homology domain itself may have been improperly folded and this provoked a cellular unfolded protein response (UFR) that interfered with normal protein secretion. The UFR is a signal transduction pathway in stressed cells that activates genes involved in protein folding such as Grp78 and HSP. Expression of the β-propeller in CHO-K1 cells did not, however, appear to induce an URF as there was no increase in immunoreactive Grp78 relative to mock-transfected cells (results not shown).

More studies are warranted to define the exact role of EGF precursor homology domain in producing a properly folded LDLr ligand-binding domain. To further address this question, we have recently created a LDLr construct that encodes the ligand-binding domain, the EGF precursor homology domain and an oligohistidine tag with and without the tryptophan 556 to serine mutation. A thrombin-cleavage site has been inserted between the last ligand-binding repeat and the first EGF repeat. Both the wild-type

receptor and the mutant receptors will be expressed in CHO-K1 cells. Cell extracts will then be treated with thrombin and analyzed by electrophoresis on non-reducing SDS-PAGE and probed with antibodies against the ligand-binding domain (C7) and the EGF precursor homology domain (α-His). If our hypothesis is correct and the EGF repeats assist in the folding of the receptor post-translationally then mutations in the EGF repeats may cause misfolding of the ligand-binding domain with the formation of inter-molecular disulfide bonds.

We predict that the folding of the receptor is a complex two-step process. The model we propose involves an EGF precursor homology domain-facilitated folding of $LDLr^{692}$ ligand-binding domain (Figure 5-2). The first step involves an initial co-translational stabilization of hydrophobic regions within the ligand-binding domain by chaperone proteins such as RAP and Grp78/Bip. The second step involves a post-translational EGF precursor homology domain-assisted folding of the ligand-binding domain. One approach to test the two-step folding model would be to determine if the folding of the ligand-binding domain in $LDLr^{692}$ is post-translational. There is indirect evidence in this study to show that repeats in the ligand-binding domain of the LDLr attain their native conformation post-translationally. Whereas, $LDLr^{331}$ is recognized by C7 (Figure 2-12), $LDLr^{331}$ with carboxy-terminal c-myc and oligohistidine tags is not (Figure 2-11). Because the C-terminal epitope tags can only influence a post-translational folding mechanism, the folding of the first LDLr ligand-binding repeat may occur only after translation and translocation of at least the entire ligand-binding domain and the first EGF precursor repeat. However, further experiments are required to definitively

prove post-translational folding of the ligand-binding domain. This can be accomplished by monitoring the kinetics of the appearance of folded $LDLr^{692}$ in a synchronized *in vitro* translational assay. Briefly, $LDLr^{692\text{-}His}$ will be cloned into an *in vitro* transcription vector such as pGEM or Bluescript. RNA of $LDLr^{692\text{-}His}$ is added to rabbit reticulocyte lysate containing dog pancreas microsomes and ^{35}S-Methione/Cysteine. To stop re-initiation of translation the system is incubated with aurintricarboxylic acid after three minutes of translation. At certain intervals, aliquots of sample are diluted in ice-cold buffer containing cycloheximide, a protein synthesis inhibitor. The folding state of $LDLr^{692}$ at each time point is then determined by C7 reactivity (conformation-dependent epitope), chicken anti-LDLr reactivity (conformation-independent epitope), LDL-binding activity, flourography and resistance to limited protease digestion.

A number of cellular control mechanisms have evolved that facilitate post-translational steps in protein biosynthesis. Chaperone proteins and folding catalysts are an important part of these cellular control mechanisms. They associate with newly synthesized proteins and assure correct folding and post-translational modifications including disulfide bridge formation, glycosylation and complex formation (Frydman et al., 1994). Recently it was shown that the molecular chaperone protein Grp78/BiP co-immunoprecipitates with both wildtype and two different mutant LDLrs (W556S & C646Y). Therefore, Grp78 may be an important factor in the quality control of the LDLr (Jorgensen et al., 2000). Another protein that may be implicated in the folding the LDLr is protein disulfide isomerase (PDI), which catalyzes disulfide formation and rearrangement by thiol/disulfide exchange. The protein, RAP is a novel type of

chaperone that is especially designed to assist in the biosynthesis and intracellular transport of endocytic receptors (Medved et al., 1999). It appears to be involved in the folding of several members of the LDLr gene family, specifically VLDLr and LRP (Obermoeller et al., 1998 Mikhailenko et al., 1999). In this project, RAP appeared to limit protein aggregation of $LDLr^{292}$. However, further studies are required to clarify the exact role of RAP in LDLr trafficking. Currently, we are in the process of producing a panel of monoclonal antibodies against the LDLr. In the future, we hope to continuously label $LDLr^{292}$ and $LDLr^{692}$ transfected cells with ^{35}S-Methione/Cysteine and immunoprecipitate with antibodies against the LDLr. In this way, we will dissect the components involved in LDLr trafficking. By pulse-chase, we also will elucidate the kinetics of aggregate formation and secretion of $LDLr^{292}$ and $LDLr^{692}$. After determining the proteins that precipitate with the LDLr, we will further confirm their importance in LDLr trafficking by performing an *in vitro* refolding assay. Purified LDLr will be denatured using guanidine HCL and urea and then allowed to refold in the presence of chaperones (eg. Grp78, RAP) and or catalysts (PDI) to see if they promote the proper *in vitro* refolding of $LDLr^{292}$ and $LDLr^{692}$. In this way we will dissect all the components required for producing a properly folded and functional LDLr.

The development of biosensor technology based on surface plasmon resonance has provided a reliable means for measuring the binding activity of biomolecules. Optical sensors have the potential to provide detailed information about binding kinetics. However, there are a number of artifacts that must be considered when designing a biosensor experiment. Collecting data under the appropriate conditions and processing

the data through the use of reference surfaces and blank injections can eliminate many system dependent artifacts such as bulk refractive index changes, matrix effects, nonspecific binding, injection noise and baseline drift. In this study, accurate binding kinetics were determined for LDL-LDLr interaction. To exclude both lattice effects and the participation of other cell components, a purified, soluble receptor was coupled onto the surface of a biosensor chip and the association and dissociation rate constants were determined. The kinetics of binding fit a model in which LDL initially bound to the receptor to form a complex with a high dissociation rate followed by a slower rearrangement to form a more stable and high affinity complex with a slower dissociation rate. This rearrangement could involve a conformational change in the ligand and/or the receptor. To determine the effect of LDL heterogeneity on the kinetics of binding, LDL from hypertriglyceridemic patients were tested. The small, dense and triglyceride-enriched particles bound with similar kinetics as native LDL. This reinforces the possibility of other cell surface components influencing the receptor/ligand interaction.

The concept that a change in conformation of a receptor-ligand complex is required for receptor activation is just emerging as a prevalent observation. For future studies we will elucidate the mechanism of the isomerization. Since LDL is heterogeneous in terms of size, density and composition, we will test the binding kinetics of LDL isolated from hyperlipidemics that has been subfractioned using density gradient ultracentrifugation according to hydrated densities. Although we have tested subfractions of normal LDL and found no difference in binding kinetics (data not shown), testing subfractions of hypertriglyceridemic LDL would prove more informative

due to their exaggerated decrease in size and density relative to normal LDL. To determine if apoB is involved in the isomerization, we will test the binding kinetics of receptor-defective LDL isolated from patients with FDB and LDL that contains apoB80, apoB88 and apoB94, truncated apoB species that have been reported to have an increased affinity for the LDLr. Based on the conformational model for LDL-LDLr interaction, these truncated LDL species may not have to undergo isomerization to achieve the high affinity complex. Lastly, we would be interested in determining whether or not the isomerization also occurs with apoE-mediated binding and in the presence of cell surface proteoglycans. It is our hope that by studying the mechanisms involved in LDL-LDLr interactions we will understand how we might intervene to facilitate capture of cholesterol-carrying lipoproteins and reduce the risk for the development of atherosclerosis.

Figure 5-1: Point mutations in the β-propeller subdomain that lead to familial hypercholesterolemia. The positions of 39 independent missense mutations were mapped within the model of the LDLr β-propeller domain. Mutations cluster on the bottom of the β-propeller domain, and the side that is connected to the EGF domains. Reproduced from Springer, 1998.


B
N
C
C
N
C

Figure 5-2: Model depicting the post-translational folding of LDLr^{692}: **(1)** As the protein is translated, hydrophobic regions are masked by the binding of chaperone proteins. **(2)** Following release of the polypeptide post-translational folding of the EGF-precursor homology domain begins, possibly assisted by chaperone proteins. **(3)** The EGF precursor homology domain facilities the folding of the ligand-binding domain. **(4)** A folded and functional LDLr^{692} is secreted.

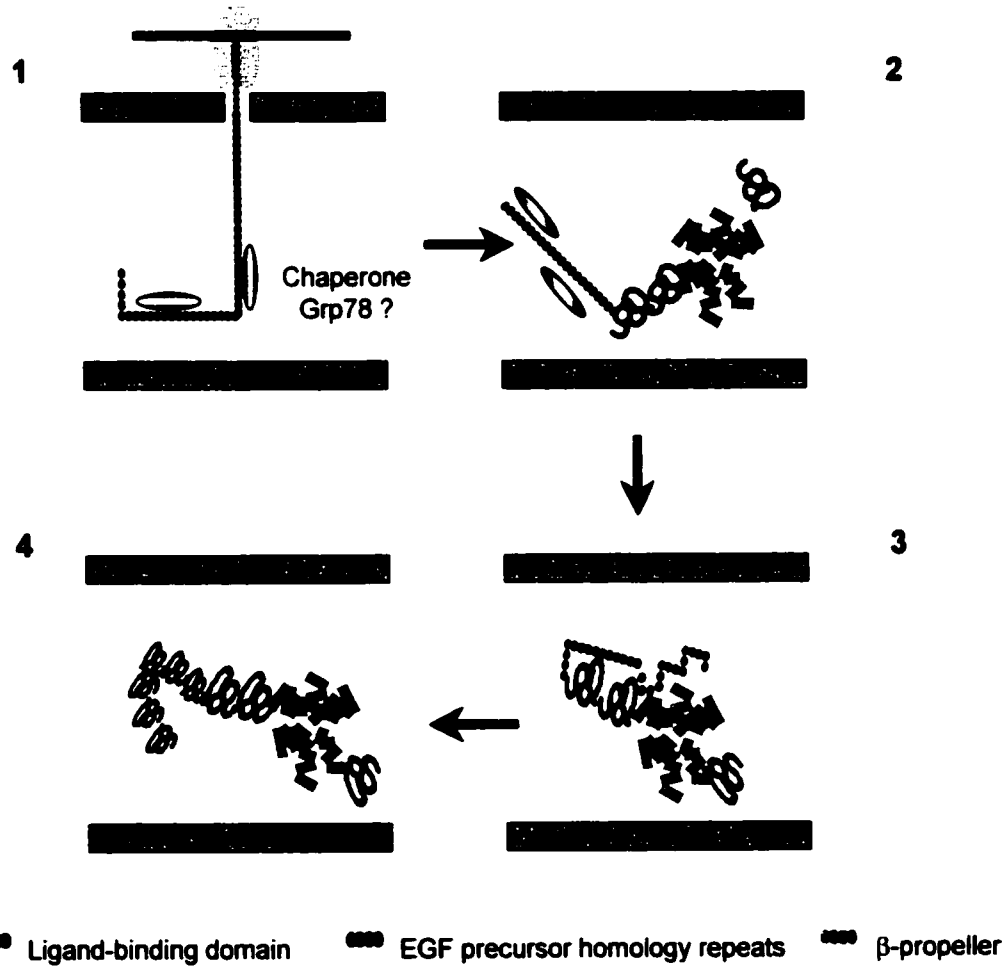
1
2
Chaperone
Grp78 ?
4
3
Ligand-binding domain
EGF precursor homology repeats
β-propeller

References

Acton, S.L., Scherer, P.E., Lodish, H.F. and Krieger, M. (1994) Expression cloning of SR-BI, a CD36-related class B scavenger receptor. *J Biol Chem.* **269**:21003-21009.

Aggerbeck, L.P., Wetterau, J.R., Weisgraber, K.H., Mahley, R.W. and Agard, D.A. (1988b) Crystallization and preliminary X-ray diffraction studies on the amino-terminal (receptor-binding) domain of human apolipoprotein E3 from serum very low density lipoproteins. *Journal of Molecular Biology.* **202**:179-181.

Aggerbeck, L.P., Wetterau, J.R., Weisgraber, K.H., Wu, C.S. and Lindgren, F.T. (1988a) Human apolipoprotein E3 in aqueous solution. II. Properties of the amino- and carboxyl-terminal domains. *Journal of Biological Chemistry.* **263**:6249-6258.

Anderson, R.G.W., Goldstein, J.L., and Brown, M.S. (1976) Localization of low density lipoprotein receptors on plasma membrane of normal human fibroblasts and their absence in cells from a familial hypercholesterolemia homozygote. *Proceeding of the National Academy of Science.* **73**:2434-2438.

Asai, D.J. and Wilder, J.K. (1993) Making monoclonal antibodies. *Methods of Cell Biology.* **37**:57-74.

Austin, M.A., Breslow, J.L., Hennekens, C.H., Buring, J.E., Willett, W.C. and Krauss, R.M. (1988) Low-density lipoprotein subclass patterns and risk of myocardial infarction. *JAMA.* **260**:1917-1921.

Aviram, M., Lund-Katz, S., Phillips, M.C. and Chait, A. (1988) The influence of the triglyceride content of low density lipoprotein on the interaction of apolipoprotein B-100 with cells. *Journal of Biological Chemisty.* **263**:16842-16848.

Aviram, M., Bierman, E.L. and Chait, A. (1988) Modification of low density lipoprotein by lipoprotein lipase or hepatic lipase induces enhanced uptake and cholesterol accumulation in cells. *Journal of Biological Chemistry.* **263**:15416-15422.

Bachrati, C.Z., Downes, C.S. and Rasko, I. (1999) Chemical reverse transformation of CHO-K1 cells induces changes in expression of a candidate tumour suppressor and of a gene not previously characterised as transformation related. *Euroupean Journal of Cell Biology.* **78**:561-566.

Baker, D., Sohl, J.L., Agard, D.A. (1992) A protein-folding reaction under kinetic control. *Nature.* **356**:263-265.

Beglova, N., North, C.L. and Blacklow, S.C. (2001) Backbone dynamics of a module pair from the ligand-binding domain of the LDL receptor. *Biochemistry*. **40**:2808-2815.

Beisiegel, U., Schneider, W.J., Goldstein, J.L., Anderson, R.G. and Brown, M.S. (1981) Monoclonal antibodies to the low density lipoprotein receptor as probes for study of receptor-mediated endocytosis and the genetics of familial hypercholesterolemia. *Journal of Biological Chemisty*. **256**:11923-11931.

Beissinger, M. and Buchner, J. (1998) How chaperones fold proteins. *Biological Chemistry*. **379**:245-259.

Belfi, C.A., Chatterjee, S., Gosky, D.M., Berger, S.J. and Berger, N.A. (1999) Increased sensitivity of human colon cancer cells to DNA cross-linking agents after GRP78 up-regulation. *Biochemical Biophysica Research Communication*. **257**:361-368.

Bieri, S., Djordjevic, J.T., Daly, N.L., Smith, R. and Kroon, P.A. (1995) Disulfide bridges of a cysteine-rich repeat of the LDL receptor ligand-binding domain. *Biochemistry*. **34**:13059-13065.

Blackhart, B.D., Ludwig, E.M., Pierotti, V.R., Caiati, L., Onasch, M.A., Wallis, S.C., Powell, L., Pease, R., Knott, T.J. and Chu, M.L., (1986) Structure of the human apolipoprotein B gene. *Journal of Biological Chemistry*. **261**:15364-15367.

Blacklow, S.C., and Kim, P.S. (1996) Protein folding and calcium binding defects arising from familial hypercholesterolemia mutations of the LDL receptor. *Nature Structural Biology*. **3**:758-762.

Borén, J., Ekstrom, U., Agren, B., Nilsson-Ehle, P., and Innerarity, T.L. (2001) The molecular mechanism for the genetic disorder familial defective apolipoprotein B100. *Journal of Biological Chemistry*. **276**:9214-9218.

Borén, J., Lee, I., Zhu, W., Arnold, K., Taylor, S., and Innerarity, T.L. (1998). Identification of the low density lipoprotein receptor – binding site in apolipoprotein B100 and the modulation of its binding activity by the carboxyl terminus in familial defective apo-B100. *Journal of Clinical Investigation*. **101**:1084-1093.

Brown, M.S. and Goldstein, J.L. (1986) A receptor-mediated pathway for cholesterol homeostasis. *Science*. **232**:34-47.

Brown, M.S. and Goldstein, J.L. (1999) A proteolytic pathway that controls the cholesterol content of membranes, cells, and blood. *Proceeding of the National Academy of Science*. **96**:11041-11048.

Brown, M.S. and Goldstein, J.L. (1997) The SREBP pathway: regulation of cholesterol metabolism by proteolysis of a membrane-bound transcription factor. *Cell.* **89**:331-340.

Brown, M.S., Kovanen, P.T., and Goldstein, J.L. (1981) Regulation of plasma cholesterol by lipoprotein receptors. *Science.* **212**:628-635.

Buja, L.M., Kita, T., Goldstein J.L., Watanabe, Y., and Brown, M.S. (1983) Cellular pathology of progressive atherosclerosis in the WHHL rabbit. An animal model of familial hypercholesterolemia. *Arteriosclerosis.* **3**:87-101.

Bungert, S., Molday, L.L., and Molday, R.S. (2001) Membrane Topology of the ATP Binding Cassette Transporter ABCR and Its Relationship to ABC1 and Related ABCA Transporters. *Journal of Biological Chemistry.* **46**:2012-2018.

Bu, G. (1998) Receptor-associated protein: a specialized chaperone and antagonist for members of the LDL receptor gene family. *Current Opinion in Lipidology.* **9**:149-55.

Campos, H., Arnold, K.S., Balestra, M.E., Innerarity, T.L. and Krauss, R.M. (1996) Differences in receptor binding of LDL subfractions. *Arteriosclerosis Thrombosis Vascular Bioliogy.* **16**:794-801.

Carrell, R.W., and Lomas, D.A. (1997) Conformational disease. *Lancet.* **350**:134-138.

Chan, L., (1992) Apolipoprotein B, the major protein component of triglyceride-rich and low density lipoproteins. *Journal of Biological Chemistry.* **267**:25621-25624.

Chappell, D.A., Fry, G.L., Waknitz, G.L., amd Berns, J.J. (1991). Evidence for isomerization during binding of apolipoprotein-B100 to low density lipoprotein receptors. *The Journal of Biological Chemistry.* **287**:270-278.

Chappell, D.A., Fry, G.L., Waknitz, M.A. and Berns, J.J. (1991) Ligand size as a determinant for catabolism by the low density lipoprotein (LDL) receptor pathway. A lattice model for LDL binding. *Journal of Biological Chemistry.* **266**:19296-19302.

Chappell, D.A., Fry, G.L., Waknitz, M.A., Muhonen, L.E., and Pladet, M.W. (1993). Low density lipoprotein receptors bind and mediate cellular catabolism of normal very low density lipoproteins *in vitro. The Journal of Biological Chemistry.* **268:** 25487-25493.

Chatterton, J.E., Phillips, M.L., Curtiss, L.K., Milne, R., Fruchart, J.C., Schumaker and V.N. (1995) Immunoelectron microscopy of low density lipoproteins yields a ribbon and bow model for the conformation of apolipoprotein B on the lipoprotein surface. *Journal of Lipid Research.* **36**:2027-2037.

Chauhan, V., Wang, X., Ramsamy, T., Milne, R.W. and Sparks, D.L. (1998) Evidence for lipid-dependent structural changes in specific domains of apolipoprotein B100. *Biochemistry*. **37**:3735-3742.

Chen, C. and Okayama, H. (1987) High-efficiency transformation of mammalian cells by plasmid DNA. *Molecular Cell Biology*. 7:2745-2752.

Chen, G.C., Liu, W., Duchateau, P., Allaart, J., Hamilton, R.L., Mendel, C.M., Lau, K., Hardman, D.A., Frost, P.H., Malloy, M.J., and Kane, J.P. (1994) Conformational differences in human apolipoprotein B-100 among subspecies of low density lipoproteins (LDL). Association of altered proteolytic accessibility with decreased receptor binding of LDL subspecies from hypertriglyceridemic subjects. *Journal of Biological Chemistry*. **269**:29121-29128.

Chen, W.J., Goldstein, J.L., and Brown, M.S. (1990) NPXY, a sequence often found in cytoplasmic tails, is required for coated pit-mediated internalization of the low density lipoprotein receptor. *Journal of Biological Chemistry*. **256**:3116-3123.

Cooper, A.D. (1997) Hepatic uptake of chylomicron remnants. *J Lipid Res*. **38**:2173-2192.

Cruz JC, Chang TY. (2000) Fate of endogenously synthesized cholesterol in Niemann-Pick type C1 cells. *J Biol Chem*. **275**:41309-41316.

Dachet, C., Cavallero, E., Martin, C., Girardot, G. and Jacotot, B. (1995) Effect of gemfibrozil on the concentration and composition of very low density and low density lipoprotein subfractions in hypertriglyceridemic patients. *Atherosclerosis*. **113**:1-9.

Daly, N.L., Scanlon, M.J., Djordijivic, J.T., Kroon, P.A., and Smith, R. (1995). Three-dimensional structure of a cysteine-rich repeat from the low-density lipoprotein receptor. *Proceedings of the National Academy of Science*. **92**:6334-6338.

Davis, G.C., Goldstein, J.L., Sudhof, T.C., Anderson, R.G.W., Russell, D.W., and Brown M.S. (1987) Acid-dependent ligand dissociation and recycling of LDL receptor mediated by growth factor homology region. *Nature*. **326**:760-765.

De Crescenzo, G., Grothe, S., Lortie, R., Debanne, M.T. and O'Connor-McCourt, M. (2000) Real-time kinetic studies on the interaction of transforming growth factor alpha with the epidermal growth factor receptor extracellular domain reveal a conformational change model. *Biochemistry*. **39**:9466-9476.

De Loof, H., Rosseneu, M., Brasseur, R. and Ruysschaert, J.M. (1986) Use of hydrophobicity profiles to predict receptor binding domains on apolipoprotein E and the low density lipoprotein apolipoprotein B-E receptor. *Proc Natl Acad Sci U S A.* **83**:2295-2299.

Dirlam, K.A., Gretch, D.G., LaCount, D.J., Sturley, S.L. and Attie, A.D. (1996) Expression and characterization of a truncated, soluble, low-density lipoprotein receptor. *Protein Expression and Purification.***8**:489-500.

Dirlam-Schatz, K.A. and Attie, A.D. (1998) Calcium induces a conformational change in the ligand binding domain of the low density lipoprotein receptor. *Journal of Lipid Research.* **39**:402-411.

Djordjevic, J.T., Bieri, S., Smith, R. and Kroon, P.A. (1996) A deletion in the first cysteine-rich repeat of the low-density-lipoprotein receptor leads to the formation of multiple misfolded isomers. *European Journal of Biochemistry.* **239**:214-219.

Eckardstein, A.V., Nofer J.R., and Assmann G. (2001) High density lipoproteins and arteriosclerosis role of cholesterol efflux and reverse cholesterol transport. *Arteriosclerosis Thrombosis Vascular Biology.* **21**:13-27.

Eder, J., Rheinnecker, M. and Fersht, A.R. (1993) Folding of subtilisin BPN': role of the pro-sequence. *Journal of Molecular Biology.* **233**:293-304.

Edwards, P.R., Gill, A., Pollard-Knight, D.V., Hoare, M., Buckle, P.E. and Lowe, P.A., (1995) Leatherbarrow RJ. Kinetics of protein-protein interactions at the surface of an optical biosensor. *Analytical Biochemistry.* **231**:210-207.

Ellis, R.J. and Hartl, F.U. (1999) Principles of protein folding in the cellular environment. *Current Opinion of Structural Biology.* **9**:102-110.

Esser, V. and Russell, D.W. (1988) Transport-deficient mutations in the low density lipoprotein receptor. Alterations in the cysteine-rich and cysteine-poor regions of the protein block intracellular transport. *Journal of Biological Chemistry.* **263**:13276-13281.

Esser, V., Limbird, L.E., Goldstein, J.L., Brown, M.S., and Russell, D.W. (1986). Mutational analysis of the ligand binding domain of the low density lipoprotein receptor. *The Journal of Biological Chemistry.* **263:**13282-13290.

Evan, G.I., Lewis, G.K., Ramsay, G. and Bishop, J.M. (1985) Isolation of monoclonal antibodies specific for human c-myc proto-oncogene product. *Molecular Cell Biology.* **5**:3610-3616.

Fass, D., Blacklow, S., Kim, P.S., and Berger, J.M. (1997) Molecular basis of familial hypercholesterolaemia from structure of LDL receptor module. *Nature*. **388**:691-693.

Fazio, S., Lee, Y.L., Ji Z.S. and Rall, S.C. Jr. (1993) Type III hyperlipoproteinemic phenotype in transgenic mice expressing dysfunctional apolipoprotein E. *Journal of Clinical Investigation*. **93**:1497-1503.

Feldman, D.E. and Frydman, J. (2000) Protein folding *in vivo*: the importance of molecular chaperones. *Current Opinion in Structural Biology*.**10**:26-33.

Fidge, N.H. (1999) High density lipoprotein receptors, binding proteins, and ligands. *Journal of Lipid Research*. **40**:187-201.

Fisher, R.J. and Fivash, M. (1994) Surface plasmon resonance based methods for measuring the kinetics and binding affinities of biomolecular interactions. *Current Opinion in Biotechnology*. **5**:389-395.

Fivash, M., Towler, E.M. and Fisher, R.J. (1998) BIAcore for macromolecular interaction. *Current Opinion in Biotechnology*. **9**:97-101.

Frydman, J., Nimmesgern, E., Ohtsuka, K. and Hartl, F.U. (1994) Folding of nascent polypeptide chains in a high molecular mass assembly with molecular chaperones. *Nature*. **370**:111-117.

Galeano, N.F., Al-Haideri, M., Keyserman, F., Rumsey, S.C. and Deckelbaum, R.J. (1998) Small dense low density lipoprotein has increased affinity for LDL receptor-independent cell surface binding sites: a potential mechanism for increased atherogenicity. *Journal of Lipid Research*. **39**:1263-1273.

Galeano, N.F., Milne, R., Marcel, Y.L., Walsh, M.T., Levy, E., Ngu'yen, T.D., Gleeson, A., Arad, Y., Witte, L. and Al-Haideri M, (1994) Apoprotein B structure and receptor recognition of triglyceride-rich low density lipoprotein (LDL) is modified in small LDL but not in triglyceride-rich LDL of normal size. *Journal of Biological Chemisty*. **269**:511-519.

Garcia, C.K., Wilund, K., Arca, M., Zuliani, G., Fellin, R., Maioli, M., Calandra, S., Bertolini, S., Cossu, F., Grishin, N., Barnes, R., Cohen, J.C. and Hobbs, H.H. (2001) Autosomal recessive hypercholesterolemia caused by mutations in a putative LDL receptor adaptor protein. *Science*. **292**:1394-1398.

Gaus, K., Basran, A. and Hall, E.A. (2001) Assessment of the fifth ligand-binding repeat (LR5) of the LDL receptor as an analytical reagent for LDL binding. *Analyst*. **126**:329-336.

Gething, M.J. (1999) Role and regulation of the ER chaperone BiP. Semin *Cell Devolment Biology*. **10**:465-472.

Gilbert, H.F. (1998) Protein disulfide isomerase. *Methods of Enzymology*. **290**:26-50.

Ginsberg, H.N., Barr, S.L., Gilbert, A., Karmally, W., Deckelbaum, R., Kaplan, K., Ramakrishnan, R., Holleran, S. and Dell, R.B. (1990) Reduction of plasma cholesterol levels in normal men on an American Heart Association Step diet or a Step 1 diet with added monounsaturated fat. *New England Journal of Medicine*. **322**:574-579.

Goldstein, J.L., and Brown, M.S. (1974) Binding and degradation of low density lipoproteins by cultured human fibroblasts: Comparison of cells from a normal subject and from a patient with familial hypercholesterolemia. *Journal of Biological Chemistry*. **259**: 5153-5162.

Goldstein, J.L., Anderson, R.G.W., and Brown, M.S. (1979) Coated pits, coated vesicles and receptor-mediated endocytosis. *Nature* **279**: 679-685.

Goldstein, J.L., Brown, M.S., Anderson, R.G., Russell, D.W. and Schneider, W.J. (1985a) Receptor-mediated endocytosis: concepts emerging from the LDL receptor system. *Annual Review in Cell Bioliogy*. **1**:1-39.

Goldstein, J.L., Hobbs, H.H. and Brown, M.S. (1985b) In the Metabolic and molecular bases of inherited disease 7th edition editors Scriver, C.R., et al. 1981-2030.

Goldstein, J.L., Kita, T. and Brown, M.S. (1983) Defective lipoprotein receptors and atherosclerosis. Lessons from an animal counterpart of familial hypercholesterolemia. *New England Journal of Medicine*. **309**:288-296.

Goldstein, J.L. and Brown, M.S. (2001) Molecular medicine. The cholesterol quartet. *Science*. **292**:1310-1312.

Gray, A.M. and Mason, A.J. (1990) Requirement for activin A and transforming growth factor--beta 1 pro-regions in homodimer assembly. *Science*. **247**:1328-30.

Greenfield, N. and Fasman, G.D. (1969) Computed circular dichroism spectra for the evaluation of protein conformation. *Biochemistry*. **8**:4108-4116.

Griffith, O.M. (1991) Cesium chloride gradients in carbon fiber fixed angle rotor for purification of viruses, organelles, and plasmid DNA. *American Biotechnological Lab*.**9**:24-26.

Havel, R.J., Eder, H.A. and Bragdon, J.H. (1955) The distribution and chemical composition of ultracentrifugally separated lipoproteins in human serum. *Journal of Clinical Investigation*. **34**:1345:1353.

Heeren, J., and Beisiegel, U. (2001) Intracellular metabolism of triglyceride-rich lipoproteins. *Current Opinion in Lipidology*. **12**:255-260.

Hinnen, A, Hicks, J.B. and Fink, G.R. (1978) Transformation of yeast. *Biotechnology*. **24**:337-341.

Hinshaw, J.E., Schmid, S.L. (1995) Dynamin self-assembles into rings suggesting a mechanism for coated vesicle budding. *Nature*. **374**:190-192.

Hobbs, H.H., Russell, D.W., Brown, M.S., and Goldstein, J.L. (1990) The LDL receptor locus and familial hypercholesterolemia: Mutational analysis of a membrane protein. *Annual Review of Genetics*. **24:**133-170.

Holstein, S.E., Ungewickell, H. and Ungewickell, E. (1996) Mechanism of clathrin basket dissociation: separate functions of protein domains of the DnaJ homologue auxilin. *J Cell Biol*. **135**:925-937.

Innerarity, T.L., Friedlander, E.J., Rall, S.C. Jr, Weisgraber, K.H. and Mahley, R.W. (1983) The receptor-binding domain of human apolipoprotein E. Binding of apolipoprotein E fragments. *Journal of Biological Chemistry*. **258**:12341-12347.

Innerarity, T.L., Hui, D.Y., Bersot, T.P., and Mahley, R.W. (1986) Type III hyperlipoproteinemia: a focus on lipoprotein receptor-apolipoprotein E2 interactions. *Advanced Experiments in Medical Biology*. **201**:273-288.

Ishibashi, S., Perrey, S., Chen, Z., Osuga, Ji., Shimada, M., Ohashi, K., Harada, K., Yazaki, Y. and Yamada, N. (1996) Role of the low density lipoprotein (LDL) receptor pathway in the metabolism of chylomicron remnants. A quantitative study in knockout mice lacking the LDL receptor, apolipoprotein E, or both. *J Biol Chem*. **271**:22422-22427.

Ito, H., Naito, C., Suzuki, Y., Nakamura, K. and Nagase M. (1994) Post-prandial triglyceride-rich lipoprotein metabolism: possible role of sialilated apolipoprotein E isoproteins. *European Journal of Clinical Investigation*. **24**:468-475.

Jeon, H. and Shipley, G.G. (2000a) Vesicle-reconstituted low density lipoprotein receptor. (2000a) Visualization by cryoelectron microscopy. *J Biol Chem*. **275**:30458-30464

Jeon, H. and Shipley, G.G. (2000b) Localization of the N-terminal domain of the low density lipoprotein receptor. *J Biol Chem.* **275**:30465-30470.

Jonsson, U., Fagerstam, L., Lofas, S., Stenberg, E., Karlsson, R., Frostell, A., Markey, F. and Schindler F. (1993) Introducing a biosensor based technology for real-time biospecific interaction analysis. *Annual Biology of Clinics* (Paris). **51**:19-26.

Jorgensen, M.M., Jensen, O.N., Holst, H.U., Hansen, J.J., Corydon, T.J., Bross, P., Bolund, L. and Gregersen, N. (2000) Grp78 is involved in retention of mutant low density lipoprotein receptor protein in the endoplasmic reticulum. *Journal of Biological Chemistry.* **275**:33861-33868.

Kane, J.P. and Havel, R.L. (1995). Disorders of the biogenesis and secretion of lipoproteins containing the B apolipoproteins. In the Scriver C.R., Beaudet, A.L., Sly, W.S., Valle, D. (eds): The metabolic basis of inherited disease, 7th ed. New York, McGraw-Hill, 1995, vol. II 1853-1885.

Kane, J.P., Hardman, D.A., and Paulus, H.E., (1980) Heterogeneity of apolipoprotein B: isolation of a new species from human chylomicrons. *Proceedings of the National Academy of Science.* **77**:2465-2469.

Kataoka, S., Paidi, M., Howard and B.V. (1994) Simplified isoelectric focusing/immunoblotting determination of apoprotein E phenotype. *Clinical Chemistry.* **40**:11-13.

Kibbey, R.G., Rizo, J., Gierasch, L.M. and Anderson, R.G. (1998) The LDL receptor clustering motif interacts with the clathrin terminal domain in a reverse turn conformation.
J Cell Biol. **142**:59-67.

Kinoshita, M., Krul, E.S. and Schonfeld, G. (1990) Modification of the core lipids of low density lipoproteins produces selective alterations in the expression of apoB-100 epitopes. *Journal of Lipid Research.* **31**:701-708.

Kleinman, Y., Eisenberg, S., Oschry, Y., Gavish, D., Stein, O. and Stein, Y. (1985) Defective metabolism of hypertriglyceridemic low density lipoprotein in cultured human skin fibroblasts. Normalization with bezafibrate therapy. *Journal of Clinical Investigation.* **75**:1796-1803.

Knott, T.J., Rall, S.C. Jr, Innerarity, T.L., Jacobson, S.F., Urdea, M.S., Levy-Wilson, B., Powell, L.M., Pease, R.J., Eddy, R., Nakai, H., Mahley, R.W. and Scott, J. (1985) Human apolipoprotein B: structure of carboxyl-terminal domains, sites of gene expression, and chromosomal localization. *Science.***230**:37-43.

Knott, T.J., Pease, R.J., Powell, L.M., Wallis, S.C., Rall, S.C. Jr, Innerarity, T.L., Blackhart, B., Taylor, W.H., Marcel, Y., Milne, R.W., Johnson, D., Fuller, M., Lusis, A.J., McCarthy, B.J., Mahley, R.W., Levy-Wilson, B., and Scott, J. (1986) Complete protein sequence and identification of structural domains of human apolipoprotein B. *Nature.* **323**:734-738.

Kobayashi, K., Nakamura, N., Sumi, A., Ohmura, T. and Yokoyama, K. (1998) The development of recombinant human serum albumin. *Ther Apher.* **2**:257-262.

Kotake, H., Li, Q., Ohnishi, T., Ko, K.W., Agellon, L.B. and Yokoyama, S. (1996) Expression and secretion of rabbit plasma cholesteryl ester transfer protein by Pichia pastoris. *J Lipid Res.* **37**:599-605.

Kozarsky, K., Kingsley, D., and Krieger, M. (1988) Use of a mutant cell line to study the kinetics and function of O-linked glycosylation of low density receptors. *Proceedings of the National Academy of Science.* **85**:4335-4339.

Krauss, R.M., and Burke, D.J. (1982) Identification of multiple subclasses of plasma low density lipoproteins in normal humans. *Journal of Lipid Research.* **23**:97-104.

Krieger, M., and Herz, J. (1994) Structures and functions of multiligand lipoprotein receptors: macrophage scavenger receptors and LDL receptor-related protein (LRP). *Annu Rev Biochem.* **63**:601-637.

Krul, E.S., Parhofer, K.G., Barrett, P.H., Wagner, R.D. and Schonfeld, G. (1992) ApoB-75, a truncation of apolipoprotein B associated with familial hypobetalipoproteinemia: genetic and kinetic studies. *Journal of Lipid Research.* **33**:1037-1050.

Kuwano, M., Seguchi, T., and Ono, M. (1991) Glycosylation mutations of serine/threonine-linked oligosaccharides in low-density lipoprotein receptor: indispensable roles of O-glycosylation. *Journal of Cellular Science.* **98**:131-134.

Law, A., and Scott, J. (1990) A cross-species comparison of apolipoprotein B domain that binds to LDL receptor. *Journal of Lipid Research.* **31**:1109-1120.

Li, Y., Marzolo, M.P., van Kerkhof, P., Strous, G.J. and Bu, G. (2000) The YXXL motif, but not the two NPXY motifs, serves as the dominant endocytosis signal for low density lipoprotein receptor-related protein. *J Biol Chem.* **275**:17187-17194.

Livnah, O., Stura, E.A., Middleton, S.A., Johnson, D.L., Jolliffe, L.K. and Wilson, I.A. (1999) Crystallographic evidence for preformed dimers of erythropoietin receptor before ligand activation. *Science.* **283**:987-990.

Lund-Katz, S., Laplaud, P.M., Phillips, M.C. and Chapman, M.J. (1998) Apolipoprotein B-100 conformation and particle surface charge in human LDL subspecies: implication for LDL receptor interaction. *Biochemistry*. **37**:12867-12874.

Mahley, R.W. and Huang, Y. (1999) Apolipoprotein E: from atherosclerosis to Alzheimer's disease and beyond. *Current Opinion in Lipidology*. **10**:207-17

Mahley, R.W., Innerarity, T.L., Rall, S.C. Jr, and Weisgraber, K.H. (1984) Plasma lipoproteins: apolipoprotein structure and function. *Journal of Lipid Research*. **25**:1277-1294.

Mahley, R.W., Innerarity, T.L., Weisgraber, K.B. and Oh, S.Y. (1979) Altered metabolism (*in vivo* and *in vitro*) of plasma lipoproteins after selective chemical modification of lysine residues of the apoproteins. *Journal of Clinical Investigation*. **64**:743-750.

Malby, S., Pickering, R., Saha, S., Smallridge, R., Linse, S. and Downing, A.K. (2001) The first epidermal growth factor-like domain of the low-density lipoprotein receptor contains a noncanonical calcium binding site. *Biochemistry*. **40**:2555-2563.

Marcoux, C., Tremblay, M., Fredenrich, A., Jacques, H., Krimbou, L., Nakajima, K., Davignon, J., and Cohn, J.S. (1998) Plasma remnant-like particle lipid and apolipoprotein levels in normolipidemic and hyperlipidemic subjects. *Atherosclerosis*. **139**:161-171.

Markwell, M.A., Haas, S.M., Bieber, L.L. and Tolbert, N.E. (1978) A modification of the Lowry procedure to simplify protein determination in membrane and lipoprotein samples. *Analytical Biochemistry*. **87**:206-210.

Marlovitis, T.C., Abrahamsberg, C., and Blaas, D. (1998). Soluble LDL minireceptors–minimal structure requirements for recognition of minor group human rhinovirus. *The Journal of Biological Chemistry*. **273**:33835-33840.

McKeone, B.J., Patsch, J.R. and Pownall, H.J. (1993) Plasma triglycerides determine low density lipoprotein composition, physical properties, and cell-specific binding in cultured cells. *Journal of Clinical Investagation*. **91**:1926-1933.

Medved, L.V., Migliorini, M., Mikhailenko, I., Barrientos, L.G., Llinas and M., Strickland, D.K. (1999) Domain organization of the 39-kDa receptor-associated protein. *Journal of Biological Chemistry*. **274**:717-727.

Mikhailenko, I., Considine, W., Argraves, K.M., Loukinov, D., Hyman, B.T. and Strickland, D.K. (1999) Functional domains of the very low density lipoprotein receptor:

molecular analysis of ligand binding and acid-dependent ligand dissociation mechanisms. *Journal of Cellular Science.* **112**:3269-3281.

Milne, R., Theolis, R. Jr, Maurice, R., Pease, R.J., Weech, P.K., Rassart, E., Fruchart, J.C., Scott, J. and Marcel, Y.L. (1989) The use of monoclonal antibodies to localize the low density lipoprotein receptor-binding domain of apolipoprotein B. *Journal of Biological Chemistry.* **264**:19754-19760.

Miyake, Y., Tajma, S., Funahashi, T., and Yamamoto, A. (1989). Analysis of a recycling-impaired mutant of low density lipoprotein receptor in familial hypercholesterolemia. *The Journal of Biological Chemistry.* **264:**16584-16590.

Mommaas-Kienhuis, A.M., Krijbolder, L.H., Van Hinsbergh, V.W., Daems, W.T. and Vermeer, B.J. (1985) Visualization of binding and receptor-mediated uptake of low density lipoproteins by human endothelial cells. *European Journal of Cell Biology.* **36**:201-208.

Netzer, W.J. and Hartl, F.U. (1998) Protein folding in the cytosol: chaperonin-dependent and -independent mechanisms. *Trends Biochemical Science.* **23**:68-73.

Netzer, W.J. and Hartl, F.U. (1997) Recombination of protein domains facilitated by co-translational folding in eukaryotes. *Nature.* **388**:343-349.

Nohturfft, A., Yabe, D., Goldstein, J.L. Brown, M.S. and Espenshade, P.J. (2000) Regulated step in cholesterol feedback localized to budding of SCAP from ER membranes. *Cell.* **102**:315-323.

North, C.L. and Blacklow, S.C. (2000) Evidence that familial hypercholesterolemia mutations of the LDL receptor cause limited local misfolding in an LDL-A module pair. *Biochemistry.* **39**:13127-13135.

Obermoeller, L.M., Chen, Z., Schwartz, A.L. and Bu, G. (1998) Ca^{2+} and receptor-associated protein are independently required for proper folding and disulfide bond formation of the low density lipoprotein receptor-related protein. *Journal of Biological Chemistry.* **273**:22374-22381.

Orci, L., Carpentier, J.L., Perrelet, A., Anderson, R.G., Goldstein, J.L. and Brown, M.S. (1978) Occurrence of low density lipoprotein receptors within large pits on the surface of human fibroblasts as demonstrated by freeze-etching. *Experimental Cell Research.* **113**:1-13.

O'Shannessy, D.J., Brigham-Burke, M., Soneson, K.K., Hensley, P. and Brooks, I. (1993) Determination of rate and equilibrium binding constants for macromolecular

interactions using surface plasmon resonance: use of nonlinear least squares analysis methods. *Analytical Biochemistry.* **212**:457-468.

Pease, R.J., Milne, R.W., Jessup, W.K., Law, A., Provost, P., Fruchart, J.C., Dean, R.T., Marcel, Y.L. and Scott, J. (1990) Use of bacterial expression cloning to localize the epitopes for a series of monoclonal antibodies against apolipoprotein B100. *Journal of Biological Chemistry.* **265**:553-568.

Pirwany, I.R., Fleming, R., Greer, I.A., Packard, C.J., and Sattar, N. Lipids and lipoprotein subfractions in women with PCOS: relationship to metabolic and endocrine parameters. (2001) *Clinical Endocrinology.* **54**:447-453.

Pitas, R.E., Friera, A., McGuire, J. and Dejager, S. (1992) Further characterization of the acetyl LDL (scavenger) receptor expressed by rabbit smooth muscle cells and fibroblasts. *Arteriosclerosis and Thrombosis.* **12**:1235-1244.

Pruzanski, W., Stefanski, E., de Beer, F.C., de Beer, M.C., Ravandi, A., and Kuksis, A. (2000) Comparative analysis of lipid composition of normal and acute-phase high density lipoproteins. *Journal of Lipid Research.* **41**:1035-1047.

Rall, S.C. Jr, Weisgraber, K.H., Innerarity, T.L. and Mahley, R.W. (1982) Structural basis for receptor binding heterogeneity of apolipoprotein E from type III hyperlipoproteinemic subjects. *Proceeding of the National Academy of Science.* **79**:4696-700.

Raffai, R., Weisgraber, K.H., MacKenzie, R., Rupp, B., Rassart, E., Hirama, T., Innerarity, T.L. and Milne, R. (2000) Binding of an antibody mimetic of the human low density lipoprotein receptor to apolipoprotein E is governed through electrostatic forces. Studies using site-directed mutagenesis and molecular modeling. *Journal of Biological Chemistry.* **275**:7109-7116.

Rapoport, I., Chen, Y.C., Cupers, P., Shoelson, S.E. and Kirchhausen, T. (1998) Dileucine-based sorting signals bind to the beta chain of AP-1 at a site distinct and regulated differently from the tyrosine-based motif-binding site. *EMBO J.* **17**:2148-2155.

Rattenholl, A., Ruoppolo, M., Flagiello, A., Monti, M., Vinci, F., Marino, G., Lilie, H., Schwarz, E. and Rudolph R. (2001) Pro-sequence assisted folding and disulfide bond formation of human nerve growth factor. *Journal of Molecular Biology.* **305**:523-533.

Raussens, V., Fisher, C.A., Goormaghtigh, E., Ryan, R.O. and Ruysschaert, J.M. (1998) The low density lipoprotein receptor active conformation of apolipoprotein E. Helix organization in N-terminal domain-phospholipid disc particles. *Journal of Biological Chemistry.* **273**:25825-25830.

Reardon, C.A., Driscoll, D.M., Davis, R.A., Borchardt, R.A., Getz and G.S. (1986) The charge polymorphism of rat apoprotein E. *Journal of Biological Chemistry.* **261**:4638-4645.

Redgrave, T.G. and Carlson, L.A. (1979) Changes in plasma very low density and low density lipoprotein content, composition, and size after a fatty meal in normo- and hypertriglyceridemic man. *Journal of Lipid Research.* **20**:217-229.

Remy, I., Wilson, I.A. and Michnick, S.W. (1999) Erythropoietin receptor activation by a ligand-induced conformation change. *Science.* **283**:990-993.

Rigotti, A., Edelman, E.R., Seifert, P., Iqbal, S.N., DeMattos, R.B., Temel, R.E., Krieger, M. and Williams, D.L. (1996) Regulation by adrenocorticotropic hormone of the in vivo expression of scavenger receptor class B type I (SR-BI), a high density lipoprotein receptor, in steroidogenic cells of the murine adrenal gland. *J Biol Chem.* **271**:33545-33549.

Robenek, H., Harrach, B. and Severs, N.J. (1991) Display of low density lipoprotein receptors is clustered, not dispersed, in fibroblast and hepatocyte plasma membranes. *Arterioscler Thromb.* **11**:261-271.

Rohlmann, A., Gotthardt, M., Hammer, R.E. and Herz, J. (1998) Inducible inactivation of hepatic LRP gene by cre-mediated recombination confirms role of LRP in clearance of chylomicron remnants. *J Clin Invest.* **101**:689-695.

Romanos, M.A., Scorer, C.A. and Clare, J.J. (1992) Foreign gene expression in yeast: a review. *Yeast.* **8**:423-488.

Russell, D.W., Brown, M.S. and Goldstein, J.L. (1989). Different combinations of cysteine-rich repeats mediate binding of low density lipoprotein receptor to two different proteins. *The Journal of Biological Chemistry.* **284:**21682-21688.

Russell, D.W., Yamamoto, T., Schneider, W.J., Slaughter, C.J., Brown, M.S. and Goldstein, J.L. (1983) cDNA cloning of the bovine low density lipoprotein receptor: feedback regulation of a receptor mRNA. *Proceedings of the National Academy of Sciences.* **80**:7501-7505.

Sarti, M., Farquhar, M.G. and Orlando, R.A. (2000) The receptor-associated protein (RAP) interacts with several resident proteins of the endoplasmic reticulum including a glycoprotein related to actin. *Experiments in Cell Research.* **260**:199-207.

Sato, A., Shimada, Y., Herz, J., Yamamoto, T. and Jingami, H. (1999) 39-kDa receptor-associated protein (RAP) facilitates secretion and ligand binding of extracellular region of very-low-density-lipoprotein receptor: implications for a distinct pathway from low-density-lipoprotein receptor. *Biochemical Journal.* **341**:377-383.

Savonen, R., Obermoeller, L.M., Trausch-Azar, J.S., Schwartz, A.L. and Bu, G. (1999) The carboxyl-terminal domain of receptor-associated protein facilitates proper folding and trafficking of the very low density lipoprotein receptor by interaction with the three amino-terminal ligand-binding repeats of the receptor. *Journal of Biological Chemistry.* **274**:25877-225882.

Saxena, K. and Shipley, G.G. (1997) Structural studies of detergent-solubilized and vesicle-reconstituted low-density lipoprotein (LDL) receptor. *Biochemistry.* **36**:15940-15948.

Scanu, A.M., Khalil, A., Neven, L., Tidore, M., Dawson, G., Pfaffinger, D., Jackson, E., Carey, K.D., McGill, H.C., and Fless, G.M. (1988) Genetically determined hypercholesterolemia in a rhesus monkey family due to a deficiency of the LDL receptor. *Journal of Lipid Research.* **12**:1671-1681.

Schneider, W.J., Basu, S.K., McPhaul, M.J., Goldstein, J.L.and Brown, M.S. (1979) Solubilization of the low density lipoprotein receptor. *Proc Natl Acad Sci U S A.* **76**:5577-5581.

Schneider, W.J., Beisiegel, U., Goldstein, J.L. and Brown, M.S. (1982) Purification of the low density lipoprotein receptor, an acidic glycoprotein of 164,000 molecular weight. *The Journal of Biological Chemistry.* **257**:2664-2673.

Schuck, P. (1997) Use of surface plasmon resonance to probe the equilibrium and dynamic aspects of interactions between biological macromolecules. *Annual Reviews of Biophysical and Biomolecular Structure.* **26**:541:566.

Schumaker, V.N., Phillips, M.L. and Chatterton, J.E. (1994) Apolipoprotein B and low-density lipoprotein structure: implications for biosynthesis of triglyceride-rich lipoproteins. *Advanced Protein Chemistry.* **45**:205-248.

Schuster, M., Einhauer, A., Wasserbauer, E., Sussenbacher, F., Ortner, C., Paumann, M., Werner, G. and Jungbauer, A. (2000) Protein expression in yeast; comparison of two expression strategies regarding protein maturation. *Journal of Biotechnology.* **84**:237-248.

Scorer, C.A., Clare, J.J., McCombie, W.R., Romanos, M.A. and Sreekrishna, K. (1994) Rapid selection using G418 of high copy number transformants of *Pichia pastoris* for high-level foreign gene expression. *Biotechnology*. **12**:181-184.

Segelke, B.W., Forstner, M., Knapp, M., Trakhanov, S.D., Parkin, S., Newhouse, Y.M., Bellamy, H.D., Weisgraber, K.H., and Rupp, B. (2000) Conformational flexibility in the apolipoprotein E amino-terminal domain structure determined from three new crystal forms: implications for lipid binding. *Protein Science*. **9**:886-897.

Segrest, J.P., Jones, M.K. and Dashti, N. (1999) N-terminal domain of apolipoprotein B has structural homology to lipovitellin and microsomal triglyceride transfer protein: a "lipid pocket" model for self-assembly of apoB-containing lipoprotein particles. *Journal of Lipid Research*. **40**:1401-1416.

Segrest, J.P., Jones, M.K., Mishra, V.K., Anantharamaiah, G.M. and Garber, D.W. (1994) ApoB-100 has a pentapartite structure composed of three amphipathic alpha-helical domains alternating with two amphipathic beta-strand domains. Detection by the computer program LOCATE. *Arteriosclerosis and Thrombosis*. **14**:1674-1685.

Shachter, N.S. (2001) Apolipoproteins C-I and C-III as important modulators of lipoprotein metabolism. *Current Opinion in Lipidology*. **12**:297-304.

Simons, K. and Ikonen, E. (2000) How cells handle cholesterol. *Science*. **290**:1721-1726.

Simmons, T., Newhouse, Y.M., Arnold, K.S., Innerarity, T.L. and Weisgraber KH. (1997) Human low density lipoprotein receptor fragment. Successful refolding of a functionally active ligand-binding domain produced in *Escherichia coli*. *Journal of Biological Chemistry*. **272**:25531-25536.

Sohl, J.L., Jaswal, S.S. and Agard, D.A. (1998) Unfolded conformations of alpha-lytic protease are more stable than its native state. *Nature*. **395**:817-819.

Springer, T.A. (1998) An extracellular beta-propeller module predicted in lipoprotein and scavenger receptors, tyrosine kinases, epidermal growth factor precursor, and extracellular matrix components. *Journal of Molecular Biology*. **283**:837-862.

Sreekrishna, K., Nelles, L., Potenz, R., Cruze, J., Mazzaferro, P., Fish, W., Fuke, M., Holden, K., Phelps, D. and Wood, P. (1989) High-level expression, purification, and characterization of recombinant human tumor necrosis factor synthesized in the methylotrophic yeast *Pichia pastoris*. *Biochemistry*. **28**:4117-4125.

Sreekrishna, K., Potenz, R.H., Cruze, J.A., McCombie, W.R., Parker, K.A., Nelles, L., Mazzaferro, P.K., Holden, K.A., Harrison, R.G., and Wood, P.J., (1988) High level

expression of heterologous proteins in methylotrophic yeast *Pichia pastoris*. *Journal of Basic Microbiology*. **28**:265-278.

Steele, J.C. and Reynolds, J.A. (1979) Molecular weight and hydrodynamic properties of apolipoproteins in guanidine hydrochloride and sodium dodecyl sulfate solutions. *Journal of Biological Chemistry*. **254**:1639-1654.

Stenberg, E., Persson, B., Ross, H., Urbaniczky, C., (1991) Quantitative determination of surface concentration of protein with surface plasmon resonance by using radiolabeled proteins. *Journal of Collidial Interface Science*.**143**:513-526.

Sudhof, T.C., Goldstein, J.L., Brown, M.S., and Russell, D.W. (1985) The LDL receptor gene: a mosaic of exons shared with different proteins. *Science*. **228**:815-822.

Swinkels, D.W., Hendriks, J.C., Demacker, P.N. and Stalenhoef, A.F. (1990) Differences in metabolism of three low density lipoprotein subfractions in Hep G2 cells. *Biochimical Biophysica Acta*. **1047**:212-222.

Tall, A.R., and Small D.M. (1978) Plasma high-density lipoproteins. *New England Journal of Medicine*. **299**:1232-1236.

Teng, B., Sniderman, A., Krauss, R.M., Kwiterovich, P.O. Jr, Milne, R.W. and Marcel, Y.L. (1985) Modulation of apolipoprotein B antigenic determinants in human low density lipoprotein subclasses. *Journal of Biological Chemistry*. **260**:5067-5072.

Van der Westhuyzen, D.R., Stein, M.L., Henderson, H.E., Marais, A.D., Fourie, A.M. and Coetzee, G.A. (1991) Deletion of two growth-factor repeats from the low-density-lipoprotein receptor accelerates its degradation. *Biochem J*. **277**:677-682.

Van Driel, I.R., Brown, M.S. and Goldstein, J.L. (1989) Stoichiometric binding of low density lipoprotein (LDL) and monoclonal antibodies to LDL receptors in a solid phase assay. *Journal of Biological Chemistry*. **264**:9533-9538.

Van Driel, I.R., Davis, C.G., Goldstein, J.L., and Brown, M.S. (1987a). Self association of the low density lipoprotein receptor mediated by the cytoplasmic domain. *The Journal of Biological Chemistry*. **262:**16127-16134.

Van Driel, I.R., Goldstein, J.L., Sudhof, T.C. and Brown, M.S. (1987b). First cysteine-rich repeat in ligand binding domain of low density lipoprotein receptor binds Ca^{2+} and monoclonal antibodies, but not lipoproteins. *The Journal of Biological Chemistry*. **262:**17443-17449.

Von Eckardstein, A., Nofer, J.R. and Assmann, G. (2001) High density lipoproteins and arteriosclerosis. Role of cholesterol efflux and reverse cholesterol transport. *Arteriosclerosis Thrombosis Vascular Biology*. **21**:13-27.

Wegner, G.H. (1990) Emerging applications of the methylotrophic yeasts. *FEMS Microbiology Review*. **7**:279-283.

Wegner, G.H. and Harder, W. (1987) Methylotrophic yeasts--1986. *Antonie Van Leeuwenhoek*. **53**:29-36.

Weisgraber, K.H. (1994) Apolipoprotein E: structure-function relationships. *Advanced Protein Chemistry*. **45**:249-302.

Weisgraber, K.H. and Mahley, R.W. (1996) Human apolipoprotein E: the Alzheimer's disease connection. *FASEB Journal*. **10**:1485-1494.

Weisgraber, K.H., Innerarity, T.L., Harder, K.J., Mahley, R.W., Milne, R.W., Marcel, Y.L. and Sparrow, J.T. (1983) The receptor-binding domain of human apolipoprotein E. Monoclonal antibody inhibition of binding. *Journal of Biological Chemisty*. **258**:12348-12354.

Weisgraber, K.H., Lund-Katz, S., and Phillips, M.C. (1992) In "High Density lipoproteins and Atherosclerosis III" (N.E. Miller and A.R. Tall, Eds), pp. 175-181. Elsivier, Amsterdam.

Weisgraber, K.H., Rall, S.C. Jr and Mahley, R.W. (1981) Human E apoprotein heterogeneity. Cysteine-arginine interchanges in the amino acid sequence of the apo-E isoforms. *J Biol Chem*. **256**:9077-9083.

Welty, F.K., Seman, L., and Yen, F.T. (1995) Purification of the apolipoprotein B-67-containing low density lipoprotein particle and its affinity for the low density lipoprotein receptor. *Journal of Lipid Research*. **36**:2622-2629.

Wernette-Hammond, M.E., Lauer, S.J., Corsini, A., Walker, D., Taylor, J.M. and Rall, S.C. Jr. (1989) Glycosylation of human apolipoprotein E. The carbohydrate attachment site is threonine 194. *Journal of Biological Chemistry*. **264**:9094-9101.

Wetterau, J.R., Aggerbeck, L.P., Rall, S.C. Jr and Weisgraber, K.H. (1988) Human apolipoprotein E3 in aqueous solution. I. Evidence for two structural domains. *Journal of Biological Chemistry*. **263**:6240-6248.

Willnow, T.E., Armstrong, S.A., Hammer, R.E. and Herz, J. (1995) Functional expression of low density lipoprotein receptor-related protein is controlled by receptor-

associated protein *in vivo*. *Proceedings of the National Academy of Science*. **92**:4537-4541.

Willnow, T.E., Rohlmann, A., Horton, J., Otani, H., Braun, J.R., Hammer, R.E. and Herz, J. (1996) RAP, a specialized chaperone, prevents ligand-induced ER retention and degradation of LDL receptor-related endocytic receptors. *EMBO Journal*. **15**:2632-2639.

Wilson, C., Mau, T., Weisgraber, K.H., Wardell, M.R., Mahley, R.W. and Agard, D.A. (1994) Salt bridge relay triggers defective LDL receptor binding by a mutant apolipoprotein. *Structure*. **2**:713-718.

Wilson, C., Wardell, M.R., Weisgraber, K.H., Mahley, R.W. and Agard, D.A. (1991) Three-dimensional structure of the LDL receptor-binding domain of human apolipoprotein E. *Science*. **252**:1817-1822.

Wang, X., Pease, R., Bertinato, J. and Milne, R.W. (2000) Well-defined regions of apolipoprotein B-100 undergo conformational change during its intravascular metabolism. *Arteriosclerosis Thrombosis and Vascualar Biology*. **20**:1301-1308.

Yamamoto, T., Davis, C.G., Brown, M.S., Schneider, W.J., Casey, M.L., Goldstein, J.L., and Russell, D.W. (1984) The human LDL receptor: a cysteine-rich protein with multiple Alu sequences in its mRNA. *Cell*. **39**:27-38.

Yang, C.Y., Gu, Z.W., Weng, S.A., Kim, T.W., Chen, S.H., Pownall, H.J., Sharp, P.M., Liu, S.W., Li, W.H., Gotto, A.M. Jr, and Chan, L. (1989) Structure of apolipoprotein B-100 of human low density lipoproteins. *Arteriosclerosis*. **9**:96-108.

Yang, C.Y., Chen, S.H., Gianturco, S.H., Bradley, W.A., Sparrow, J.T., Tanimura W.L., Sparrow, D.A., DeLoof, Rosseneu, M., Lee, J.S., Gu, Z.W., gotto, A.M., and Chan, L. (1986) Sequence, structure, receptor-binding domains and internal repeats of human apolipoprotein B-100. *Nature*. **323**:738:742.

Ybe, J.A., Brodsky, F.M., Hofmann, K., Lin, K., Liu, S.H., Chen, L., Earnest, T.N., Fletterick, R.J. and Hwang, P.K. (1999) Clathrin self-assembly is mediated by a tandemly repeated superhelix. *Nature*. **399**:371-375.

Zaiou, M., Arnold, K.S., Newhouse, Y.M., Innerarity, T.L., Weisgraber, K.H., Segall, M.L., Phillips, M.C. and Lund-Katz S. (2000) Apolipoprotein E-low density lipoprotein receptor interaction. Influences of basic residue and amphipathic alpha-helix organization in the ligand. *Journal of Lipid Research*. **4**:1087-1095.

Ziak, M., Meier, M., Etter, K.S. and Roth, J. (2001) Two isoforms of trimming glucosidase II exist in mammalian tissues and cell lines but not in yeast and insect cells. *Biochem Biophys Res Commun.* **280**:363-367.